THE AMERICAN JOURNAL OF PATHOLOGY

VOLUME XXXVIII APRIL, 1961 NUMBER 4

ELECTRON MICROSCOPIC STUDIES OF NORMAL AND PROLIFERATED BILE DUCTULES

FENTON SCHAFFNER, M.D., AND HANS POPPER, M.D.

From the Department of Pathology, The Mount Sinai Hospital, New York, N.Y.

Tubules lined by flat or cuboidal epithelium connect bile canaliculi between the liver cells with the smallest bile ducts in the portal tracts. They lie partly in the portal tract and partly in the parenchyma, mainly in its periportal zone, and have been designated as cholangioles, canals of Hering, ampullas or intermediate pieces. The name "bile ductule" seems to be preferable [1] to differentiate it from the smallest interlobular duct accompanied by terminal branches of portal vein and hepatic artery. Under abnormal circumstances in both human beings and experimental animals, these ductules exhibit excessive proliferation, appear in a variety of shapes, and the cells may be quite undifferentiated ("oval cells").[2] The proliferation is usually associated with the accumulation of inflammatory cells, and the combined lesion has been designated as "ductular cell reaction." [3] The derivation of normal and particularly of proliferated ductules has not been established. They have been assumed by some to originate from liver cells, and by others to be derived from pre-existing ducts or ductules. Connections between ductules and liver cell plates have been demonstrated repeatedly by injection methods.[4] Histochemical reactions,[5,6] including staining for various phosphatases,[7] have shown them to differ from liver cells. Since interpretations have been controversial, we have utilized electron microscopy in order to investigate the ductules in man and in representative examples of experimental hepatic injury in animals (a) to determine the basic cytology of these structures

Supported by Research Grant A-3846 Path. from the National Institute of Arthritis and Metabolic Diseases of the United States Public Health Service, and by the United States Army Medical Research and Development Command under Contract DA-49-007-MD-790.

Presented in part at the Annual Meeting of the American Society of Experimental Pathology, Chicago, April 13, 1960.

Accepted for publication, November 28, 1960.

which might permit conclusions as to their function; (b) to compare their appearance with that of neighboring liver cells and mesenchymal cells; and (c) to describe their relation to the surrounding stroma.

Material and Methods

Liver sections containing ductules were chosen for this study from collected specimens prepared for electron microscopy. The human tissues were from cases of acute viral hepatitis (2 cases), subacute hepatitis (1 case), postnecrotic cirrhosis (2 cases), primary biliary cirrhosis (2 cases), Wilson's disease (1 case), idiopathic hemochromatosis (1 case), nonspecific portal inflammation (2 cases), extrahepatic biliary obstruction (2 cases), and chlorpropamide-induced cholestasis (1 case). The animal specimens came from 2 normal rats and 1 normal dog, 1 rat fed a low choline-low protein-high fat diet[8] for 3 months, 4 rats fed a diet containing 0.5 per cent ethionine[9] for 1 to 2 months, and 1 fed a diet with 5,000 ppm. of Aramite[10] for 1 month.

Liver tissue was obtained with a Menghini biopsy needle[11] from both patients and animals and immediately fixed in a 1.5 per cent aqueous osmium tetroxide solution adjusted to pH 7.4 with sodium hydroxide. In animals this was done at a laparotomy preceding sacrifice. Tissue was dehydrated and embedded in a mixture of methyl and n-butyl methacrylate and sectioned with the Porter-Blum microtome. After mounting on copper grids, some of the sections were floated face down for 20 minutes on a 1 per cent solution of phosphotungstic acid for staining collagen fibers.[12] The sections were examined and photographed with a Philips EM 100 electron microscope. Thicker sections were examined with the phase contrast microscope or with the light microscope after staining with chromotrope aniline blue. Paraffin sections from the same biopsy specimens were examined by conventional methods.

Observations

Normal Ductules

Since ductules were not seen in the small electron microscopic specimens of normal human liver, the normal ductules in the rat and dog are described. In cross section, with the light microscope, the ductule appeared as an acinar structure lined by cuboidal epithelium. By electron microscopy it consisted of 3 to 10 cells, each about 10 μ in diameter, arranged around a 1 to 3 μ lumen (Figs. 1, upper, and 2, upper left). The ductular cell border directed toward the lumen exhibited 5 to 30 projecting microvilli; these measured 0.3 μ in length and 0.1 μ in thickness. They were somewhat shorter than the canalicular microvilli of liver cells but were of similar thickness. Fine filaments appeared to traverse the length of the microvillus, but no definite central canal was seen. The filaments appeared to connect with an irregular cytoplasmic network which was much finer than the endoplasmic reticulum and was well recognized only in optimal specimens (Fig. 3). Occasional cells also showed bleb formation replacing microvilli along part of the lumen surface (Fig. 2, upper left). The nucleus was round to oval, about 5 μ in diameter, and occupied the central half of the cell. Nuclear chromatin appeared homogeneous, and a small and irregular nucleolus was usually eccentric.

Within the cytoplasm, 5 to 10 small mitochondria appeared in cross section. These were considerably smaller than the mitochondria in parenchymal liver cells and had few cristae. Ergastoplasm was scant, and ribonucleoprotein or Palade granules appeared as a few scattered clusters not necessarily near endoplasmic reticulum. Between adjacent cells radiating from the lumen of the ductule, the borders were straight. Canaliculi draining near-by liver cells occasionally extended between two ductular cells (Fig. 2, upper right). The outer border of the ductule was gently curved and devoid of microvilli. It was separated by a thin light zone about 500 Å in width from an electron-dense homogeneous layer of about equal width. This was enveloped by another less distinct and narrower light zone. The dense layer was continuous around the entire ductular structure; it resembled a basement membrane and, on occasion, was duplicated (Fig. 2, lower half). External to the outer light zone of the membrane, small bundles of collagenous fibrils were occasionally seen; similar fibrils were not found inside the basement membrane. Adjacent to the ductule a lymphatic space, one or two small blood vessels and a few mesenchymal cells were manifest.

In the patient with Wilson's disease, a normal intralobular ductule was encountered. This exhibited microvilli projecting into the lumen (Fig. 4). A few mitochondria were noted in each cell, and one cell contained a fat droplet. A few fibrils lay outside the basement membrane.

Ductular Proliferation Without Inflammation or Fibrosis

The fatty liver of the rat on a low protein-high fat diet exhibited many ductules. The cells in these were smaller and flatter than in the normal rat. The lumens were more frequently cut tangentially or even longitudinally, suggesting that they were no longer cylindrical but were rather flattened or irregular. Increased numbers of microvilli projected into the lumens although they were the same size and shape as in the normal liver. The nuclei were oval, with the long axis parallel to the lumen; nucleoli were small. Mitochondria were sparse, but ergastoplasm seemed to be increased in amount. Neither fibrils nor mesenchymal cells were in proximity to the thin basement membrane. The ductule usually lay in the space of Disse, which extended between sinusoidal endothelium and the liver cell margins. No comparable ductules were seen in the human tissues.

Ductular Proliferation with Periductular Inflammation of Short Duration

In rats receiving ethionine or Aramite, ductular proliferation began within 2 to 3 weeks. These ductules were larger than normal and occa-

sionally had larger though rounded lumens (Fig. 1, lower). The cells varied in size and shape, but microvilli were present. Occasionally the entire lumen surface of a cell formed a bleb. The nuclei were often irregularly shaped. Some mitochondria contained increased numbers of cristae. The basement membrane was unaltered but was surrounded by a continuous layer of intertwined fibrils and many parenchymal cells. The periodicity of the fibrils was that of collagen. Some mesenchymal cells were large and contained phagosomes and lipofuscin granules. The relations to lymphatics and blood vessels were preserved. Neither fibrils nor mesenchymal cells lay within the space encircled by the basement membrane.

In acute viral hepatitis somewhat similar ductules were found although with a greater amount of periductular fibrosis. In some instances surface bleb formation was more prominent. Focally, the basement membrane was separated from the ductular cell. Since the surrounding structures were intact, this empty space presumably was not artifact but probably represented edema. In several patients small black globules, probably lipid, lay in the ductular cell cytoplasm. In addition, vacuolated or dense granular bodies similar to the lipofuscin pigment granules in liver cells were seen. Reticulated and osmiophilic areas were noted in some ductular cells in jaundiced patients. These resembled bile imbibition in parenchymal cells.

Long Standing Ductular Proliferation

Many normal-sized ductules were found in rats given ethionine for two months or longer. The lumens were small and round or elongated; microvilli were normal. The nuclei were quite irregular and occasionally eccentric. The cytoplasm was generally disrupted and occasionally contained finely granular electron-dense deposits. These resembled ferritin [13] although they were not clearly contained within organelles. The basement membrane often was not a sharp thin line but a smudgy band measuring up to 0.2 μ in thickness. Surrounding the ductule were many mesenchymal cells and a tangled mass of fibers in large bundles. Lymphatic spaces were not discerned, and no near-by blood vessels were found. Mesenchymal cells were smaller than ductular cells and had irregular nuclei with scant cytoplasm. Fine filaments lacking periodicity and not impregnated by phosphotungstic acid occasionally extended from the cytoplasm through the cell wall and were intermixed with collagen fibrils outside the cell. These cells had the characteristic crenated nuclei of Kupffer cells, but the cytoplasm differed by the absence of phagocytized content. Fibroblasts were not seen.

Similar ductules were seen in livers with postnecrotic cirrhosis, hemochromatosis, nonspecific portal inflammation and chronic cholangitis secondary to common duct stone (Fig. 5). These also had small, round lumens and were surrounded by thickened basement membranes, fiber bundles and inflammatory cells. Lymphatics or blood vessels were at a distance. The nuclei often varied considerably in size, shape and density in the same ductule. Nucleoli were larger than in rats, and occasionally two appeared in a single nucleus. In hemochromatosis, ferritin[13] was present in the ductular cell cytoplasm. Only in this condition were the ductular cell nucleoli prominent.

Canalicular-Ductular Junction

In one patient with inactive postnecrotic cirrhosis, two ductular cells lay in close apposition to two parenchymal cells to which they bore no similarity (Fig. 6). The cell borders between ductular and parenchymal cells were straight, and neither a space nor a basement membrane separated them. A lumen containing microvilli was evident between the two ductular cells and another between the two ductular cells and one of the parenchymal cells. The cytoplasm of the parenchymal cell had the usual abundant and orderly profiles of endoplasmic reticulum and showed numerous Palade granules as well as many normal mitochondria containing fairly dense material. The ductular cells appeared empty; they had little endoplasmic reticulum and few small mitochondria with scant content. Ductular cells were separated from the tissue space by a thin basement membrane which extended over the surface of the two liver cells for a distance of 10 to 20 μ and then ended in a frayed fashion (Fig. 7). The extension of the basement membrane seemed to serve as an anchor holding the ductule in place. Microvilli, normally present on the sinusoidal surface of the parenchymal cell, could be seen under the basement membrane.

Bleb Formation in the Lumen Membrane of the Ductular Epithelium

In some instances with more rapid ductular proliferation (a rat with Aramite intoxication, a 10-year-old child with very active postnecrotic cirrhosis, and an infant with severe subacute hepatitis and cholangiolitis) numerous blebs projected into the ductule lumen (Fig. 8). The blebs usually involved the entire lumen surface of an affected cell. The cell membrane appeared lifted up, the bleb containing cell sap and a few Palade granules. Organelles were not seen. When bleb formation was extensive, blebs were also encountered in the parenchymal cell canalicular lumens.

Discussion

The electron microscope shows the ductular cell to have a far less elaborate cytoplasmic structure than the parenchymal cell, indicating a less complex metabolic function. The paucity and smallness of mitochondria suggest little energy production, and the sparsity of endoplasmic reticulum reflects minimal biosynthesis.[14] Despite great individual variations in the same ductule under abnormal circumstances, the appearance of the cells differs from that of liver cells. Intermediate forms between the two types of cells were not seen although ductules were in process of excessive proliferation. These findings do not support the concept that ductular cells proliferating in postnatal life originate from liver cells by modulation.[15] Rather, the viewpoint that they are derived from pre-existing ductular cells is favored.[16] This does not negate the possibility that during embryonal development ductular cells may develop from liver cells.[17] The most distinctive feature of the ductule is the basement membrane; this is lacking about liver cell plates except where the membrane seems to serve as an anchor at the point of ductule origin. Even when surrounded by excessive fiber deposit, liver cells do not have a basement membrane although the existence of such a membrane is suggested in conventional sections stained with the periodic acid-Schiff stain.[18] An apparently continuous membrane impregnated with silver stain, as judged by very thin sections examined by both light and electron microscopy, results from overlap of individual collagen fibers.

The structural features common to both ductular and liver epithelium are the microvilli, which extend from the surfaces exposed to bile flow into the lumens of ductules and those of hepatic cell canaliculi. The basal surfaces of ductular epithelium are straight and rest on basement membranes while the sinusoidal surfaces of liver cells are thrown into irregularly projecting microvilli which extend into the pericellular tissue spaces and occasionally into the sinusoidal blood stream. Since liver cells secrete bile and ductule cells apparently do not, microvilli probably do not reflect secretion of bile but represent a function common to both cells, presumably secretion or reabsorption of water. While the appearance of the basal surface of ductular epithelium indicates considerably less exchange activity than the sinusoidal surface of liver cells, water transport is suggested by the close proximity to lymphatic spaces and blood vessels. Several reported observations imply the secretion of fluid by ductular epithelium. Secretin increases the flow of a bile containing bicarbonate but one poor in bile salts. If biliary content exemplified by bile salts is formed in liver cells, bicarbonate-containing fluid may be

secreted by the ductular epithelium.[19,20] Moreover, in the face of ductular proliferation, as in subacute ethionine intoxication, bile flow is increased but the bile salt concentration is low, thus supporting the view that the ductule secretes water.[21] Finally, in other intoxications, water, bilirubin and dye excretion are affected in different fashions.[22,23] A role in bile secretion has been ascribed to the ductules. Bleb formation has been related to apocrine secretion, and this has also been seen in liver cell bile canaliculi.[24] However, the significance of these blebs requires further investigation. Evidence for reabsorption by ductules can also be cited. That the gallbladder can resorb water has long been known. In intrahepatic cholestasis and in hamartomas (Meyenberg complexes), inspissation of bile in canaliculi and ductules bespeaks water removal. Ductules may therefore determine the final water and electrolyte content of hepatic bile.

With light microscopy it may be difficult to recognize ductular epithelium. In experimental animals, particularly, the cells may appear flattened and resemble fibroblasts or appear oval or clustered like mesenchymal cells. However, by electron microscopy their true nature is readily revealed by the demonstration of microvilli and basement membranes. The close proximity of inflammatory cells and fibers to proliferating ductules comprised of irregular epithelial cells ("ductular cell reaction") suggests a causal interrelationship. It may be claimed that portal inflammation leads to ductular proliferation. On the other hand, it is likely that under abnormal circumstances a factor which provokes growth of bile ductules may be excreted into the bile, possibly by damaged parenchymal cells.[25] If this escapes into the surrounding stroma, possibly as part of a fluid interchange mechanism, it may prove to be an irritant, thus accounting for the inflammation demonstrated.

Summary

Intrahepatic biliary ductules in man and experimental animals were investigated in normal and abnormal livers by electron microscopy. The ductular cells varied greatly, particularly under abnormal circumstances, and differed from liver cells in the appearance of the cell organelles and the presence of basement membranes. Cells intermediate between ductular and parenchymal elements were not encountered. Thus, there was no evidence that the former were derived from the latter in postnatal life. The occurrence of microvilli in the lumens of liver cell canaliculi and of ductules also indicates a common function, presumably the regulation of water content of bile.

References

1. Popper, H., and Schaffner, F. Liver: Structure and Function. Blakiston Div., McGraw-Hill Book Co., Inc., New York, 1957, p. 103.
2. Farber, E. Similarities in the sequence of early histological changes induced in the liver of the rat by ethionine, 2-acetylaminofluorene and 3′-methyl-4-dimethylaminoazobenzene. *Cancer Res.*, 1956, **16**, 142–148.
3. Popper, H.; Kent, G., and Stein, R. Ductular cell reaction in the liver in hepatic injury. *J. Mt. Sinai Hosp.*, 1957, **24**, 551–556.
4. Herxheimer, G., and Thölldte, M. Regeneration und Hypertrophie (Hyperplasie) der Leber. In: Handbuch der speziellen pathologischen Anatomie und Histologie. Henke, F., and Lubarsch, O. (eds.). J. Springer, Berlin, 1930, Vol. 5, Verdauungsdrüsen, Pt. 1, Leber, Chapt. 11, pp. 988–1037.
5. Melnick, P. J. Polycystic liver; analysis of seventy cases. *A.M.A. Arch. Path.*, 1955, **59**, 162–172.
6. Rosenholtz, M. Use of the histochemical demonstration of aminopeptidase to distinguish small bile ducts and hepatic parenchymal cells. (Abstract) *Gastroenterology*, 1960, **38**, 794.
7. Wachstein, M. Enzymatic histochemistry of the liver. *Gastroenterology*, 1959, **37**, 525–537.
8. Hoffbauer, F. W. Fatty cirrhosis in the rat. I. A method of grading specimens. *A.M.A. Arch. Path.*, 1959, **68**, 160–170.
9. Singer, E. J.; Hutterer, F.; Kent, G.; Zak, F. G., and Popper, H. Hepatic fibrosis; chemical and histologic studies during subacute ethionine intoxication. *A.M.A. Arch. Path.*, 1959, **68**, 103–112.
10. Popper, H.; and Sternberg, S. S.; Oser, B. L., and Oser, M. The carcinogenic effect of Aramite in rats; a study of hepatic nodules. *Cancer*, 1960, **13**, 1035–1046.
11. Parets, A. D.; Schaffner, F., and Black, H. Percutaneous liver biopsy with the Menghini needle. *Am. J. Digest. Dis.*, 1959, N.S. **4**, 693–699.
12. Watson, M. L. Staining of tissue sections for electron microscopy with heavy metals. *J. Biophys. & Biochem. Cytol.*, 1958, **4**, 475–478.
13. Richter, G. W. A study of hemosiderosis with the aid of electron microscopy; with observations on the relationship between hemosiderin and ferritin. *J. Exper. Med.*, 1957, **106**, 203–218.
14. Novikoff, A. B., and Essner, E. The liver cell; some new approaches to its study. *Am. J. Med.*, 1960, **29**, 102–131.
15. Leduc, E. H. Cell modulation in liver pathology. *J. Histochem.*, 1959, **7**, 253–255.
16. Ungar, H., and Goldberg, M. G. The nature of bile duct proliferations in the liver following ingestion of DL-ethionine. Lab. Invest., 1959, **8**, 1523–1534.
17. Horstmann, E. Entwicklung und Entwicklungsbedingungen des intrahepatischen Gallengangsystems. *Arch. f. Entwicklngsmech. d. Organ.*, 1939, **139**, 363–392.
18. Popper, H.; Paronetto, F., and Barka, T. PAS-positive structures of nonglycogenic character in normal and abnormal liver. *Arch. Path.*, 1960, **70**, 300–313.
19. Sperber, I. Secretion of organic anions in the formation of urine and bile. *Pharmacol. Rev.*, 1959, **11**, 109–134.
20. Wheeler, H. O.; Ramos, O. L., and Whitlock, R. T. Electrolyte excretion in bile. *Circulation*, 1960, **21**, 988–996.

21. POPPER, H.; SCHAFFNER, F.; HUTTERER, F.; PARONETTO, F., and BARKA, T. Parenchymal fibrogenesis: the liver. *Ann. New York Acad. Sc.*, 1960, **86**, 1075–1088.

22. ANDREWS, W. H. H. Excretory function of the liver; a re-assessment. *Lancet*, 1955, **2**, 166–169.

23. VANLERENBERGHE, J.; MILBLED, G., and GUERRIN, F. Étude du mécanisme sécrétoire de la cholérèse. *Path. et Biol.*, 1960, **8**, 1231–1234.

24. KITANI, T. Morphologic Studies on Cholestasis. Pamphlet of the Department of Internal Medicine, Osaka University Medical School, Japan; distributed at presentation at the first meeting of the International Association for the Study of the Liver, London, April 25–26, 1960.

25. GILLMAN, J.; GILBERT, C., and SPENCE, I. Some factors regulating structural integrity of the intrahepatic bile ducts with special reference to primary carcinoma of the liver and vitamin A. *Cancer*, 1954, **7**, 1109–1154.

Thanks are due to the staff of the Cell Research Laboratory of The Mount Sinai Hospital for assistance in the performance of this study.

[*Illustrations follow*]

Legends for Figures

FIG. 1. Electron micrographs of bile ductules in rats. Upper: Ductule in a normal rat; V, microvilli; MC, a mesenchymal cell. The small arrows indicate the basement membrane while the large arrow on the left points to a fiber bundle. × 10,000. Lower: Ductule in a rat fed a diet containing Aramite. The ductular epithelium is surrounded by a basement membrane and an envelope of fibers (arrows), endothelial and mesenchymal cells (MC), and blood vessels (BV); the latter contain erythrocytes. × 3000.

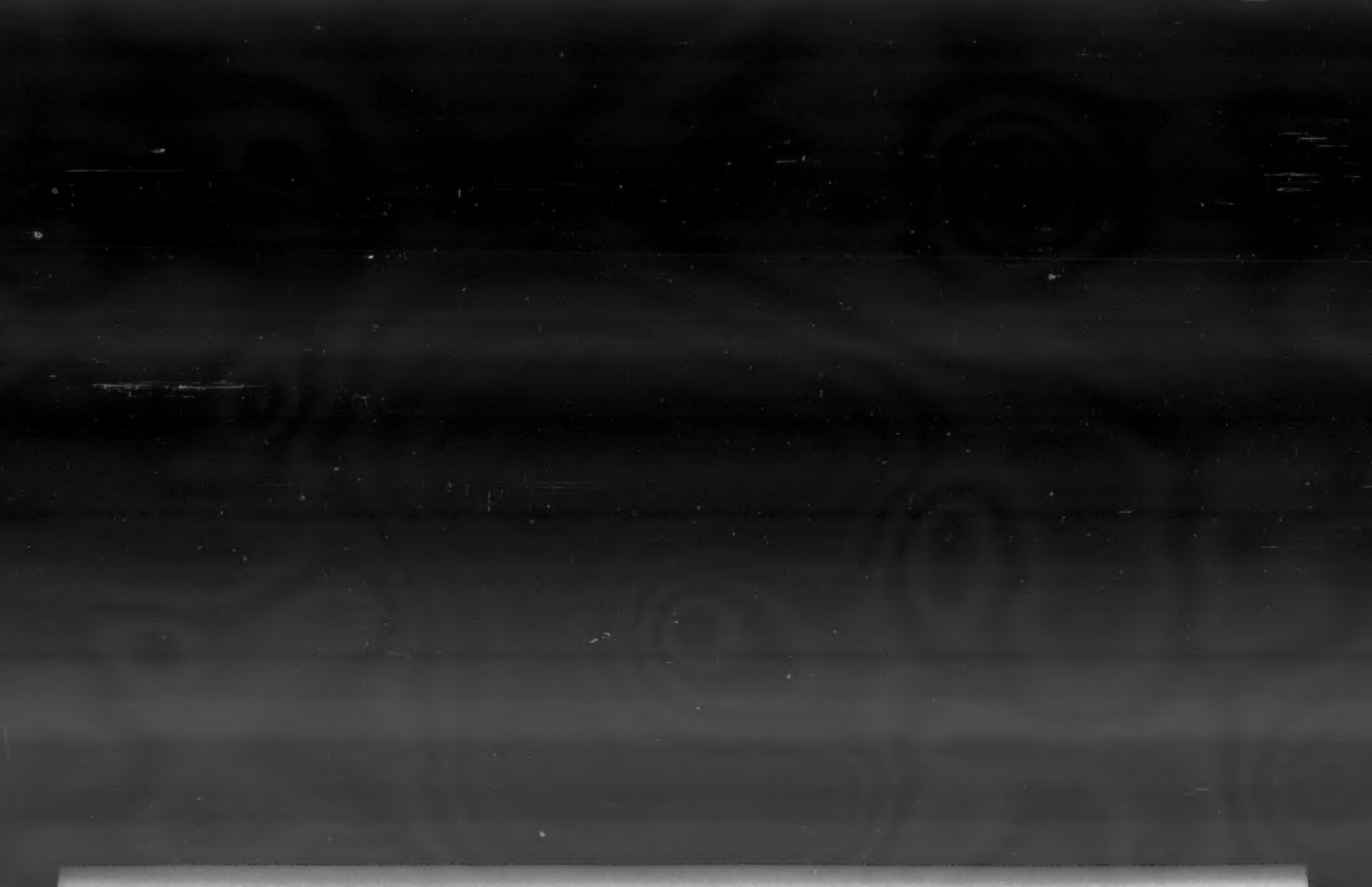

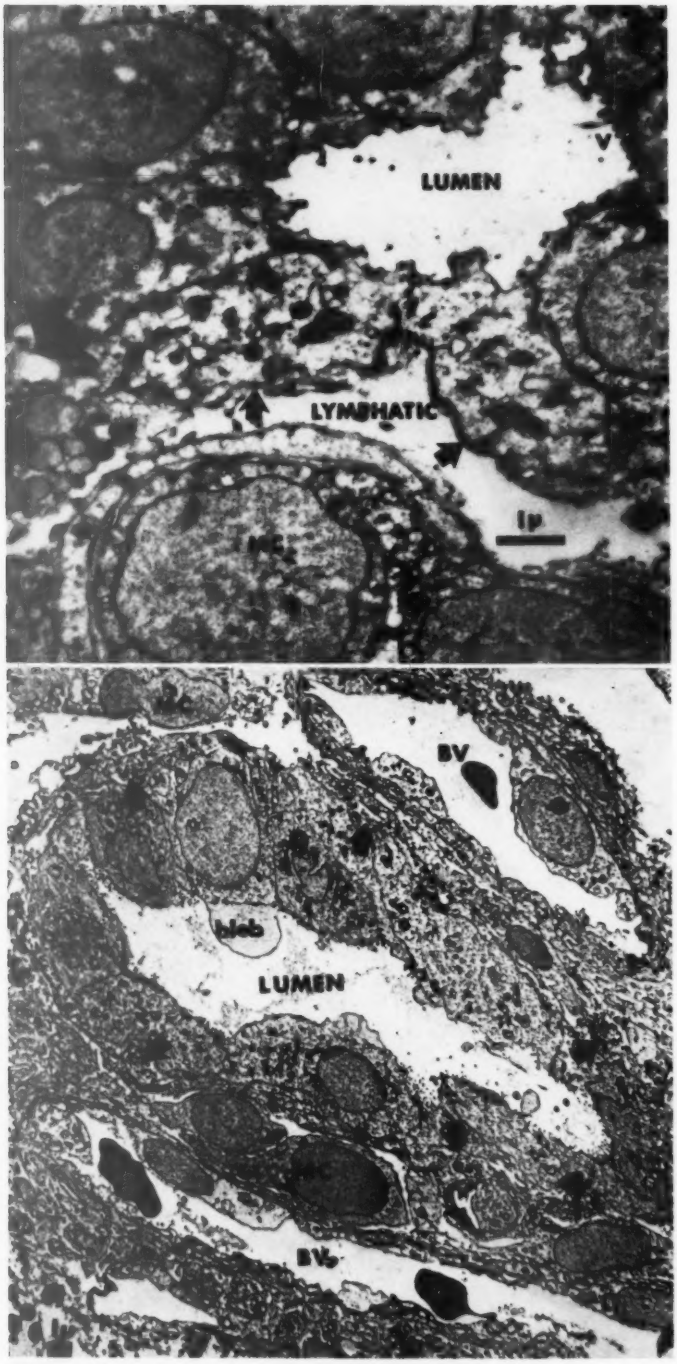

1

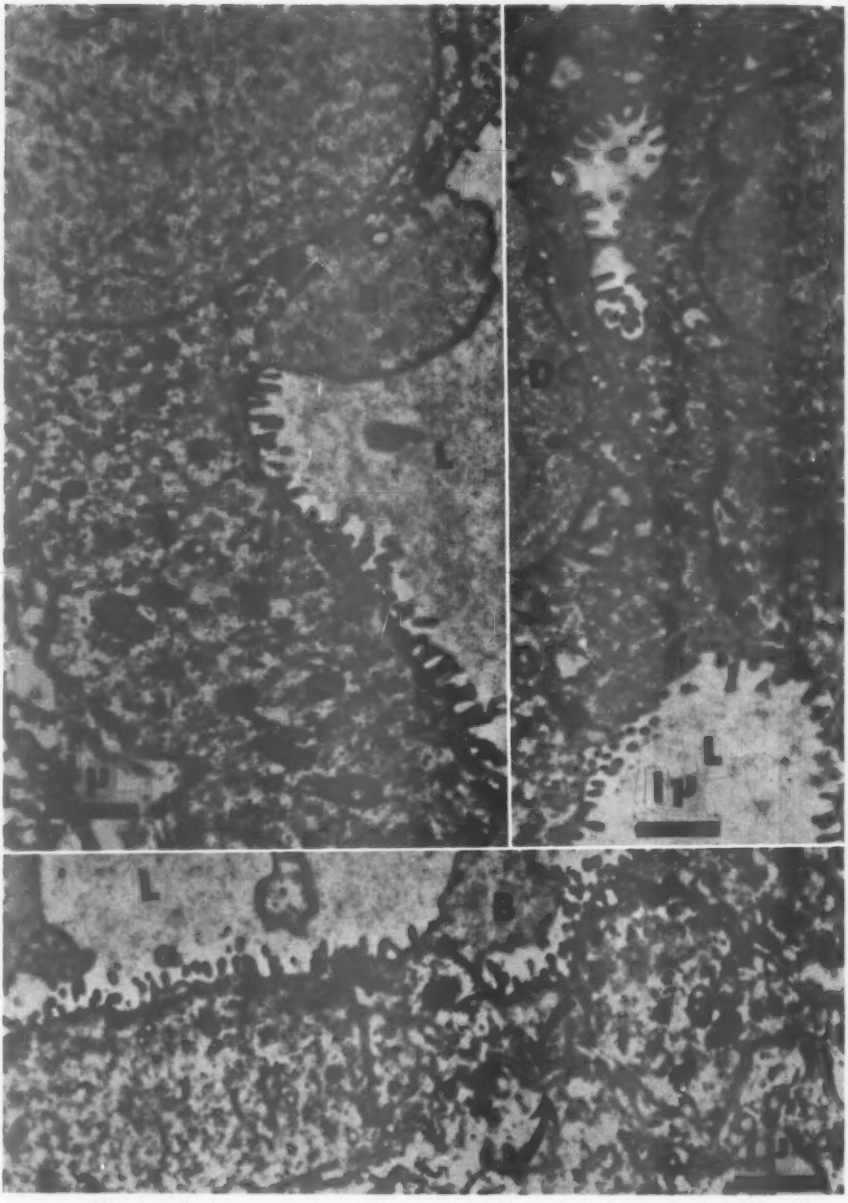

FIG. 2. Bile ductule in a normal rat. Upper left: Bleb formation in the location of the lumen surface. Upper right: Canaliculus (arrow) between neighboring parenchymal cells. Lower half: Duplication of the basement membrane (arrows). L, lumen; DC, ductular epithelium; B, bleb. × 13,000.

3

FIG. 3. Detail of lumen border of a ductular cell, showing fine filaments (arrows) in microvilli which appear to be connected to a fine cytoplasmic network (Fi). The latter is thinner than the endoplasmic reticulum (ER) and is not related to mitochondria (m). × 95,000.

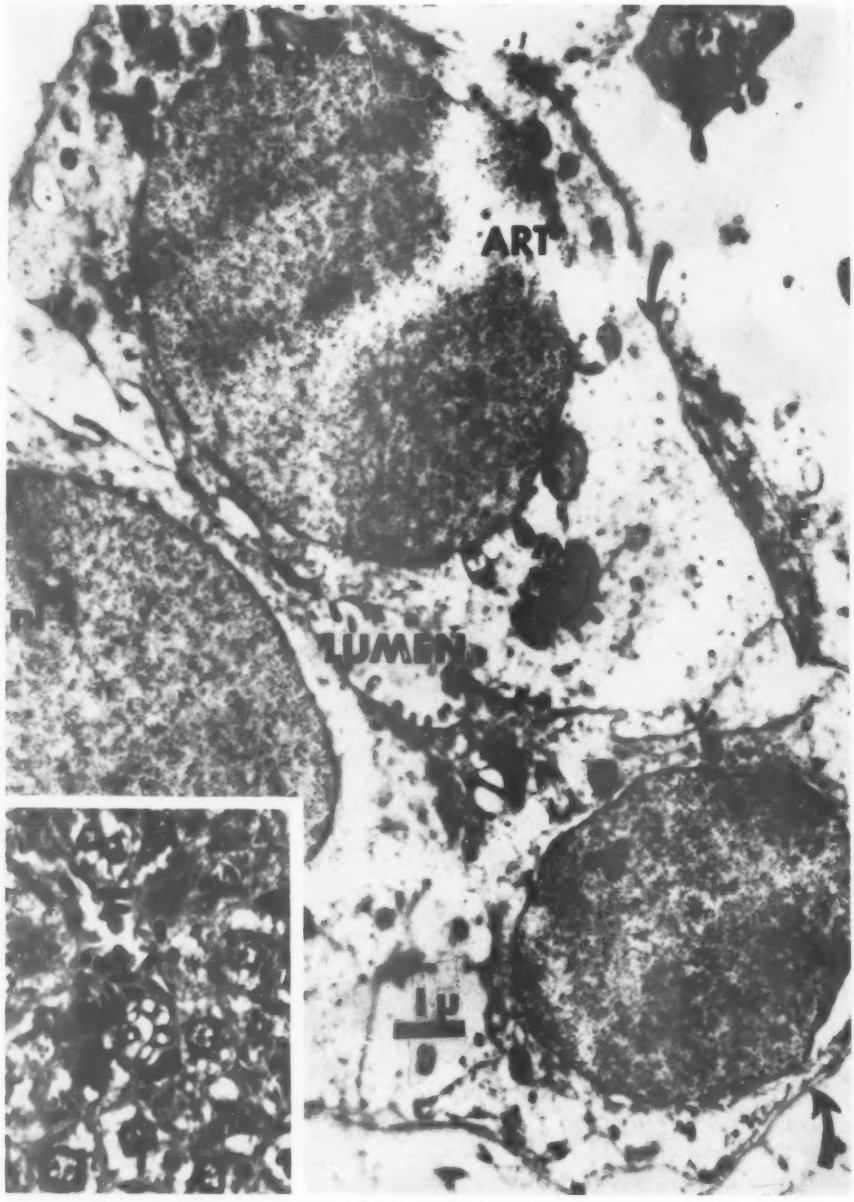

FIG. 4. Liver in a 12-year-old boy with Wilson's disease. An almost normal ductule has a lumen about 2 μ in diameter. There are apparently 4 to 8 microvilli per cell. One of the nuclei has a small nucleolus (nl). The mitochondria in the ductular cells are small, and a fat droplet (fd) is seen in one. The basement membrane (arrows) is surrounded by a few reticulum fibers (F). The borders between ductular cells are more irregular than is usual, and the cells are separated from one another. An artifact (ART) is present in the collodion grid. × 10,000. Insert: Conventional microscopic section in the same specimen, showing a ductule (arrow) in the parenchyma. Hematoxylin and eosin stain. × 400.

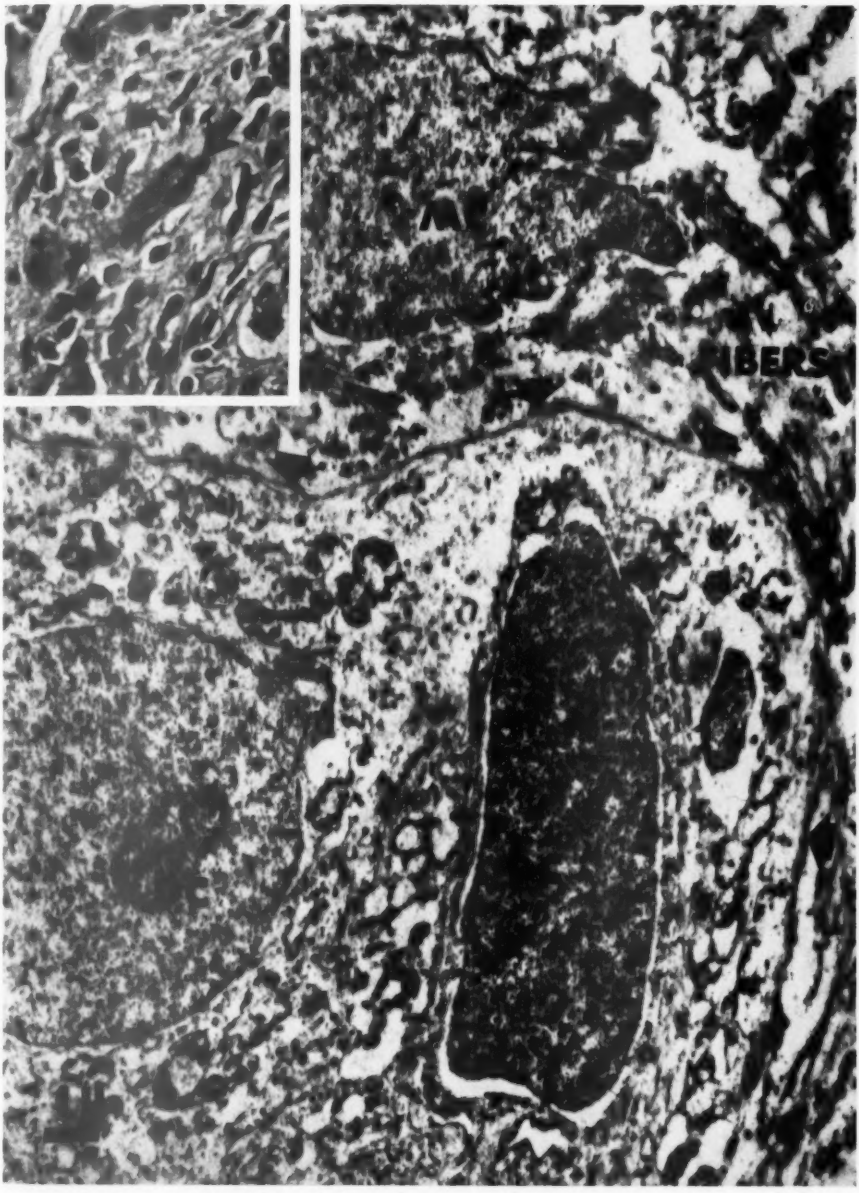

FIG. 5. A ductule in the liver of a 10-year-old girl with active postnecrotic cirrhosis. There is variation in ductular cell nuclei (DC). Fibers appear to be coming from a mesenchymal cell (MC) outside the basement membrane (arrows). × 8000. Insert: A proliferated ductule (arrow) in the same specimen. Hematoxylin and eosin stain. × 400.

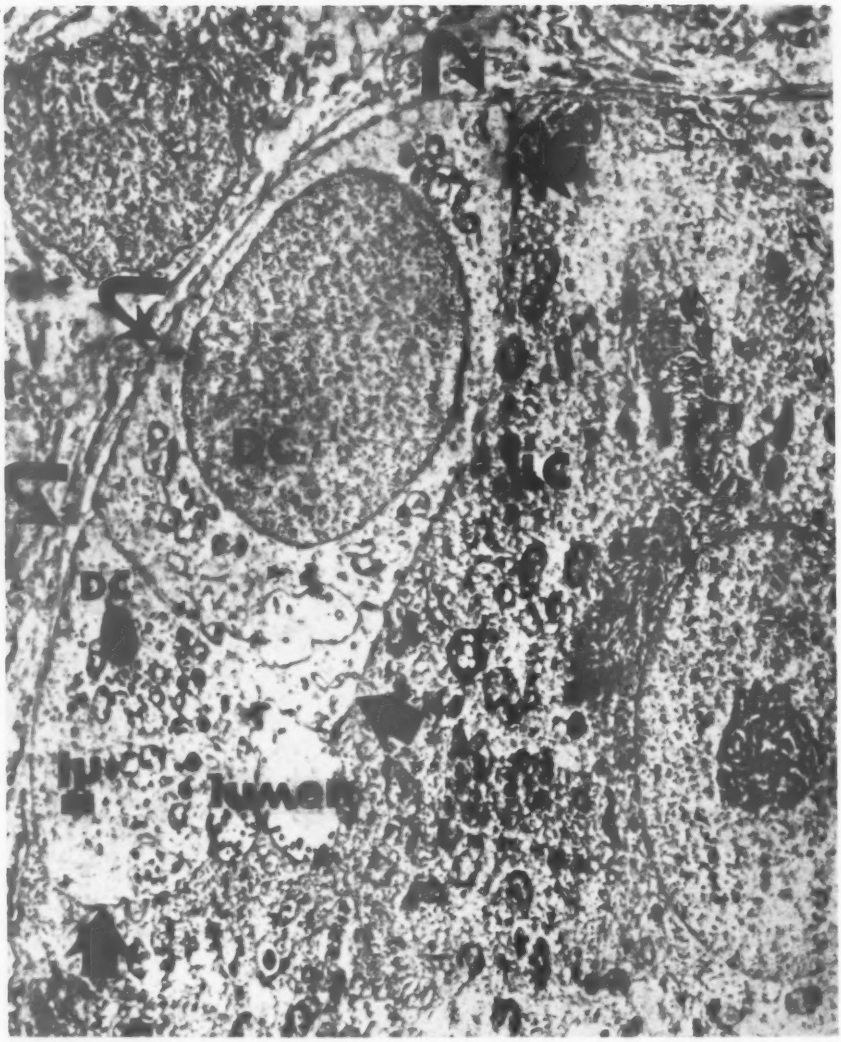

6

FIG. 6. A liver specimen from a 54-year-old man with inactive postnecrotic cirrhosis. Two ductular cells (DC) border a parenchymal cell (LC) and share a common lumen with it. The ductular-parenchymal cell border (straight arrows) is straight, and no basement membrane is present although one is seen on the outside border of the ductular cells (curved arrows). × 3500.

FIG. 7. Detail of the right upper portion of Figure 6. There is extension of the basement membrane (solid arrows) along the surfaces of the ductular cell (DC), the parenchymal cell (LC) and the mesenchymal cell (MC). Microvilli may be seen on the surface of the parenchymal cell beneath the basement membrane extension (curved arrows). The membrane terminates after appearing to fray slightly (open arrow). × 8000.

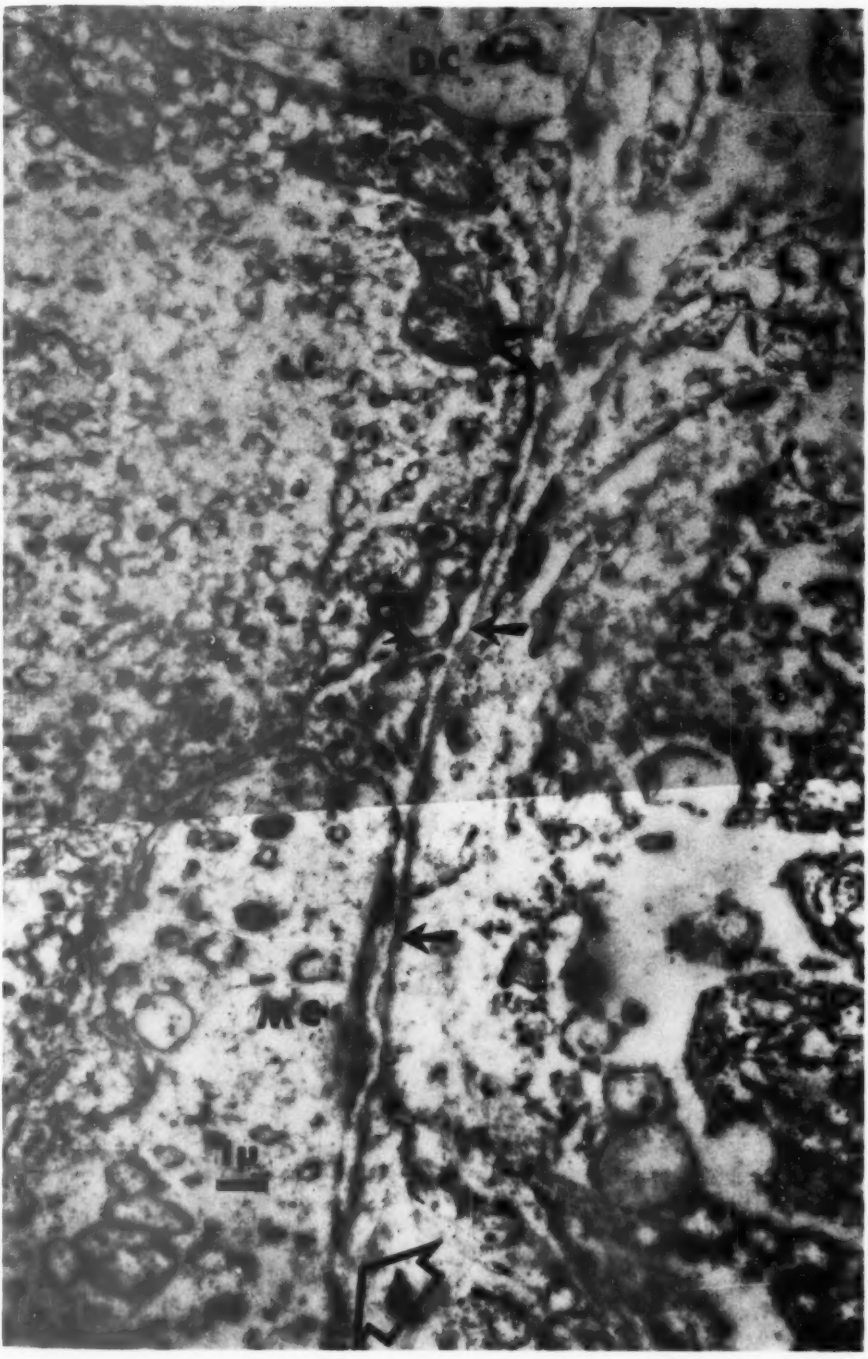

7

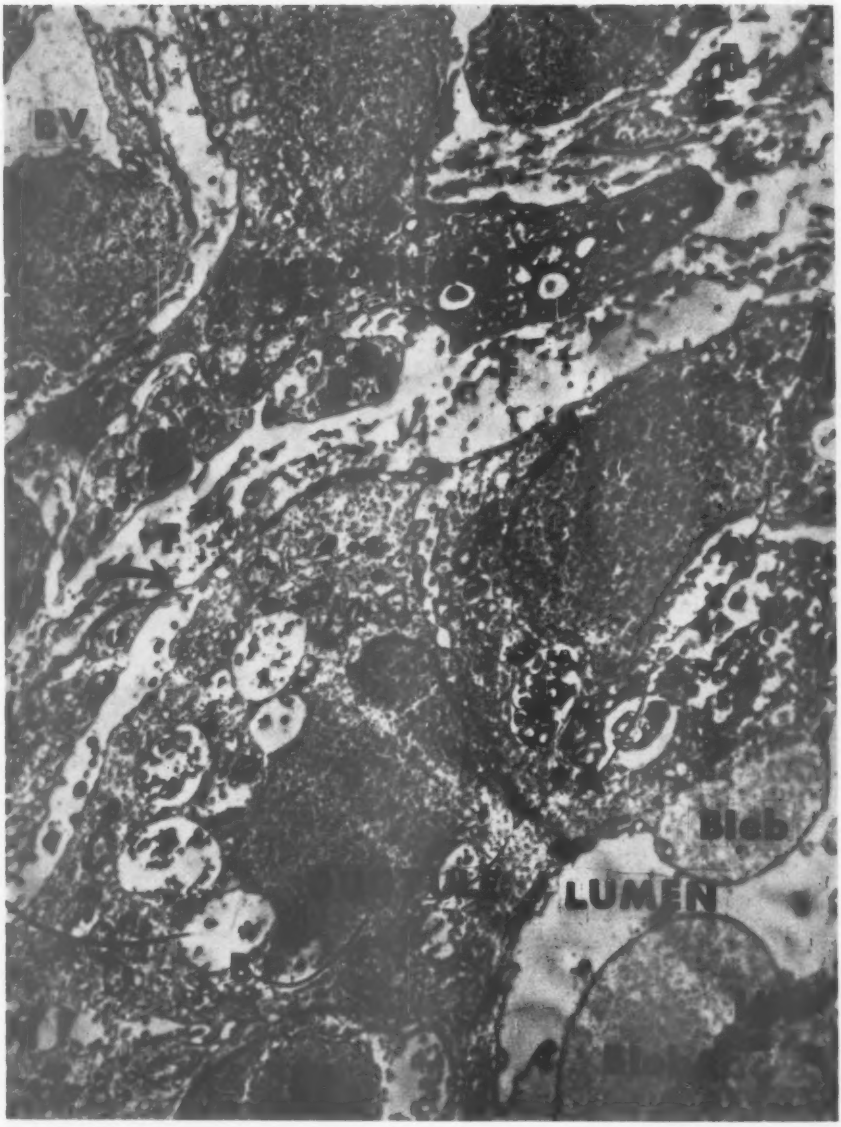

FIG. 8. A liver specimen from a patient with subacute cholangiolitis. A ductule is surrounded by a basement membrane (arrows). Fibrils (F), a macrophage containing pigment (P), and a blood vessel (BV) are evident near by. Vessels in ductular cells contain osmiophilic material that may be bile pigment (BP). The lumen shows two large blebs. Artifacts (A) are in the collodion grid. × 5000.

INVESTIGATIONS OF ALLERGIC LIVER INJURY

I. Light, Fluorescent and Electron Microscopic Study of the Effects of Soluble Immune Aggregates

Jan W. Steiner, M.D.

From the Department of Pathology, University of Toronto, Banting Institute, Toronto, Canada

The immediate or Arthus type allergic reaction has been shown to lead to so-called eosinophilic necrosis of parenchymal liver cells.[1–7] The mechanism of this injury has been attributed to: (a) the formation of particulate complexes of antigen and antibody, resulting in vascular occlusion and ischemic necrosis[6,7]; (b) the direct injury resulting from the interaction of free antigen and cell-bound antibody[3]; and (c) the indirect injury resulting from the interaction of free antigen and antibody within the sinusoidal circulation.[5]

Recent studies have shown that in organs other than the liver, preformed soluble immune aggregates primarily produced an endothelial injury.[8–10] These observations apply to tissues in which an effective barrier separates vascular lumens from the parenchyma. The hepatic lobule has been shown to differ from other organs since it possesses neither a continuous endothelium nor a basement membrane.[11–17] Thus it was the purpose of this study to investigate the response of liver tissue to the injection of such immune complexes.

The investigation by light and fluorescent microscopy was concerned with the over-all features of the resulting lesions. The observations indicated that soluble complexes of antigen and antibody produced an injury morphologically indistinguishable from that resulting from the injection of particulate, precipitated immune aggregates into the portal circulation.[6,7] The electron microscopic observations were confined to the fine structural modulations of the constituents in the space of Disse during the early phases of such injury. The accumulation of an eosinophilic substance in this region, noted by others and designated as one component of the process of serous hepatitis,[18] has been shown to consist in this instance of intracellular edema of Kupffer cells and microvilli of liver cells, leading to distention of the perisinusoidal space.

Supported by a grant of the National Research Council of Canada (MA-785).
Accepted for publication, October 6, 1960.

Material and Methods

Animals. Female rabbits, weighing 2 to 2.5 kg., of mixed New Zealand and Giant White stock, were used. Animals found to be suffering from hepatic coccidiosis were excluded from the study.

Antigen. Purified human serum albumin (HSA), Connaught Laboratories, Toronto, Canada, was used.

Antiserum. Anti-human serum albumin serum (anti-HSA) was prepared in rabbits immunized by the method of Kabat and Mayer,[19] preceded by two injections of 10 mg. of HSA emulsified with an equal volume of complete Freund's adjuvant.[20] Antiserums were pooled and analyzed for antibody content by the quantitative precipitin technique.[19] The final concentration of the pool was 2.8 mg. of antibody protein per ml.

Immunization Schedule (*Experiment I*). Rabbits were immunized by repeated courses of injections of HSA, using the method of Kabat and Mayer.[19] Freund's adjuvant was omitted in this instance.

Preparation of Complexes of HSA-Anti-HSA (*Experiment II*). The point of optimal precipitation was determined by the method of Dean and Webb,[21] using twofold dilutions of the antigen as determined by preliminary trials and a constant dilution of antiserum. Determinations of the point of equivalence were made by visual observation as well as by titrations of the supernatants for excess antigen and antibody respectively. Precipitated complexes were allowed to form overnight at 4° C. After centrifugation and removal of the supernatant, the precipitates were washed 4 times with physiologic saline at 4° C. Soluble complexes were then prepared by the addition of excess antigen (expressed as a multiple of the amount present at equivalence) to the washed precipitate formed at equivalence and incubated for 4 to 6 hours at 37° C. until the precipitate was dissolved. Where total solubilization did not occur after this time, the supernatant was used after centrifugation. Each injection contained 3 times or 25 times excess antigen.

Fluorescein Labeling. Antigen was labeled, where appropriate, with fluorescein isothiocyanate by the modified method of Marshall, Eveland and Smith.[22] This was carried out prior to injection or before incorporation into complexes.

Histologic Methods. Tissues were obtained immediately upon induction of sodium Nembutal anesthesia. Those used for light microscopy were fixed in 10 per cent buffered formalin (pH 7) and embedded in paraffin. Sections were stained with hematoxylin and eosin, Lillie's azure eosin, Unna-Pappenheim's methyl green-pyronin and Masson's trichrome stains. Sections containing fluorescent tracer material were treated by the method of McKinnon, Andrews, Heptinstall and Germuth.[6] They were examined with a Leitz Ortholux microscope fitted with an ultraviolet light source. Preliminary photographs were obtained by means of a Polaroid A.S.A. 3000 film. Definitive photographs were taken on Kodak Panatomic-X film. Tissues intended for electron microscopy were fixed in Palade's cold buffered (pH 7.4) osmium tetroxide in physiologic saline, and kept for ½ hour in the cold at 4° C. and for 1 hour at room temperature. A few fragments of tissue from each specimen were incubated subsequently in a 5 per cent alcoholic solution of uranyl acetate for 1 hour at room temperature. All tissues were embedded in butyl-methyl methacrylate (8:1) after dehydration in graded alcohols. Ultra-thin sections were cut on a Porter-Blum microtome with glass and diamond knives and examined unstained or after flotation on protargol, silver methenamine with and without prior periodic acid oxidation, or on phosphotungstic acid. The sections were mounted on Formvar-coated grids and examined in an RCA EMU 3 electron microscope.

Experiment I

Animals were immunized by the method of Kabat and Mayer.[19] Alum-precipitated HSA, neutralized with N/10 NaOH, was administered intravenously, in quantities

of 100 mg. of protein over 4 weekly periods. Where appropriate, the course was repeated after an interval of 7 days. Upon attaining a titer of 2.8 mg. of antibody protein per ml., animals were challenged with 10 mg. of HSA in the skin of the flank. All rabbits showing a 2+ or better Arthus reaction at the end of 24 hours received injections with 250 mg. of HSA 5 days later directly into the portal vein under sodium Nembutal anesthesia. Two animals dying of anaphylactic shock immediately following injection were not included in the final assessment.

TABLE I

EXPERIMENT I. STUDY OF THE EFFECTS OF A LARGE CHALLENGING DOSE OF ANTIGEN ON THE LIVERS OF HYPERIMMUNE ANIMALS

Rabbit no.	Antibody (mg./ml.)	Amount of HSA * administered systemically (mg.)	Challenging dose (mg.)	Time of sacrifice following challenge (hr.)
11	2.8	500	250	24
12	2.8	400	250	48
13	2.9	600	250	72
25	2.8	500	250 †	24
26	2.9	400	250 †	72

* Human serum albumin.
† Fluorescein-labeled.

Experiment II

Normal rabbits were given direct injections into the portal vein of soluble complexes of HSA-anti HSA formed in 3 × and 25 × antigen excess respectively. Each injection contained approximately 8 mg. of antibody protein.

TABLE II

EXPERIMENT II. STUDY OF THE EFFECTS OF SOLUBLE COMPLEXES FORMED IN ANTIGEN EXCESS ON LIVERS OF NORMAL ANIMALS

Rabbit no.	Complexes formed in	Fluorescent tracer HSA * in complex	Time of sacrifice following injection (hr.)
20	3 × antigen excess	—	24
33	3 × antigen excess	—	48
39	3 × antigen excess	—	72
40	25 × antigen excess	—	24
42	25 × antigen excess	—	72
22	3 × antigen excess	Fluorescent	24
23	3 × antigen excess	Fluorescent	72
2	25 × antigen excess	Fluorescent	24
3	25 × antigen excess	Fluorescent	72

* Human serum albumin.

Controls

Sections of liver from 4 normal animals kept under identical conditions of care and maintenance were examined with the light and electron microscopes. No comparable lesions were found in these.

Two animals were injected with 250 mg. of HSA and two others with 10 ml. of

rabbit anti-HSA respectively directly into the portal vein. No lesions were demonstrable in these at the conclusion of 24 and 48 hours respectively.

The dialysate, containing large quantities of fluorescein isothiocyanate, obtained during preparation of the protein tracer material, was injected directly into the main trunk of the portal vein of two animals in 10 ml. quantities. No lesions were demonstrable in these with light microscopy after 24 and 48 hours respectively. Small quantities of the fluorescent substance were found in hepatic sinusoids, presumably localized within Kupffer cells.

Results

Since the lesions were found to be essentially identical in both experiments, the observations will be described simultaneously.

Gross Observations

In the livers of all animals were found focal and diffuse areas of necrosis situated mainly in subcapsular locations. Petechial hemorrhages were present in the margins of lesions in a number of animals.

Observations with Light Microscopy

The main components of the lesions were maplike areas of midzonal coagulative necrosis with occasional extensions to peripheral and centrilobular regions. The over-all size of these varied from large, diffuse lesions, involving several adjacent lobules in continuity (Fig. 1), to foci involving no more than a dozen liver cells. Peripheral liver plates and cells in the vicinity of central veins were almost invariably spared (Fig. 1). The sinusoids in the very centers of necrotic areas appeared totally occluded by cells and debris (Fig. 2). At the margins of the necrotic foci, narrowing of sinusoids was noted, but further outwards toward portal tracts and central veins, sinusoids were often found to be widely dilated.

At 24 hours Kupffer cells were preserved and were often increased in number in the central portions of the necrotic zones (Fig. 2). In the marginal portions of these regions parenchymal cells were seen in various stages of degeneration, showing cloudy swelling, and hydropic and vacuolar changes.

At 48 and 72 hours the number of surviving Kupffer cells was considerably reduced. There was evidence of resorption of necrotic parenchymal cells. Deeply basophilic, possibly regenerating liver cells made their appearance in such areas (Fig. 3). Degenerative changes were still noted in the marginal zones. The over-all size of the lesions did not increase beyond the limits noted at 24 hours.

The cellular reaction consisted of a scanty infiltration by various mesenchymal cells intermingled with Kupffer cells (Figs. 2 and 3). At 72 hours plasma cells were prominent in hyperimmune animals both in the margins of the necrotic lesions and in portal tracts. In the normal animals in experiment II little portal area reaction was noted at this

time. Cytoplasmic basophilia was seen in many Kupffer cells at 72 hours and was more prominent in the hyperimmune group (experiment I).

Immunohistochemical Observations

Normal liver cells possess a distinct pale blue autofluorescence. Necrotic areas were easily recognizable by the loss of this quality (Figs. 4 and 5). In both experiments where fluorescent tracer-labeled antigen was injected either in its free form (experiment I) or in the form of antibody-bound complexes (experiment II), aggregates of intensely and specifically (apple-green) fluorescent material were found in sinusoids throughout the necrotic zones and their marginal areas (Figs. 4 and 5). The material could not be identified in Kupffer cells with certainty. The quantity of the aggregates remained approximately constant between 24 and 72 hours. The particles ranged from extremely small rounded or elongated bodies to others measuring nearly 7 μ in diameter. The amount of aggregated fluorescent substance was somewhat greater in the hyperimmune animals of experiment I (Fig. 5) than in the normal animals of experiment II (Fig. 4).

No fluorescent tracer was found within liver cells, in the portal tracts or in the radicles of portal veins outside of lobules. Exact localization of the fluorescent tracer in totally necrotic lesions was difficult because of the marked disruption of the architecture.

Electron Microscopic Observations

Owing to limitations of space, these observations are limited to the normal and pathologic constituents of the blood-liver barrier. A later publication will deal with the changes in parenchymal liver cells. A further limitation was imposed by restricting observations to the marginal zones of necrotic areas and, in the main, to those remote from portal tracts. This course of action was dictated partly by histologic considerations which will be dealt with anon and partly by knowledge acquired from light and fluorescent microscopy. The latter indicated that cells in prenecrotic phases of the process were most likely to be found in these locations.

The fine structure of the liver has been extensively investigated,[15,23–28] and some reports have dealt more specifically with the sinusoidal lining and the perisinusoidal space.[11–14,17,29,30] Further studies have elucidated certain aspects of the phagocytic function of Kupffer cells and of the transport mechanism of colloidal particles from the blood stream into parenchymal liver cells and vice versa.[24,31,32]

The fine structure of the rabbit liver has not been dealt with in detail in other publications.

Cross sections of sinusoids (Fig. 6) show them to be angular in shape,

the angles occurring at points of contact of neighboring liver cells which form the outer wall of sinusoids. The contact edges of liver cells have rounded contours since such areas are almost invariably sectioned tangentially, producing a pyramid-shaped gap between them; the apex of

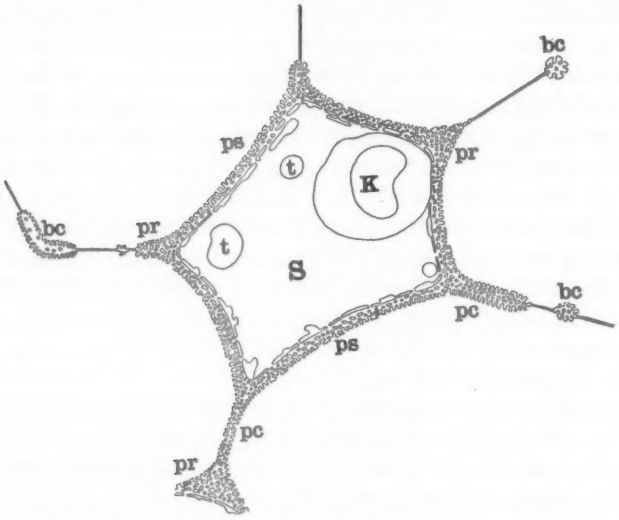

TEXT-FIGURE 1. Structure of the blood-liver barrier of the rabbit. An angulated sinusoid (S) is seen. Trabeculae (t) extend around the periphery of the sinusoid from the main body of the Kupffer cell (K). Between the endothelium and the liver cell lie the microvilli of the latter. The intervening area constitutes the perisinusoidal space of Disse (ps). At the points of contact of neighboring parenchymal cells, wedge-shaped perisinusoidal recesses are present (pr). These occasionally extend for some distance outward from the sinusoid to form perisinusoidal canals (pc). Bile canaliculi (bc) form as a result of focal separations of parenchymal cell membranes. Neither perisinusoidal canals nor bile canaliculi possess an endothelial lining.

the wedge points away from the lumen. This is referred to as the perisinusoidal recess.

Kupffer cells tend to be located over these angular recesses (Fig. 6). The shape of the main body of these cells varies from round or ovoid to elongated, depending on the angle of sectioning. The cell is visualized as an octopus-like structure with widely extending flat trabeculae. The trabeculae are wide ribbon-like branches of cytoplasm extending alongside the sinusoidal wall or projecting into the sinusoidal lumen where they are often seen as isolated, cross-sectioned villi. The ultimate branches of the trabeculae form elongated sheetlike profiles which line most of the sinusoidal periphery (Fig. 14). Gaps are clearly demonstrable in the endothelial lining of the sinusoids, bringing liver cells into direct contact with the blood stream (Fig. 14). The sinusoid lining is

visualized as being in continual restless motion, producing intercellular spacings which are transient and of varied sizes. A surfeit of endothelial lining is seen in some areas where terminal trabeculae of Kupffer cells overlap like tiles on a roof, suggesting that they had retracted from neighboring denuded areas. Plasma can be demonstrated in the perisinusoidal space in relation to such gaps while in other areas the endothelium appears to seal off the underlying spaces effectively.

It has been noted previously [15] that the attachment of Kupffer cells to the sinusoid wall is only tenuous if indeed it exists at all. Others [12–14] have stated that the attachment is accomplished by villous processes of the Kupffer cells interlocking with microvilli of the underlying liver cells. This latter concept could not be confirmed in the rabbit (Fig. 8), nor could any attachment be demonstrated between neighboring Kupffer cells.

The structural organization of Kupffer cells normally shows little evidence of their specialized function (Fig. 8). The nucleus, bounded by a nuclear membrane, shows a few infoldings. Closely applied to the membrane is an outer zone of condensed karyoplasm. The nuclear center is less osmiophilic and homogeneous except for denser areas resulting from tangential sections through the peripheral condensed zones. This nuclear configuration is in accord with the usual structure of mesenchymal cell nuclei. The nucleolus is generally inconspicuous. Under conditions of normal activity, cytoplasmic organelles are rather scanty. The Golgi complex is small and the endoplasmic reticulum poorly developed, only occasional elongated or vesicular profiles being found in random locations in the cytoplasm. The ergastoplasmic vesicles are mostly smooth with no identifiable granules of ribonucleoprotein on their external surface although such microsomal fractions are found fairly abundantly through the cytoplasm. Mitochondria are found both in the perinuclear region and in outlying portions of the cytoplasm. Their small numbers and simple structure suggest that the normal energy requirement of the cell is low.

The perisinusoidal space (space of Disse; Figs. 9 and 14), noted by others,[11–14,17,29,30] occupies the position immediately subadjacent to the endothelial lining. Its lumen boundary consists of the cytoplasm of Kupffer cells, the outer one being formed by the parenchymal liver cells. Innumerable, ramified and overlapping microvilli of the latter project into the space (Figs. 9 and 14). In sections stained with protargol, cell membranes stain intensely except in areas where structures are sectioned tangentially. Material can be found in the space of Disse which has the characteristics of condensed plasma (Fig. 9). This is difficult to distinguish from the smudgy outlines of some microvilli. In sections stained

with periodic acid-silver methenamine (PASM) a deeply black, argentophilic material of granular appearance and elongated shape can be seen in the space of Disse (Fig. 7). This corresponds to the periodic acid-Schiff (PAS)-positive substance demonstrated in this location by Wassermann[17] and to the PASM-positive material in this location in thin sections examined with the light microscope (Fig. 10). Although the PASM method is insensitive to small quantities of aldehydes,[33] it nevertheless stains intensely glycoproteins and mucopolysaccharides containing the necessary concentration of 1,2-glycol groups. This substance when present in small quantities is not demonstrable by the protargol method of staining sections for the electron microscope, suggesting some more specific affinity than simple argentophilia. The PASM-positive material is thought to represent ground substance in which the fibrillar components of the sinusoid wall are found (Figs. 11 to 13). Contrary to Wassermann's statement,[17] the fibrils are easily demonstrable in thin sections provided they are stained with phosphotungstic acid or uranyl acetate (Figs. 11 to 13). Their diameter approximates 500 Å, and the striations along their long axes are spaced at intervals of approximately 640 Å (Fig. 11). They are seen mostly in cross section in compact bundles suggesting a circumferential position in relation to the sinusoid. Neither the PASM-positive material nor the fibers were demonstrable within Kupffer or liver cells. In the vicinity of the portal tract the PASM-positive material and fibers are normally abundant, producing a wide perisinusoidal space (Figs. 9 and 13). In such areas caution must be exercised when interpreting lesions since the material in unstained or protargol-stained sections suggests a pathologically distended space of Disse (Fig. 9).

From the perisinusoidal recesses there extend between liver cells for variable distances perisinusoidal canals which appear either to end blindly or to communicate with a neighboring sinusoid. These canals have a lining of parenchymal cell microvilli but no endothelial covering, and they contain few fibrillar and amorphous argentophilic components. Rouiller[28] suggested that communications existed between sinusoids and bile capillaries. This could not be substantiated in the livers of rabbits, although some perisinusoidal canals reached to within a very short distance of the bile canaliculi (Fig. 6). It should be emphasized, however, that the distinction between these structures and the perisinusoidal canals in normal tissues is topographic rather than structural. The main histologic features of the blood-liver barrier are summarized schematically in Text-figure 1.

Pathologic Observations. In the marginal zones of the necrotic areas, perisinusoidal spaces were the seat of marked alterations. These were well developed at 24 hours.

The most striking alteration was the almost total obliteration of the

space of Disse by distended microvilli of liver cells (Figs. 15 to 17). Within 24 hours the tips of these became pear-shaped and their matrices lost their usual electron density. At this stage they still remained attached to their parent cells by thin stalks of intact cytoplasm. By the end of 48 hours many of these structures became rounded and detached from their moorings (Figs. 16 to 18). Some were seen at this time in the gaps between the terminal trabeculae of Kupffer cells. In many instances they were distorted, possibly because of the narrow gap through which they passed (Fig. 17). As free bodies in the lumens of sinusoids, they were rounded. At 72 hours large numbers of such bodies were found within the vascular channels, both on the upstream and downstream sides of the necrotic foci (Fig. 19).

In some areas detachment of edematous microvilli failed to occur, and in these cases the space became markedly distended by huge masses of ballooned cytoplasm (Fig. 15). This was partly the result of fusion of neighboring microvilli, since several pedicles were seen at times entering such masses. In other instances the bases were broad and pedicles could no longer be recognized. The internal structure of the swollen microvilli presented a monotonous, finely granular structure with no detectable cytoplasmic organelles. In areas where detachment did occur, the spaces of Disse appeared markedly narrowed though this was a difficult phenomenon to assess with certainty (Fig. 19).

Some terminal tentacles of Kupffer cells participated in this ballooning transformation. They were difficult to distinguish from swollen microvilli except for their lack of attachment to liver cells (Figs. 16 and 18). At 24 hours the change mainly affected the organelles of these trabeculae. Mitochondria were distended and their matrices clear. The cristae mitochondriales appeared too short and retracted. Pinocytosis vesicles within the cytoplasm were distended, the trabeculae assuming a "Swiss-cheese" appearance (Figs. 16 and 18).

At 48 hours the ballooning often affected the cytoplasmic matrix outside the confines of the organelles (Fig. 18). Rounded trabeculae protruded into the sinusoid lumen, and the intercellular gaps appeared larger than usual. This change probably facilitated the migration of detached microvilli. At 72 hours many large terminal trabeculae were found floating freely in sinusoid lumens, though actual detachment could not be proved. The changes in microvilli and the trabeculae of Kupffer cells did not always occur *pari passu*. The former were seen in all the areas studied, to a greater or less degree; the latter were variable, and the time sequence described above could not be as clearly established as in the case of the microvillous alterations.

Large, electron-dense, crenated masses of material measuring approximately 1 to 3 μ were found free within sinusoidal lumens and in Kupffer

cells (Figs. 20 and 21). These were considered to correspond to the antigenic material visualized with fluorescent microscopy. Similar aggregates could be seen in large numbers in animals into whose portal vein precipitated immune complexes had been injected.[34] A high degree of magnification showed them to consist of fairly evenly spaced, denser particles lying in a lighter matrix. The spacings of 200 to 400 Å were reminiscent of the internal structure of antigen-antibody complexes.[35] The substance was not considered to be lipid since in unstained sections it showed relatively little osmiophilia.

When phagocytosed, the substance tended to become concentrated in large Kupffer cell trabeculae (Figs. 20 and 21). At 48 hours many of these outrunners retracted into perisinusoidal recesses and were often found extending deeply into perisinusoidal canals (Fig. 20). This gave the cells a star-shaped appearance (*Sternzellen*). At 72 hours the aggregates within the trabeculae became surrounded by large, distended endoplasmic cisternas not unlike those found in mature plasma cells (Fig. 20). It was thought possible that this prominence of rough-surfaced vesicles corresponded to the development of cytoplasmic basophilia of Kupffer cells at 72 hours. It is noteworthy that lipid and other particulate matter phagocytosed by Kupffer cells did not evoke such an ergastoplasmic response at this time. This suggested that the reaction might be related to the easily catabolizable nature of this material or to the possible capacity of Kupffer cells to become transformed into antibody-producing cells in the presence of an exogenous foreign protein.

The precipitated complexes occasionally entered the space of Disse (Fig. 22). When this phenomenon occurred in marginal areas of the necrotic zones, the swelling of Kupffer cell trabeculae and of microvilli made interpretation of the effects of the precipitated complexes difficult. However, when entry occurred in areas far removed from the necrotic zones, it became apparent that they behaved as an inert substance in such locations. Thus it was concluded that the mere presence of such precipitated complexes in proximity to the constituents of the space of Disse could not be responsible *per se* for the changes cited above.

Other changes in the region of the blood-liver barrier consisted of phagocytosis by Kupffer cells of released cell debris from necrotic areas, entry of exogenous mesenchymal cells and erythrocytes into the space of Disse and mobilization of Kupffer cells. These phenomena will be dealt with in a later publication.

Discussion

Recent studies have shown that soluble immune complexes formed in antigen excess possess a pathogenic potential. Apart from their ana-

phylactogenic property in guinea pigs [36] and mice,[37] they produced inflammatory changes in the skin.[38–40] Large amounts of such aggregates injected intravenously caused characteristic lesions of serum sickness in mice [9,10] and acute glomerulonephritis in rats.[8] The injury in these experiments was primarily endothelial.

Previous investigations of allergic liver injury have shown that the interaction of antigen and antibody in hepatic sinusoids leads to the development of necrotizing "eosinophilic" lesions.[1–7] It was suggested that such injury in the rabbit was dependent upon the intravascular formation of particulate immune precipitates initiating focal ischemic necrosis.[6,7] This view was based partly on studies of interaction of antigen and antibody *in vivo* where the respective proportions of these constituents were not known,[3,5] and partly on the result of portal vein injections of precipitated immune aggregates prepared *in vitro*.[6,7] In the latter experiments hepatic necroses were anticipated since it was known that even inert particulate matter injected into the portal circulation could produce such lesions.[41]

The purpose of the experiments reported in this paper was to determine the effects of portal vein injections of soluble antigen-antibody complexes formed in the presence of an excess of the former component. This *in vitro* preparation of immune aggregates was supplemented by a study of the result of antigen-antibody reactions *in vivo* when theoretical conditions of antigen excess were created in the portal circulation of hyperimmune rabbits by means of large injections of specific antigen.

Observations by light microscopy showed that the midzonal "eosinophilic" necrosis of liver lobules which resulted was identical with that produced by the injection of precipitated complexes.[6,7] When fluorescent tracer antigen was used (either free or incorporated into complexes), aggregation of this substance at the site of the lesions occurred in a manner similar to that noted when fluorescent tracer-labeled antigen was incorporated into precipitated immune aggregates.[6,7] Thus, "antigenic thrombi" formed even when the presence of an antigen excess medium was expected to lead to solubilization of the complexes.

Two explanations are suggested to account for this phenomenon: (a) as a result of the initial injury by soluble complexes, circulatory stasis develops which favors the aggregation of antigen in its free or antibody-bound form at the site of lesions; or (b) owing to the possible dissociation of the components of the complexes within the lobules [42] and preferential uptake of antigen by liver or Kupffer cells, rapid equilibration or perhaps actual slight antibody preponderance may prevail, favoring precipitation. Thus, formation of precipitated complexes in this manner would present a situation the reverse of that found in serum

sickness where precipitation may be the result of an active increase in endogenous antibody.[43]

The second explanation is at present less acceptable since antigen could not be demonstrated conclusively in liver or Kupffer cells. It should be noted that the precipitation phenomenon in this experiment is in some way related to the development of necrosis since antigenic thrombi were found only in or in the immediate vicinity of the lesions. This was not the case after particulate complexes prepared *in vitro* were injected; in this circumstance their presence was noted even in the larger radicles of the portal venous system.[6,7]

The studies by light and fluorescent microscopy did not resolve the question of the possible ischemic nature of the initial injury. A search was therefore made on an ultrastructural level for evidence of any change which could not be accounted for by either ischemia or the direct contact of precipitated complexes with tissues. It was presumed that if such evidence was found, a justifiable suggestion could be made that the injury might be attributed to the activity (toxicity) of soluble complexes.

The findings may be summarized as follows: Within 24 hours following the intrasinusoidal interaction of antigen and antibody in antigen excess, alterations developed in the constituents of the perisinusoidal space. These consisted of ballooning of the terminal trabeculae of Kupffer cells and of the microvilli of liver cells where these projected into the space (Figs. 15 to 18). The outcome of this process was twofold. At 72 hours in some areas most of the swollen microvilli became detached and extruded into the lumen of sinusoids, leaving a narrowed and collapsed perisinusoidal space. In others, detachment failed to occur and the distended villi formed a wide barrier between the blood stream and liver cells.

Several mechanisms may be operative in the production of these changes. It is possible that the essential alteration was a disturbance of cell membrane permeability with a subsequent imbibition of plasma by the trabeculae and microvilli. It is also possible that the edema was related to a disturbance of water elimination or to changes in intracellular electrolyte values. Finally, the change could have been an expression of faulty distribution of water within the cells. It is noteworthy that similar changes have not been observed in any of the electron microscopic investigations of hepatic injury. They were not found in starvation[44] or radiation injury,[45] and no mention was made of them in papers dealing with histotoxic liver injury,[46,47] Simple anoxia,[48,49] although producing alterations in the width of the space of Disse, did not lead to this type of change. Experimentally induced alterations in the width of the peri-

sinusoidal space by injections of glucose and adrenalin,[13] respectively, were not accompanied by injury to Kupffer cell trabeculae or to the microvilli of liver cells. It is nevertheless possible that these alterations may have been overlooked unless they had been specifically searched for.

Thus, on the basis of the available evidence, it is suggested that the changes noted in the constituents of the space of Disse in these experiments may be a specific manifestation of allergic liver injury due to the activity of soluble complexes of antigen and antibody formed in antigen excess. Large amounts of such soluble immune aggregates may prove rapidly lethal to parenchymal liver cells in midzonal locations as a result of hemodynamic factors which control their concentration and the duration of their contact with such cells. In the periphery of these areas the concentrations of the complexes may be considerably smaller and the injury correspondingly more subtle. The possibility must be borne in mind that the widening of the blood-liver barrier may constitute an obstacle to the diffusion of oxygen and induce secondary ischemic damage to the parenchyma. The alterations of liver cells were found to be in most respects indistinguishable from those due to anoxic and histotoxic anoxia.[34]

Summary

Soluble complexes of antigen and antibody (human serum albumin-rabbit anti-human serum albumin) prepared *in vitro* were injected into the portal circulation of a group of normal rabbits. Theoretical conditions of antigen excess were created in another group of hyperimmune rabbits who received a large injection of specific antigen into the portal vein. The resulting midzonal necrosis of liver cells in both groups of animals was indistinguishable from the injury produced when precipitated particulate immune aggregates were administered. When fluorescent tracer-labeled antigen was used in these experiments, precipitates of this material were found in the necrotic areas even when soluble complexes were injected. The question of a possible ischemic basis for the necrosis remained unresolved.

The electron microscopic investigation disclosed a change in the terminal trabeculae of Kupffer cells and in the microvilli of liver cells, where these protruded into the space of Disse. This consisted of a ballooning of these structures and led to detachment of large numbers of microvilli from their parent cells and to their extrusion into the sinusoidal blood stream. These features were not reported in any examples of anoxic or histotoxic liver injury previously examined by electron microscopy. It was suggested that the alterations might represent a specific com-

ponent of allergic liver injury possibly related to the toxicity of soluble immune complexes.

References

1. Choi, C. The local anaphylactic reaction of liver tissue. *Soc. path. jap. (Tokyo)*, 1930, **20**, 587–589.
2. Cornil, L., and Mosinger, M. Sur les réactions hépatiques consécutives à l'injection intraabdominale répétée de sérum hétérogène. *Compt. rend. Soc. de biol.*, 1936, **121**, 61–63.
3. Hartley, G., Jr., and Lushbaugh, C. C. Experimental allergic focal necrosis of the liver. *Am. J. Path.*, 1942, **18**, 323–331.
4. Hawn, C. V., and Janeway, C. A. Histological and serological sequences in experimental hypersensitivity. *J. Exper. Med.*, 1947, **85**, 571–590.
5. Longcope, W. T. Cirrhosis of the liver produced by chronic protein intoxication. *Tr. A. Am. Physicians*, 1913, **28**, 497–512.
6. McKinnon, G. E.; Andrews, E. C., Jr.; Heptinstall, R. H., and Germuth, F. G., Jr. An immunohistologic study on the occurrence of intravascular antigen-antibody precipitation and its role in anaphylaxis in the rabbit. *Bull. Johns Hopkins Hosp.*, 1957, **101**, 258–280.
7. McKinnon, G. E. Role of *In Vivo* Antigen-antibody Precipitation in Hypersensitivity Reactions. In: Mechanisms of Hypersensitivity. Shaffer, J. H.; LoGrippo, G. A., and Chase, M. W. (eds.). Henry Ford Hospital International Symposium. Little, Brown & Co., Boston and Toronto, 1959, pp. 163–172.
8. Benacerraf, B.; Potter, J. L.; McCluskey, R. T., and Miller, F. The pathologic effects of intravenously administered soluble antigen-antibody complexes. II. Acute glomerulonephritis in rats. *J. Exper. Med.*, 1960, **111**, 195–200.
9. McCluskey, R. T., and Benacerraf, B. Localization of colloidal substances in vascular endothelium. A mechanism of tissue damage. II. Experimental serum sickness with acute glomerulonephritis induced passively in mice by antigen-antibody complexes in antigen excess. *Am. J. Path.*, 1959, **35**, 275–295.
10. McCluskey, R. T.; Benacerraf, B.; Potter, J. L., and Miller, F. The pathologic effects of intravenously administered soluble antigen-antibody complexes. I. Passive serum sickness in mice. *J. Exper. Med.*, 1960, **111**, 181–194.
11. Bennett, H. S.; Luft, J. H., and Hampton, J. C. Morphological classifications of vertebrate blood capillaries. *Am. J. Physiol.*, 1959, **196**, 381–390.
12. Cossel, L. Beitrag zur Ultrastruktur der Blutgewebsgrenze in der Leber. (Elektronenmikroskopische Untersuchungen an Lebern von Mäusen und Leberpunktaten vom Menschen.) *Beitr. path. Anat.*, 1959, **120**, 133–158.
13. Cossel, L. Elektronenmikroskopische Befunde an Lebersinusoiden und epithelien bei verschiedenen Funktionszuständen der Leber. *Verhandl. deutsch. Ges. Path.*, 1959, **43**, 204–208.
14. Cossel, L. Elektronenmikroskopische Untersuchungen zur Frage des Disseschen Raumes in der Leber. *Klin. Wchnschr.*, 1959, **37**, 743–753.
15. Fawcett, D. W. Observations on the cytology and electron microscopy of hepatic cells. *J. Nat. Cancer Inst.*, 1955, **15**, Suppl., 1475–1503.
16. Parks, H. F. The Hepatic Sinusoidal Endothelial Cell and Its Histological Relationships. In: European Regional Conference on Electron Microscopy, 1st, Stockholm, 1956. Sjöstrand, F. S., and Rhodin, J. (eds.). Academic Press, Inc., New York, 1957, pp. 151–153.

17. WASSERMANN, F. The structure of the wall of the hepatic sinusoids in the electron microscope. *Ztschr. Zellforsch.*, 1958, **49**, 13–32.

18. RÖSSLE, R. Über die serösen Entzündungen der Organe. *Virchows Arch. path. Anat.*, 1944, **311**, 252–284.

19. KABAT, E. A., and MAYER, E. M. Experimental Immunochemistry. Charles C Thomas, Springfield, Ill., 1948, 567 pp.

20. STEINER, J. W.; LANGER, B., and SCHATZ, D. The local and systemic effects of Freund's adjuvant. *A.M.A. Arch. Path.*, 1960, **70**, 424–434.

21. DEAN, H. R., and WEBB, R. A. The influence of optimal proportions of antigen and antibody in the serum precipitation reaction. *J. Path. & Bact.*, 1926, **29**, 473–492.

22. MARSHALL, J. D.; EVELAND, W. C., and SMITH, C. W. Superiority of fluorescein isothiocyanate (Riggs) for fluorescent-antibody technic with a modification of its application. *Proc. Soc. Exper. Biol. & Med.*, 1958, **98**, 898–900.

23. CLAUDE, A., and FULLAM, E. F. The preparation of sections of guinea pig liver for electron microscopy. *J. Exper. Med.*, 1946, **83**, 499–504.

24. HAMPTON, J. C. An electron microscope study of the hepatic uptake and excretion of submicroscopic particles injected into the blood stream and into the bile duct. *Acta anat.*, 1958, **32**, 262-291.

25. PALADE, G. E., and SIEKEVITZ, P. Liver microsomes; an integrated morphological and biochemical study. *J. Biophys. & Biochem. Cytol.*, 1956, **2**, 171–200.

26. POHL, W. Zur Substruktur und Funktion von Leberzellorganellen. *München med. Wchnschr.*, 1959, **101**, 334–336.

27. ROUILLER, C. Contribution de la microscopie électronique à l'étude du foie normal et pathologique. *Ann. d'anat. path.*, 1957, **2**, 548–562.

28. ROUILLER, C. Les canalicules biliaires; étude au microscope électronique. *Acta anat.*, 1956, **26**, 94–109.

29. CACHERA, R., and DARNIS, F. Examen du foie humain au microscope électronique. *Semaine hôp. Paris*, 1955, **31**, 2187–2200.

30. RÜTTNER, J. E., and VOGEL, A. Elektronenmikroskopische Untersuchungen an der Lebersinusoidwand. *Verhandl. deutsch. Ges. Path.*, 1957, **41**, 314–320.

31. PARKS, H. F.; PEACHEY, L. D., and CHIQUOINE, A. D. Submicroscopic morphology of cytoplasmic inclusions of phagocytosed colloidal particles in Kupffer cells of mice. (Abstract) *Anat. Rec.*, 1956, **124**, 428.

32. PARKS, H. F., and CHIQUOINE, A. D. Observations on Early Stages of Phagocytosis of Colloidal Particles by Hepatic Phagocytes of the Mouse. In: European Regional Conference on Electron Microscopy, 1st, Stockholm, 1956. SJÖSTRAND, F. S., and RHODIN, J. (eds.). Academic Press, Inc., New York, 1957, pp. 154–156.

33. JONES, D. B. The Kidney. Inflammatory and Vascular Disease of the Glomerulus. In: Analytical Pathology. MELLORS, R. C. (ed.) The Blakiston Division, McGraw-Hill Book, Co., Inc., New York, Toronto and London, 1957, Chapt. 3, pp. 161–217.

34. STEINER, J. W. Unpublished observations.

35. EASTY, G. C., and MERCER, E. H. Electron microscopic studies of the antigen-antibody complex. *Immunology*, 1958, **1**, 353–364.

36. GERMUTH, F. G., JR., and MCKINNON, G. E. Studies on the biological properties of antigen-antibody complexes. I. Anaphylactic shock induced by soluble antigen-antibody complexes in unsensitized normal guinea pigs. *Bull. Johns Hopkins Hosp.*, 1957, **101**, 13–44.

37. Tokuda, S., and Weiser, R. S. Production of anaphylaxis in the white mouse with soluble antigen-antibody complexes. *Science*, 1958, **127**, 1237–1238.

38. Cochrane, C. G., and Weigle, W. O. The cutaneous reaction to soluble antigen-antibody complexes; a comparison with the Arthus phenomenon. *J. Exper. Med.*, 1958, **108**, 591–604.

39. Ishizaka, K., and Campbell, D. H. Biological activity of soluble antigen-antibody complexes. I. Skin reactive properties. *Proc. Soc. Exper. Biol. & Med.*, 1958, **97**, 635–638.

40. Ishizaka, K.; Ishizaka, T., and Campbell, D. H. The biological activity of soluble antigen-antibody complexes. II. Physical properties of soluble complexes having skin-irritating activity. *J. Exper. Med.*, 1959, **109**, 127–143.

41. Mallory, F. B. Necroses of liver. *J. Med. Res.*, 1901, **6**, 264–279.

42. Walter, H., and Zipper, H. Dissociation of some injected antigen-antibody complexes *in vivo*. *Proc. Soc. Exper. Biol. & Med.*, 1960, **103**, 221–223.

43. Dixon, F. J.; Vazquez, J. J.; Weigle, W. O., and Cochrane, C. G. Pathogenesis of serum sickness. *A.M.A. Arch. Path.*, 1958, **65**, 18–28.

44. Gansler, H., and Rouiller, C. Modifications physiologiques et pathologiques du chondriome. Étude au microscope électronique. *Schweiz. Ztschr. allg. Path.*, 1956, **19**, 217–243.

45. Glauser, O. Elektronenmikroskopische Untersuchungen an Rattenlebern nach Röntgenbestrahlung. *Schweiz. Ztschr. allg. Path.*, 1956, **19**, 150–161.

46. Mölbert, E. Das elektronenmikroskopische Bild der Leberparenchymzelle nach histotoxischer Hypoxydose. *Beitr. path. Anat.*, 1957, **118**, 203–227.

47. Oberling, C., and Rouiller, C. Les effets de l'intoxication aiguë au tétrachlorure de carbone sur le foie du rat; étude au microscope électronique. *Ann. d'anat. path.*, 1956, **1**, 401–427.

48. Bassi, M., and Bernelli-Zazzera, A. Vacuolar degeneration of rat liver cells by electron microscopy. (Letter to the editor) *Nature, London*, 1957, **179**, 256–257.

49. Mölbert, E., and Guerritore, D. Elektronenmikroskopische Untersuchungen am Leberparenchym bei akuter Hypoxie. *Beitr. path. Anat.*, 1957, **117**, 32–49.

The author is indebted to Dr. Arnold R. Rich and to Dr. John D. Hamilton for their interest and many helpful suggestions; to Drs. B. Langer, E. Sterns and D. Jaffe for technical assistance; to Miss M. de Wolf for the preparation of fluorescent antigen; and to Miss B. Lambert and Mrs. L. Marmash for the preparation of sections.

[*Illustrations follow*]

Legends for Figures

Key to abbreviations used in Figures 6 to 22.

am = argentophilic (PASM-positive) material (ground substance)
bc = bile canaliculus
bd = bile duct
gl = glycogen
LC = parenchymal liver cell
lf = lipofuscin body
m = mitochondrion
mv = microvillus
N = nucleus
ps = perisinusoidal space
S = sinusoid
t = terminal trabecula of Kupffer cell
tr = trabecula of Kupffer cell
v = vacuole

Fig. 1. Rabbit 11 (experiment I). Widespread midzonal necrosis 24 hours after the injection of antigen (250 mg.) into the portal vein of a hyperimmune animal. Note the scanty cellular reaction. Azure eosin stain. × 48.

Fig. 2. Rabbit 20 (experiment II). The margin of a necrotic zone 24 hours after the portal vein injection of soluble complexes formed in 3 × antigen excess. Note the survival of some mesenchymal cells in the center of a necrotic area (right) and the scanty cellular reaction at the periphery. The marginal zone contains cells in various stages of degeneration. Azure eosin stain. × 234.

Fig. 3. Rabbit 39 (experiment II). Seventy-two hours after the portal vein injection of soluble complexes formed in 3 × antigen excess. There is evidence of resorption of necrotic liver cells and several deeply basophilic, possibly regenerating, liver cells appear scattered through the central portion of the lesion. Hematoxylin and eosin stain. × 285.

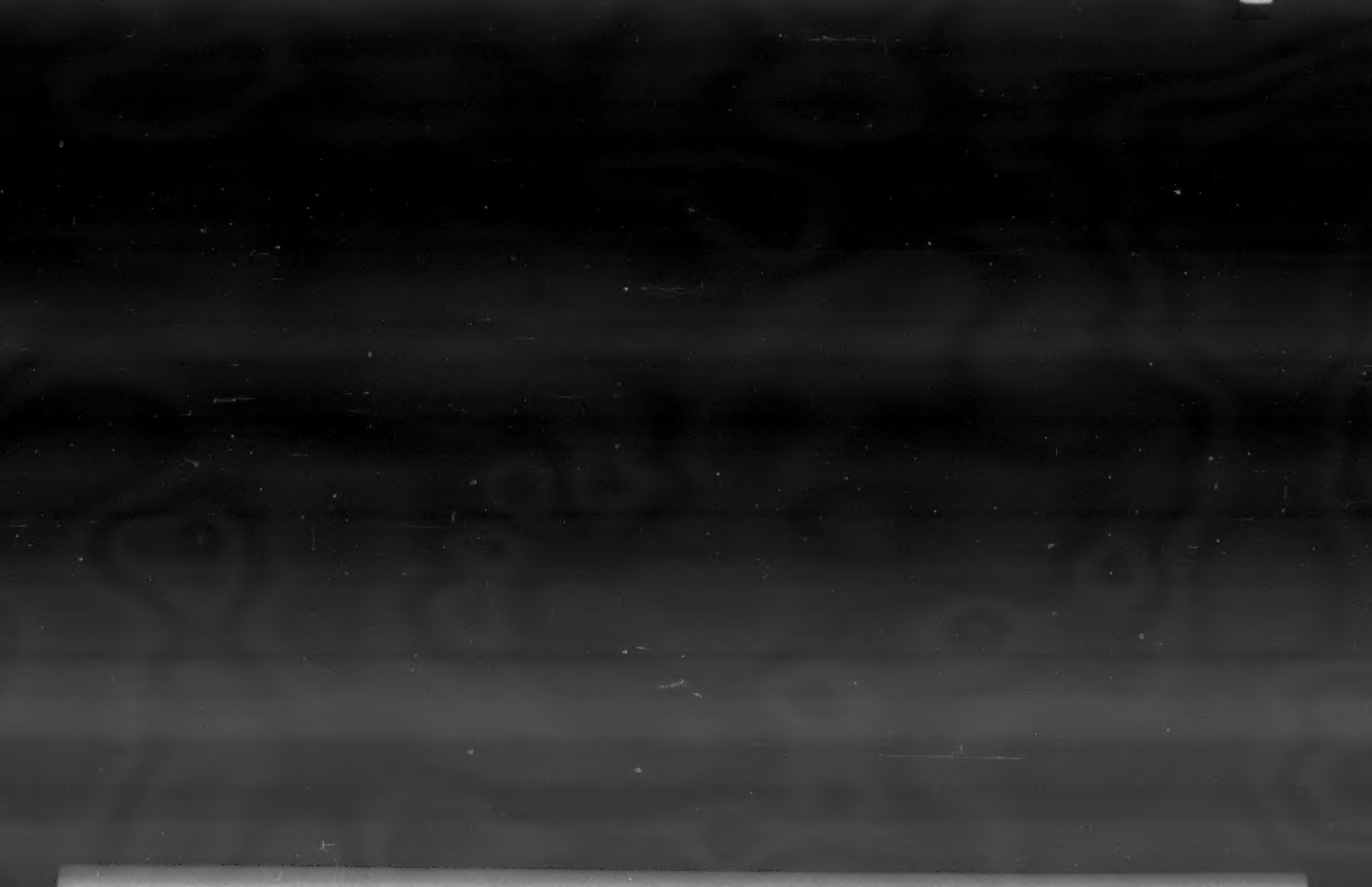

1

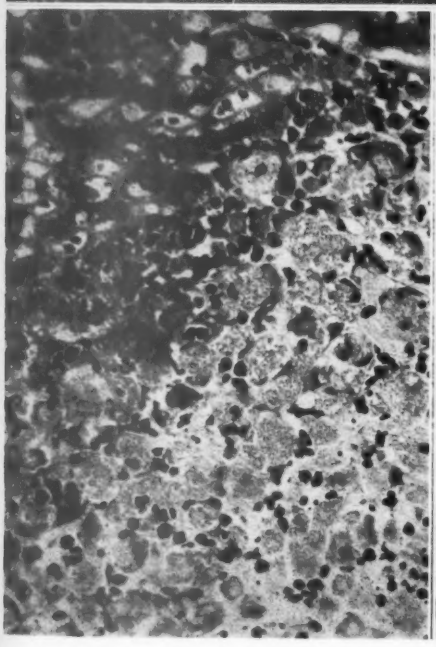

2

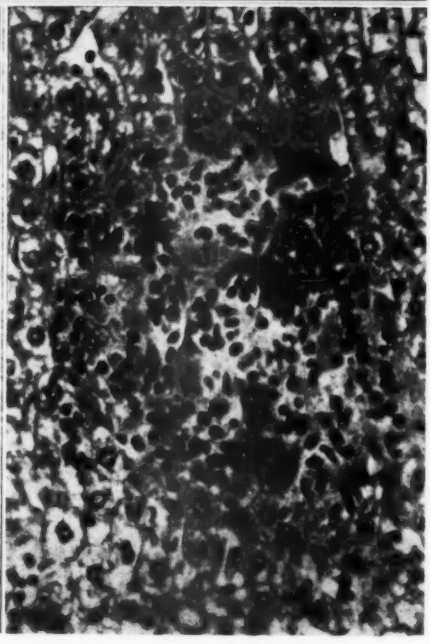

3

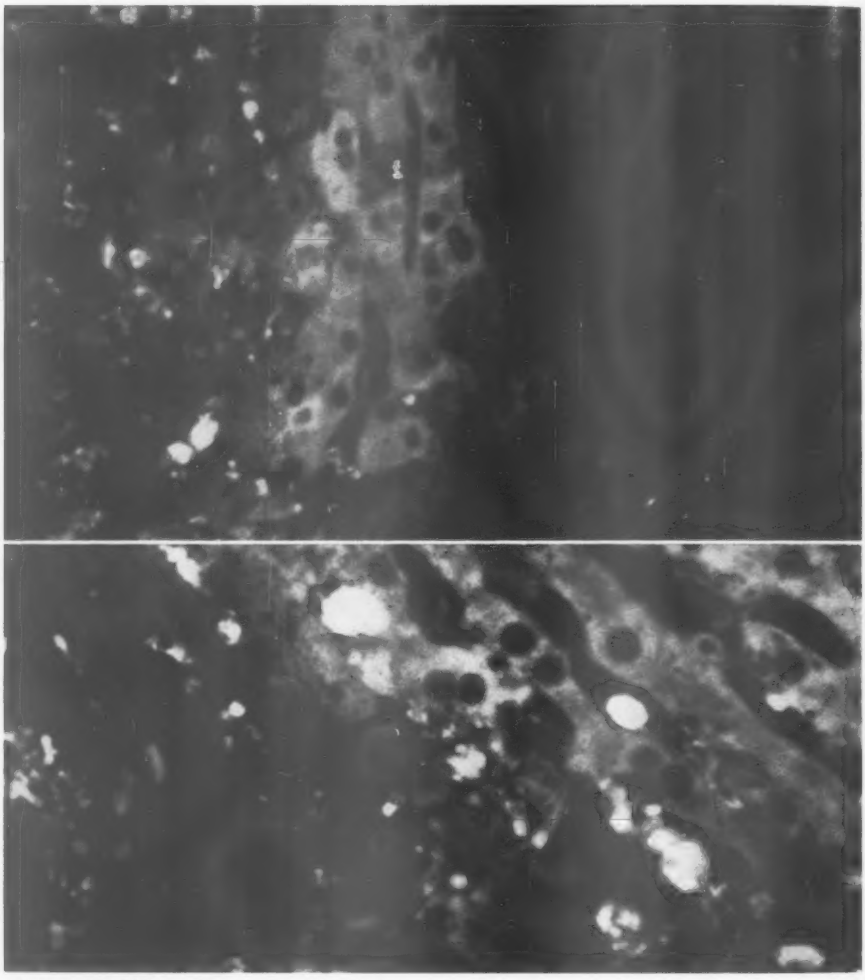

FIG. 4. Rabbit 23 (experiment II). Fluorescent photomicrograph of the margin of a necrotic zone 72 hours after the portal vein injection of soluble complexes formed in 3 × (fluorescent tracer-labeled) antigen excess. A portal tract is on the right. Intact cells of a liver plate maintain their nonspecific autofluorescence (center). The area of necrosis (left) shows loss of this property. Aggregates of antigen (specific apple-green fluorescence; white in photomicrograph) are present in sinusoids but not in the cytoplasm of necrotic parenchymal cells. Their location in Kupffer cells is difficult to determine. Unstained. × 374.

FIG. 5. Rabbit 25 (experiment I). The margin of a necrotic zone 24 hours after the portal vein injection of a challenging (fluorescent tracer-labeled) dose of antigen to a hyperimmune rabbit. Necrotic liver cells (left) show loss of autofluorescence. Large aggregates of antigen (specific apple-green fluorescence; white in photomicrograph) are seen within sinusoids both in the necrotic and marginal areas. Their size is somewhat larger than in Figure 4. Fluorescent photomicrograph, unstained. × 387.

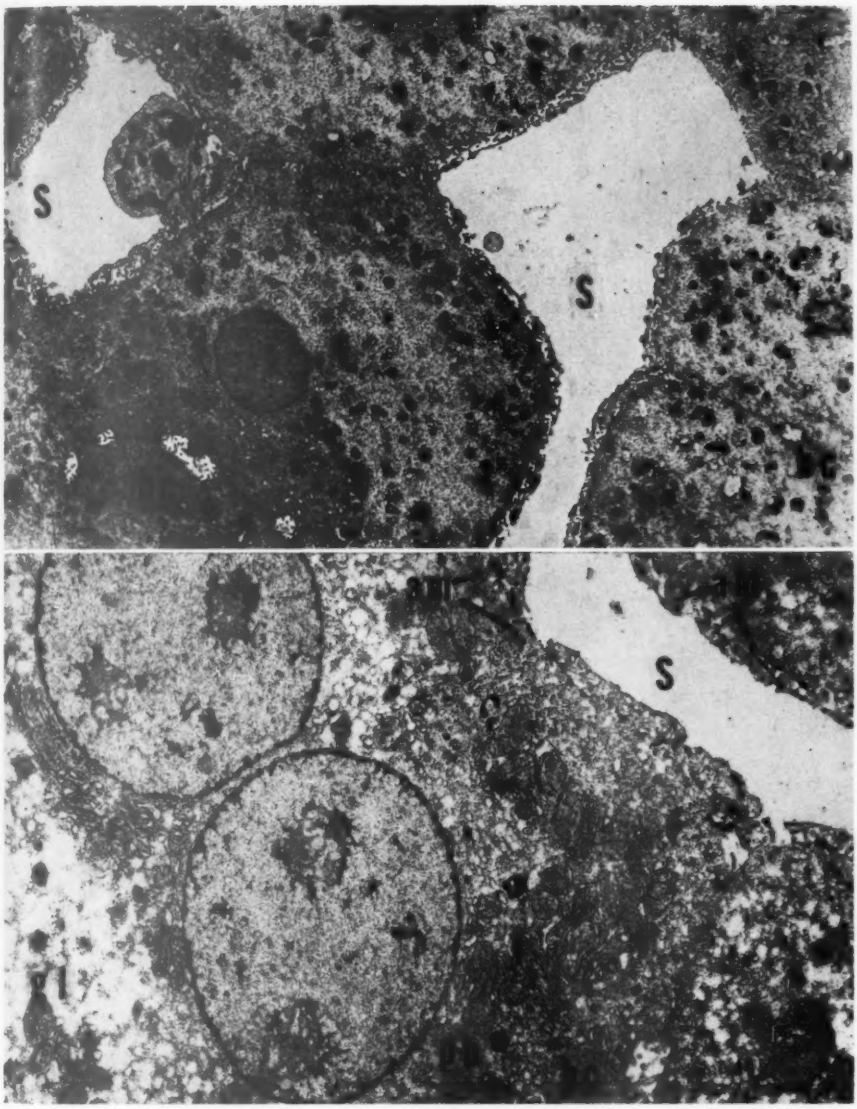

6

7

FIG. 6. Normal rabbit liver. Two angulated sinusoids border upon a central liver cell. The space of Disse surrounding both sinusoids is of even width. Several small perisinusoidal recesses are seen. A Kupffer cell lies in one of these in the left-hand sinusoid. A row of bile canaliculi extends along the intercellular boundary of two liver cells. Protargol. × 4,200.

FIG. 7. Normal rabbit liver. A binucleated liver cell containing the usual complement of finely granular glycogen. The organelles lie in the vicinity of the nuclei and between them and the sinusoid. The space of Disse is difficult to make out, owing to the presence of fine filaments of argentophilic (PASM-positive) material within it. Periodic acid-silver methenamine. × 8,960.

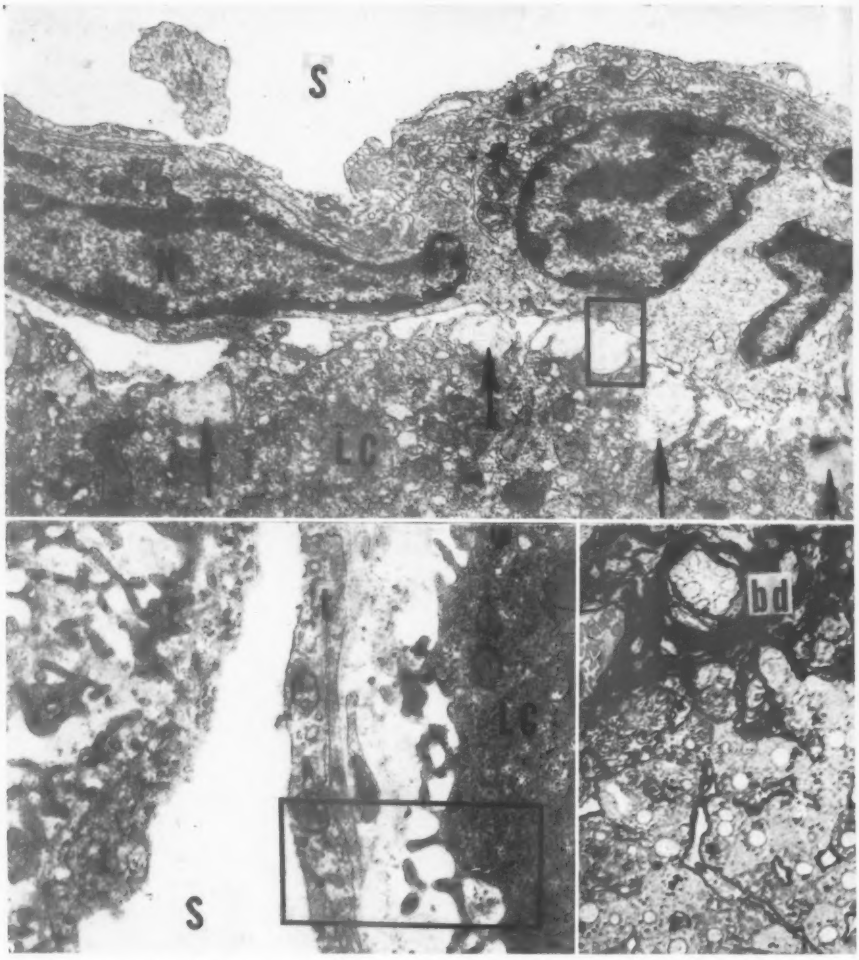

FIG. 8. Normal rabbit liver. A sinusoid near the portal tract is lined by a Kupffer cell (left) and an exogenous mesenchymal cell which is covered by an outrunner of the former. There is no evidence of an attachment of the Kupffer cell to the liver cell. The microvilli of the latter, projecting into the space of Disse, are separated from each other by a faintly argentophilic material (arrows.) An area similar to that enclosed in a square is seen in Figure 12. Protargol. × 13,200.

FIG. 9. Normal rabbit liver. The angle of a sinusoid in the vicinity of a portal tract. A faintly argentophilic, plasma-like material lies between the endothelium and the microvilli of liver cells. This represents the ground substance with its content of reticulin fibers. These can be seen in Figure 13 in an area corresponding to the one enclosed in a square. Protargol. × 19,040.

FIG. 10. Normal rabbit liver. The sinusoids in the vicinity of a portal tract are lined by a strongly PASM-positive material corresponding to that seen in Figure 9 in the electron micrograph. Thin section (0.5 μ), osmium acid-fixed tissue. Periodic acid-silver methenamine stain. × 360.

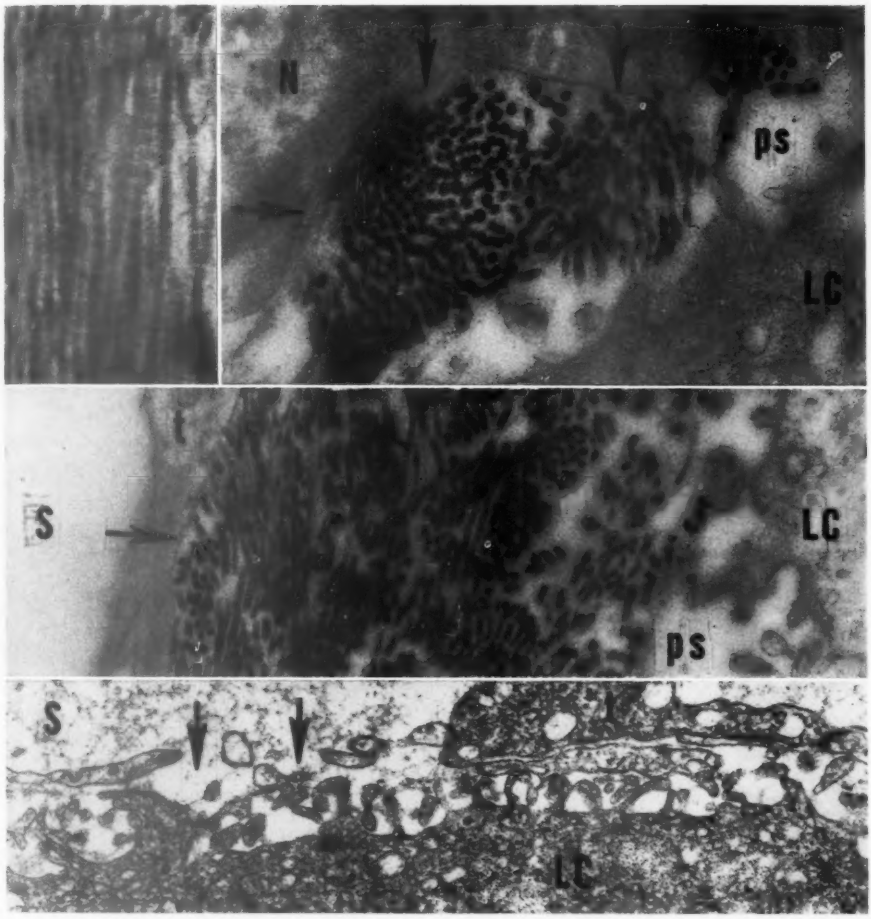

FIG. 11. Normal rabbit liver. A bundle of fibers in a perisinusoidal space shows the characteristic cross-striations of reticulin. Phosphotungstic acid stain. × 36,300.

FIG. 12. Normal rabbit liver. A bundle of cross-sectioned reticulin fibers occupies the space of Disse in an area similar to that enclosed in a square in Figure 8. The arrows point to the cell boundary of the Kupffer cell. The fibers are entirely extracellular in location. Uranyl acetate stain. × 33,000.

FIG. 13. Normal rabbit liver. A space of Disse similar to that seen in the squared area in Figure 9 is occupied by numerous uniformly polarized reticulin fibers. The arrow points to the cell membrane of the terminal trabecula of a Kupffer cell. The fibers have an entirely extracellular location. Phosphotungstic acid stain. × 33,000.

FIG. 14. Normal rabbit liver. A portion of a space of Disse bounded by terminal trabeculae of a Kupffer cell and parenchymal cell microvilli. Arrows point to gaps in the endothelial lining. Protargol stain. × 12,000.

15

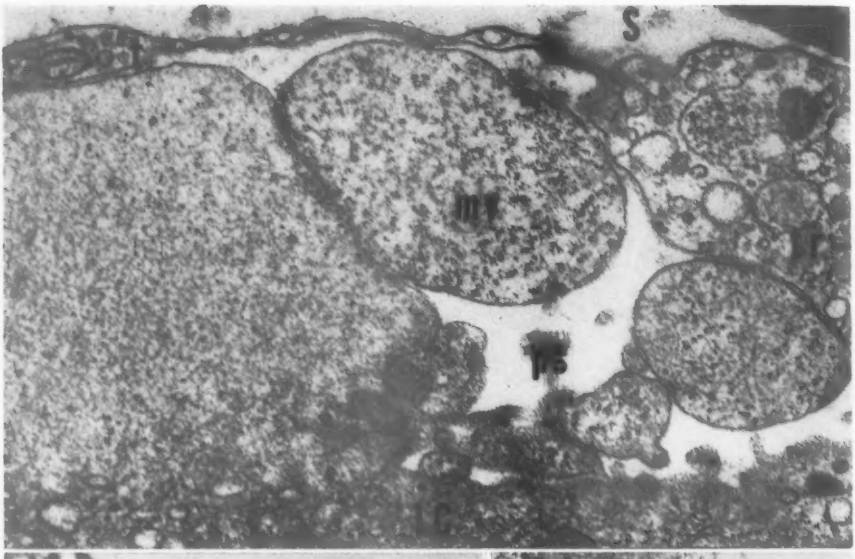

16

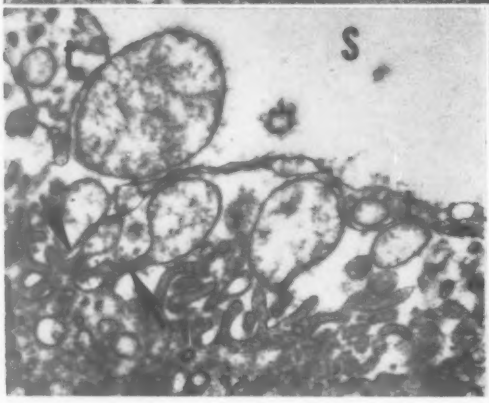

17

FIG. 15. Rabbit 39 (experiment II; 72 hours). A perisinusoidal space in the marginal area of a lobular lesion. The space is distended by ballooned, membrane-enclosed microvilli. In their internal structure organelles are absent and there are widely separated RNP granules. The villus on the left of the picture shows a broad base. An endothelial trabecula separates the space entirely from the sinusoid lumen. Note the "Swiss cheese" appearance of a larger trabecula on the right. Protargol stain. × 32,000.

FIG. 16. Rabbit 12 (experiment I; 48 hours). A perisinusoidal space from an area similar to that shown in Figure 15. The pedicles of liver cell microvilli are still unaffected (arrows). The tips are distended, however, and form pear-shaped clubs. The cytoplasm of a neighboring liver cell shows a slight vacuolar change. Protargol stain. × 24,800.

FIG. 17. Rabbit 33 (experiment II; 48 hours). A perisinusoidal space from an area similar to that shown in Figure 10. A ballooned microvillus is in process of being extruded from a space of Disse into a sinusoid lumen. Protargol stain. × 25,600.

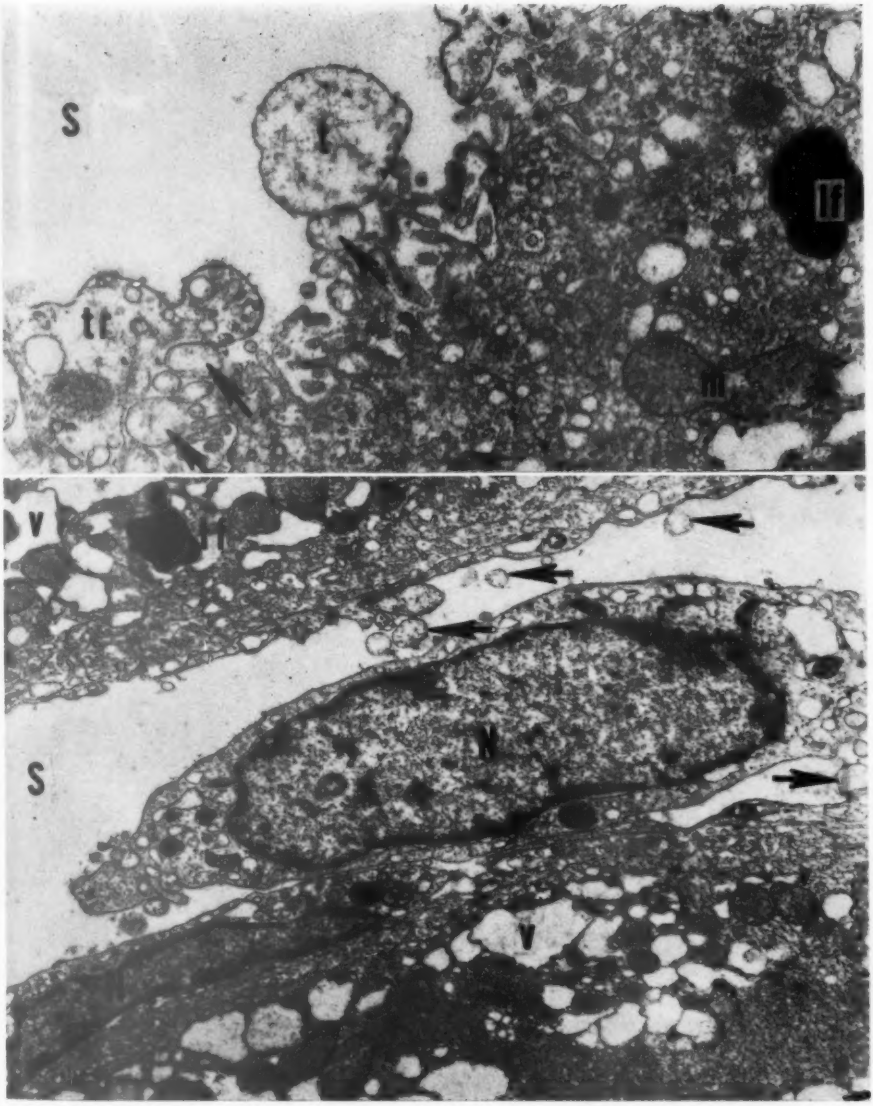

FIG. 18. Rabbit 33 (experiment II; 48 hours). The perisinusoidal space from an area similar to that shown in Figure 15. The trabeculae of Kupffer cells are affected by the ballooning change as well as by distention of microvilli (arrows). There are wide gaps in the Kupffer cell lining and a "Swiss cheese" appearance on the left. The underlying parenchymal cell shows an early vacuolar change. Protargol stain. × 16,800.

FIG. 19. Rabbit 13 (experiment I; 72 hours). A sinusoid in the marginal area of a necrobiotic zone. In the left lower corner a Kupffer cell lies in close apposition to the space of Disse. A second large Kupffer cell is seen almost entirely loose within the sinusoid lumen. Several rounded bodies (arrows) are floating in the sinusoid. These are detached liver cell microvilli. The space of Disse is collapsed. The cytoplasmic matrix between the vacuoles in a parenchymal cell in the right lower corner is markedly condensed. Protargol stain. × 12,000.

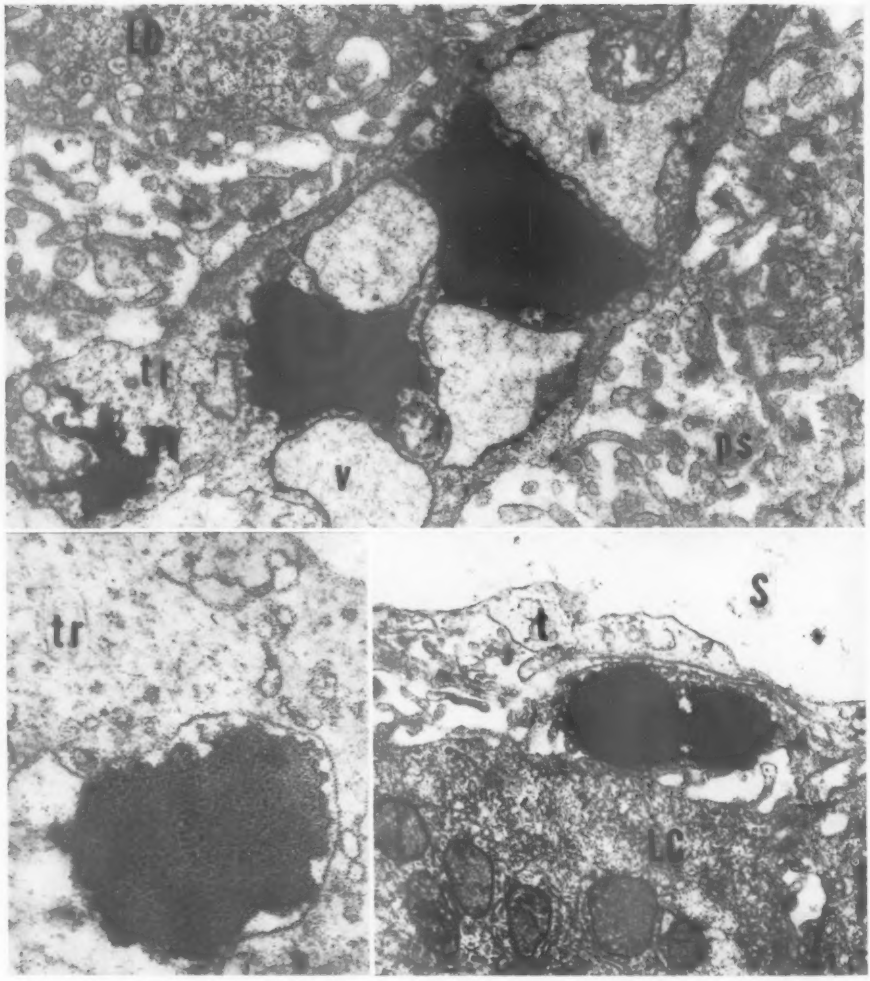

20

21

22

FIG. 20. Rabbit 3 (experiment II; 72 hours). A trabecula of a Kupffer cell at the margin of a necrobiotic zone. The densely argentophilic masses within the cytoplasm are thought to be precipitated antigen-antibody complexes. Dilated endoplasmic cisternas containing a faintly argentophilic material encompass the masses. The trabecula is retracted into a perisinusoidal recess. The labyrinthine character of the microvilli in the recess is evident in a tangential section on the right of the trabecula. Protargol stain. × 24,000.

FIG. 21. Rabbit 11 (experiment I; 24 hours). A trabecula of a Kupffer cell in process of engulfing an argentophilic mass similar to those seen in Figure 20. Protargol stain. × 44,800.

FIG. 22. Rabbit 42 (experiment II; 72 hours). Argentophilic masses similar to those in Figures 20 and 21 are found in the space of Disse. The Kupffer cell trabecula has closed off the space from the sinusoid lumen. Protargol stain. × 22,400.

CELL RENEWAL IN ADULT MOUSE TISSUES

JOSHUA L. EDWARDS, M.D., AND ROBERT E. KLEIN, M.D.

From the Department of Pathology, University of Florida College of Medicine, Gainesville, Fla.

One of the most important factors that determines the end results of tissue injury is the capacity of a tissue for replacement of its dying cells by new ones. Methods for precise measurement of this capacity are now available, and the employment of radioactive precursors of nucleic acids and proteins in labeling individual cells has begun to yield a wealth of new information concerning the kinetics of morphologic growth and biochemical synthesis in growing cells.

Fitzgerald, Eidinoff, Knoll and Simmel [1] first used tritium in radioautography, and Eidinoff and Knoll [2] first labeled the deoxyribonucleic acid (DNA) precursor, thymidine, in stable manner with tritium. Before and since then numerous studies [3–13] have established that radioautography of tissues from animals injected with tritiated thymidine or other DNA precursors provides a method for the detection of nuclei of cells that are synthesizing DNA during the period of exposure to the isotope. One can estimate accurately the relative rates at which cells proceed through the division cycle if (a) equal amounts of tritiated thymidine are available to all cells in equal concentrations for equal periods of time; (b) the duration of the period of synthesis in each cell type is approximately the same; and (c) all cells proceed through the division cycle. Under these conditions, the rate at which cells in a population are renewed is directly proportional to the incidence of cells in the population that incorporate tritiated thymidine and are thus "labeled" in radioautographs.

Normal cell proliferation in adult tissues, appropriately designated "renewal growth" by Leblond,[14,15] is periodic, highly variable in respect to rate among different cell types, and associated with characteristic patterns of cell migration. These facts became generally known through earlier studies [16–23] of the incidence and distribution patterns of mitotic figures in different tissues. The fact that mitosis usually occupies such a small fraction of the growth cycle results in most tissues having an extremely low mitotic index. In all tissues so far investigated it seems that the period of DNA synthesis is considerably longer than the period occu-

This work was supported by Research Grants E-1566 and E-1542 from the National Institutes of Health, United States Public Health Service, Bethesda, Md.

Accepted for publication, October 10, 1960.

pied by mitosis.[24–32] The "synthesis index" is, therefore, a more sensitive indicator of the rate of cell renewal than is the mitotic index.

Until recent years quantitative studies of the kinetics of cell renewal were limited to mechanical methods [33–36] and studies of the effects on the division cycle of staphmokinetic agents such as colchicine [37–39] and x-radiation.[25] Most studies employing radioactive isotopes have been limited to the investigation of single populations, and these, for the most part, have been cells of the hematopoietic system or superficial epithelium.[13,40–43]

The aims of the experiments reported here are to assess the relative rates of renewal of 34 different types of cells in the normal adult mouse and to determine the characteristic distribution pattern of cells synthesizing DNA within various organs and tissues.

Material and Method

Tritiated Thymidine (H³TDR)

The tritiated thymidine used in all experiments had a specific activity of 360 curies per mole, was labeled in the pyrimidine ring, and was free of labeled impurities and labile tritium atoms. It was prepared and purified by Schwarz Bioresearch, Inc., Mt. Vernon, New York. Dilutions suitable for injection were made in 1 per cent sodium chloride, and all injections were intravenous.

Experimental Animals

These consisted of normal male and female Swiss albino mice of a hybrid "Webster" strain, each being 64 to 72 days of age and weighing 20 to 24 gm. All were bred in our own colony and maintained on a diet of Ralston-Purina Rabbit Chow supplemented with weekly feedings of cod-liver oil saturated oat cereal. All mice used in this experiment followed the typical growth curve for this strain of mouse and were maintained at a constant temperature of 20° to 23° C.

Experimental Procedure

Each mouse received an intravenous injection of 0.7 μc. of tritiated thymidine per gm. of body weight and was killed by sudden exsanguination at varying intervals of time between 30 minutes and 16 hours following the injection. In each case a necropsy was performed immediately. To eliminate the possibility of variance associated with diurnal variations in the division cycle, all mice were killed and necropsied at the same time of day, 10:00 a.m. Blocks of 26 different tissues were taken from each mouse and fixed in Helly's fluid and cold 10 per cent formaldehyde buffered at pH 7.4.

Ribbons of approximately 6 sections were cut from each paraffin block of the formaldehyde fixed tissues. These were mounted on glass slides that were covered with a thin dry film of chrome alum gelatin. After removal of the paraffin, each section was covered with AR 10 stripping film (Kodak Limited) according to the method of Doniach and Pelc.[44] Exposure of film to the section varied from 21 to 64 days in order to determine the optimal exposure time for identification of labeled cells and grain counting over individual nuclei. After development in D 19 for 10 minutes, the radioautographs were processed further under standard conditions and finally stained through the gelatin film with hematoxylin and eosin.

Selection of Cell Types for Study

Thirty-four different cell types were selected for study. Some of these—for example, liver parenchymal cells, acinar epithelium of the thyroid gland, basal cells of the

epidermis and cardiac muscle cells—are clearly defined separate cell types. In other organs or tissues the cell populations were selected as to spatial distribution. For example, cortical cells of the outer mantle of the adrenal cortex were set apart as a population from the cells of the innermost layer, and cells comprising epithelium at the base of the intestinal crypts were distinguished as a population from the more superficial cells lining the villi. In other cases, cells composing the alveoli of certain glands, such as the salivary gland and pancreas, were considered as a population different from the ductal epithelium of that gland. All nucleated cells of the bone marrow were arbitrarily lumped together as a population, as were all neurons in the cerebrum and basal ganglia and the epithelial cells of the renal tubules. A listing of all cell types investigated is given in Table IV.

Estimation of Background and Counting of Labeled Nuclei

In all radioautographs some of the cell nuclei had incorporated the tritiated thymidine, and these cells were identified in the radioautographs by the presence of reduced silver grains in the film overlying the nuclei. These are hereinafter referred to as "labeled cells." Background under the conditions of this experiment was insignificant, and labeled and unlabeled cells were clearly distinguishable. There was no significant difference in the incidence of labeled cells in a given tissue when the period of exposure to the film varied from 21 to 72 days.

RESULTS

Liver

In studies of the radioautographs of liver, all observations reported here are based on the examination of radioautographs from livers of 4 different mice, 2 males and 2 females. Each was necropsied 2 hours after the intravenous injection of tritiated thymidine. Observations were made on 69,595 labeled and unlabeled cells in the following categories: liver parenchymal cells, Kupffer cells, and "other types," including endothelium, transient leukocytes in the sinusoids, bile duct epithelium and unidentified cells. The proportions of cell types, the percentages of labeled cells in each population, and the relative contribution of each population to DNA synthesis in the liver are presented in Tables I through III.

TABLE I

PERCENTAGES OF CELL TYPES IN MOUSE LIVER

	Percentages					
	Mouse 6	Mouse 7	Mouse $8M_1$	Mouse $8M_2$	Mean	Standard deviation
All parenchymal cells	53.02	68.05	51.69	47.25	54.99	8.70
All Kupffer cells	39.06	29.66	36.08	46.80	37.89	7.11
All other type cells	7.14	2.27	12.23	5.95	6.86	4.11
Ratio of parenchymal to Kupffer cells (P/K)	1.36	2.29	1.43	1.01	1.45	.54

Some variation in the relative size of each population in different mice is shown in Table I. It is evident that in the normal mouse approximately

TABLE II

LABELING OF CELL TYPES IN THE LIVER; MICE INJECTED INTRAVENOUSLY WITH 0.7 μC. OF H^3TDR PER GM. OF MOUSE; NECROPSY 2 HOURS LATER

	Mouse 6	Mouse 7	Mouse $8M_1$	Mouse $8M_2$	Mean	Standard deviation
Total parenchymal cells	19615	4398	7201	5995	9302	
Total labeled parenchymal cells	188	30	37	110	91	
Per cent of parenchymal cells labeled	.96	.68	.51	1.83	.98	.58
Total Kupffer cells	14250	1917	5026	5938	6783	
Total labeled Kupffer cells	553	85	304	75	254	
Per cent of Kupffer cells labeled	3.88	4.43	6.05	1.26	3.74	2.0
Total other type cells	2647	147	1703	755	1313	
Total labeled other cells	153	12	97	42	76	
Per cent of other cells labeled	5.78	8.16	5.69	5.56	5.79	1.38
Total all cells	36512	6462	13930	12688	17398	
Total labeled (all cells)	894	127	438	227	421	
Per cent of total cells labeled	2.45	1.97	3.14	1.79	2.42	.61

TABLE III

RELATIVE CONTRIBUTION OF CELL TYPES TO DNA SYNTHESIS IN LIVER; MICE INJECTED INTRAVENOUSLY WITH 0.7 μC. OF H^3TDR PER GM. OF MOUSE; NECROPSY 2 HOURS LATER

	Mouse 6	Mouse 7	Mouse $8M_1$	Mouse $8M_2$	Mean	Standard deviation
Per cent labeled parenchymal cells of all labeled cells	21.03	23.62	8.45	48.46	23.39	18.32
Per cent labeled Kupffer cells of all labeled cells	61.86	66.93	69.41	33.04	57.81	16.81
Per cent labeled other cells of all labeled cells	17.11	9.45	22.15	18.50	16.80	5.35

90 per cent of the liver consisted of 2 cell types, the liver parenchymal cells (P) and the Kupffer cells (K) lining the sinusoids. These 2 populations existed in a mean P/K ratio of 1.5 ± 0.54. Comparison of the incidence of thymidine incorporation in these 2 populations (Table III) indicated that the contribution by Kupffer cells to the total synthesis of DNA at any given time was greater than that of parenchymal cells by a factor of approximately 2 and that the contribution by cells in the liver other than these types was usually less than 20 per cent of the total. This, as well as the data given in Table II, indicated that the Kupffer cell popu-

lation was turning over at a more rapid rate than the parenchymal cell population. There was a slight preponderance of labeled parenchymal cells in the neighborhood of portal spaces. The significance of this observed difference within the lobule is difficult to assess. Data supporting the preponderant periportal distribution of parenchymal cells incorporating thymidine in regenerating liver is available[45, 46] and fully supported by our own studies.[47] No evidence that the distribution of the labeled Kupffer cells was anything but random was found.

In every case where binucleated cells were labeled, both nuclei were invariably labeled and to approximately the same extent, as indicated by the number of grains overlying each nucleus. Thus the nuclei of binucleated cells were obviously synchronized in respect to DNA synthesis.

Kidney

Cell populations in the kidney were categorized by location into the following 4 groups: (a) cells of the interstitial tissue; (b) cortical tubular epithelium; (c) medullary tubular epithelium; and (d) cells of glomeruli (all types). Cells of the interstitial tissue were composed predominantly of mononuclear cells, fibroblasts and endothelial cells. Interstitial cells were more heavily labeled than any other group in the kidney. Approximately 4 per cent of these cells were labeled. Less than 0.5 per cent of the epithelial cells composing the renal tubules incorporated thymidine under these conditions, and no significant difference existed in the labeling of epithelium in different segments of the nephron. Cell types present in the glomeruli were labeled as a group to approximately 0.8 per cent.

Adrenal

Significant differences existed between the numbers of labeled cells in the outer half of the adrenal cortex (1.7 per cent) and the inner half (0.7 per cent). That 2½ times as many cells in the outer half of the cortex were labeled as compared with the inner half suggests that either the cells tended to migrate from the outer region to the inner or that these cells were different in respect to the rate of renewal in the different regions. Approximately 2 per cent of the cells of the adrenal medulla were labeled.

Other Solid Epithelial Viscera

Cells comprising the alveolar and ductal epithelium in the salivary glands contained equal and small numbers (one per cent) of cells that were labeled. Indeed, no striking differences existed among parenchymal

cells of the thyroid, pancreas, liver, kidney or adrenal glands in respect to the fraction of these populations that incorporated thymidine. All these epithelial cells were, to some extent, continuously undergoing replacement, as was indicated by the fact that none were ever free of cells incorporating thymidine in contrast to some types of cells that rarely, if ever, synthesized DNA under normal conditions of growth.

Germinal Epithelium

Except for an occasional connective tissue cell and interstitial cells, thymidine incorporation in the testis was limited to the basal cells of the seminiferous tubules (primary spermatogonia). Of this population 34.8 per cent were labeled, and the histologic pattern of distribution of labeled cells was one of sharp localization to different segments of a tubule. In a cross section of a seminiferous tubule, either all of the cells of the basal layer of the germinal epithelium were labeled or none of this group incorporated thymidine in that cross section. The periodicity of mitosis along the length of a seminiferous tubule has been described.[48] That the distribution of cells synthesizing DNA was sharply defined along histologic lines is demonstrable in Fig. 2.

In the ovary, cells of the ovarian follicle, the cortex and the medulla were grouped as 3 separate populations. The incidence of labeling of granulosa cells in the ovarian follicle was 30 per cent, and the same sharply defined periodicity comparable to that seen in cells of the seminiferous tubules was noted in the granulosa cell population. Four and one-tenth per cent of cortical cells other than those associated with follicles were labeled. A high proportion of these were in the outermost layers of cells.

Surface Epithelium

Marked differences existed in respect to the incidence of thymidine incorporation and the distribution of labeled cells among different types of surface epithelium such as skin, intestinal mucosa, epithelium of the urinary tract and respiratory tract. Of all these tissues, the epithelium lining the crypts of the small intestine consistently contained the highest proportion of labeled cells (Fig. 3). The pattern of distribution and kinetics of this population has been carefully and quantitatively studied by Quastler, Sherman, Brecher and Cronkite [13] and Friedman.[49] In contrast to this high incidence of labeled cells in the epithelium of the small intestine, the basal epithelium of the large intestine had a much lower value (4 per cent) which, on the other hand, was significantly higher than the value obtained for other surface epithelium.

The endometrial cells incorporating thymidine were for the most part

confined to the deep glands. It was, thus, difficult to make comparisons between the incidence of labeling in this epithelium and others that have more sharply defined germinal layers. In 2 female mice multiple sections of the fallopian tube revealed almost no epithelium labeled. This was in striking contrast to a high activity of thymidine incorporation in the epithelium of the deep glands of the endometrium.

Lymphoid and Hematopoietic Tissue

These were among the most active tissues in respect to incorporation of thymidine. They were exceeded in this activity only by the germinal layer of the epithelium of the small intestine, the germinal epithelium of the testis and granulosa cells of the ovarian follicle. The distribution of radioactivity in radioautographs of these tissues was not random and was, for the most part, confined under the conditions of these experiments to large mononuclear cells. Relatively few lymphocytes or granulocytes in lymph nodes or bone marrow were labeled. Megakaryocytes and cells of the erythrocytic series were labeled more frequently. The follicular centers of both lymph nodes and spleen contained respectively, 22.3 per cent and 19.2 per cent of labeled cells as opposed to the cells of the follicular mantle which in the lymph node showed an incidence of labeling of 4.1 per cent and in the spleen of 3.8 per cent.

Seventeen and five-tenths per cent of the cells in the red pulp of the spleen and 9.8 per cent of the cells in the medulla of the mesenteric lymph nodes were labeled. The grain counts over individual nuclei of cells of both splenic red pulp and lymph node medulla were consistently higher than over similar nuclei in the centers of the follicles of both tissues.

Lung Parenchyma

Of the cells comprising the lung parenchyma, macrophages and connective tissue cells were labeled more often than any other type. A surprisingly low incidence of labeled cells was found in the respiratory epithelium. Bertalanffy [50] has made a definitive study of cell renewal in the lung.

Bone Marrow

A high degree of consistency was obtained in counts of percentages of labeled cells in the bone marrow. All nucleated marrow cells were considered as a single population without separation of various cell types. Eighteen and nine-tenths per cent was the mean value obtained in separate counts of 3 different animals. Hematopoietic tissues have been studied by this method in great detail.[13,41–43]

Thymus

A high consistency was obtained between different animals in estimating percentages of labeled cells in both cortex and medulla of the thymus. A mean value of 6.1 per cent was obtained for cortical cells and 2.2 per cent for cells in the medulla. Usually the labeled cells had large vesicular nuclei.

Heart

Cells in the heart distinguished as groups were those of endocardium, myocardium and epicardium. In no case was labeling noted in cardiac muscle cells. Capillary endothelial cells constituted those which were labeled in highest proportion. The values for endocardium were 1.9 per cent; myocardium, 1.8 per cent; and epicardium, 0.7 per cent.

Bone

Cells of the periosteum, osteocytes, and endosteum were considered as separate groups. The incidence of labeling of cells in these tissues was 0.35 per cent, 0 per cent and 0.7 per cent, respectively. Connective tissue cells, largely fibroblasts, were the cells labeled in bone; no osteocytes or osteoblasts were labeled.

Central Nervous System

Numerous sections of the brains and spinal cords in 12 mice were examined carefully, but no labeled cells were found in radioautographs of brain tissue that could be identified as nerve cells. A small proportion of microglia incorporated thymidine under these conditions.

Skin

Ten per cent of cells comprising the root of the hair follicle incorporated thymidine after a 2-hour exposure. This was in sharp contrast to the epithelium of the hair canal and the basal cells of the epidermis which were labeled to the extent of 2 per cent and 0.4 per cent respectively.

Stomach and Esophagus

Three per cent and 2 per cent of the cells, respectively, of the mucosa of the stomach and esophagus were labeled. Most of the labeled cells in the gastric mucosa were confined to the midzone between the deepest and most superficial cells 2 hours after the injection of tritiated thymidine.

Discussion

Cell populations of the adult mammalian organism have been classified in respect to cell renewal into 3 major categories.[14,15,49] At one extreme

are those cells in the adult mammal which rarely or never undergo cell division such as neurons and cardiac muscle cells. The blast forms of these fully differentiated cells do not persist past the embryonic stages of development of the organism; thus the mean life span of these cells approximates that of the organism. At the other extreme are those cell populations having a relatively high mitotic index—for example, cells of the epidermis, intestinal epithelium, hematopoietic tissues and germinal cells of the gonads. All these tissues are characterized by rapid renewal and easily recognizable stages of differentiation which may be distinguished by morphologic differences, as in erythropoiesis, by unique patterns of migration in intestinal epithelium, or by both of these characteristics of differentiation, as shown by epidermis. Marked differences exist between these cell types in respect to their mean life span, the degree to which cell division is synchronized, and the factors in the internal and external environment that affect their rate of division.

In a category between these 2 extreme groups, i.e., those cells that never divide and those undergoing rapid renewal, a third classification includes cell populations of the liver and other solid epithelial viscera and connective tissue cells in general. These are types whose parent cell is not sharply delineated spatially or morphologically from the fully differentiated cells. These are tissues also in which the mitotic rate is relatively low. On the basis of these observations it has been assumed that the rate of division of these cells is no more than just sufficient to account for the normal increase in body weight that occurs in the adult animal and that these tissues renew themselves only following injury or partial removal.[49] In contrast to this view, our observations indicate that the renewal of these tissues is also in a steady state; indeed, with the exception of neurons and cardiac muscle cells, apparently all tissues are renewing themselves at a fairly steady rate over and above that required for growth. The most obvious justification for this conclusion is that normal tissues which have ceased to grow in terms of increase in mass or cellularity still have a significant proportion of their cells that synthesize new DNA and divide. Table IV presents a list of all the tissues investigated in these experiments in order of the frequency of nuclear labeling with tritiated thymidine. It is assumed that labeled cells represent cells in the process of synthesizing new DNA and are thus in preparation for division. In the case of cells of all types that are clearly in the end stages of differentiation, none are labeled. On the other hand, marked differences exist between certain cell populations in respect to the proportion of cells labeled. These differences are, in some cases, of particular interest and significance.

The fact that Kupffer cells make a greater contribution to the total synthesis of new DNA in the liver than the parenchymal cells reaffirms

the importance of carrying out cytologic studies when conclusions are to be drawn from biochemical analyses of complex tissue homogenates. The high incidence of thymidine incorporation into fibroblasts of most tissues suggests that these cells have a potential for differentiating into a wide range of more highly specialized types of cells. The differences

TABLE IV

INCIDENCE OF LABELED CELLS; MICE INJECTED INTRAVENOUSLY WITH 0.7μC. OF H^3TDR PER GM. OF MOUSE; NECROPSY 2 HOURS LATER

Cell type	Labeled cells (%)	Standard error
Small intestine, epithelium base of crypts	50.0	4.1
Testis, primary spermatogonia	34.8	
Ovary follicle	30.0	8.1
Mesenteric lymph node, follicular center	22.3	2.7
Spleen, follicular center	19.2	10.7
Bone marrow (all nucleated cells)	18.9	1.2
Spleen, red pulp	17.5	10.6
Mesenteric lymph node, medulla	9.8	5.0
Ovary, cortex	6.4	4.1
Thymus, cortex	6.1	2.0
Mesenteric lymph node, follicular mantle	4.1	2.6
Large intestine, crypt epithelium	4.0	5.9
Thymus, medulla	2.2	0.59
Adrenal, outer cortex	1.7	0.17
Kupffer cells	1.36	0.95
Salivary gland, alveolar epithelium	1.0	0.6
Salivary gland, duct epithelium	1.0	0.2
Adrenal, medulla	0.7	0.2
Hepatic parenchymal cells	0.53	0.36
Thyroid, alveolar epithelium	0.5	0.35
Adrenal, inner cortex	0.5	0.07
Kidney, cortical tubules	0.4	0.35
Skin, basal cell layer	0.4	0.3
Bronchus, respiratory epithelium	0.4	0.1
Trachea, mucosa	0.3	0.35
Bladder, transitional epithelium	0.15	0.8
Kidney, medullary tubules	0.11	0.11
Small intestine, superficial epithelium	0	
Large intestine, superficial epithelium	0	
Cardiac muscle	0	
Skeletal muscle	0	
Neurons	0	
Bone	0	
Cartilage	0	

that exist between different types of surface epithelium—for example, small versus large intestine, and intestinal, respiratory and transitional epithelium—are striking. The reasons underlying these differences between surface epithelia are, at the present time, unknown.

The difficulty in recognizing stages in the cytogenesis of some cell types makes the task of determining the actual rate at which these cells are

renewed a complicated one. Where a clear morphologic pattern of migration or differentiation exists, one can directly measure the rate of differentiation, cell death or renewal. More than one of its several spatial or morphologic compartments must be recognized or the rate of progression through that compartment cannot be measured. This has been the primary difficulty in the measurement of the life span of the lymphocyte.

From the relative incidence of thymidine incorporation in a variety of populations, one can determine only the relative rates of renewal of the tissues studied. Except in the case of tissues such as epidermis and intestinal epithelium, determination of the actual rates of renewal have been derived hitherto by indirect calculation, requiring, in each case, an accurate estimate of the duration of mitosis. An accurate estimate of this is not easily obtained, with the possible exception of a few cell types. The hypothesis that all cells in a species have the same mitotic duration has little or no evidence in its support.

The metabolic stability of deoxyribonucleoprotein in living cells, the exclusiveness of the process of thymidine incorporation into new DNA, the stability of the tritium label in the pyrimidine ring, and the high degree of resolution obtained in radioautographs of tissues when this isotope is employed are all now well established facts. Together, these facts make it possible to determine the rate of renewal of any cell type that can be identified in tissue sections. This can be accomplished by applying the principle of isotope dilution secondary to cell division. The mean grain counts over cell nuclei will change with time at a rate that is directly proportionate to the rate of cell division. Experiments designed to measure the actual rates of renewal of mammalian cell types accurately are in progress in this laboratory.

In some cases cell populations differ considerably in the mean number of grains that overlie their respective nuclei even though the duration of their exposure to the isotope is identical. This difference between two populations in the same tissue is most obvious in comparing the labeling of large vesicular nuclei in the follicular centers of spleen and lymph nodes to those of cells outside the follicles. If the assumption is made that cells of the follicular centers are progenitors of the medullary cells, then it may be hypothesized that migration of these cells occurs during the period of DNA synthesis. If this is a valid statement, then the period of time required for migration must be less than the duration of the labeling period. A critical test of this hypothesis would be the observation of any change in the ratio of the mean grain counts over these two spatially separated groups of cells of the same type as the period of exposure to tritiated thymidine is shortened.

The high degree of constancy of the mean grain count over nuclei of

morphologically well defined populations such as the primary spermatogonia and intestinal crypt cells indicates that some cell types are quite uniform and consistent in respect to duration and mean rate of DNA synthesis. Another significant observation is the striking evidence of synchronization of certain cells in respect to thymidine incorporation, DNA synthesis and cell division. This is most obvious in the testis and ovary as shown in Figs. 1 and 2. The only cell type studied in which the thymidine incorporating cells appear to have a random distribution is the fibroblasts. The factors which predispose to these varied patterns of distribution are unknown, but it seems clearly indicated that the control of DNA synthesis and thereby of cell division is accomplished by a mechanism more complicated than by a mere direct effect, humoral or of another kind, on the cell itself. Whatever kind of control mechanisms exist must be correlated with or dependent upon the histologic structure of the tissue involved. A reasonable hypothesis is that adjacent cells influence each other in this respect, possibly by an exchange of metabolites that are essential to initiation of DNA synthesis. These are observations that must be taken into account in any satisfactory explanation of this important synthetic process.

References

1. Fitzgerald, P. J.; Eidinoff, M. L.; Knoll, J. E., and Simmel, E. B. Tritium in radioautography. *Science*, 1951, **114**, 494–498.
2. Eidinoff, M. L., and Knoll, J. E. The introduction of isotopic hydrogen into purine ring systems by catalytic exchange. (Note) *J. Am. Chem. Soc.*, 1953, **75**, 1992–1993.
3. Reichard, P., and Estborn, B. Utilization of deoxyribosides in the synthesis of polynucleotides. *J. Biol. Chem.*, 1951, **188**, 839–846.
4. Friedkin, M.; Tilson, D., and Roberts, D. Studies of deoxyribonucleic acid biosynthesis in embryonic tissues with thymidine-C^{14}. *J. Biol. Chem.*, 1956, **220**, 627–637.
5. Davidson, J. N.; Smellie, R. M.; Keir, H. M., and McArdle, A. H. Synthesis of deoxyribonucleic acid in extracts of mammalian cells. *Nature, London*, 1958, **182**, 589–590.
6. Verly, W. G., and Hunnebelle, G. Préparation de thymidine marquée avec du tritium. *Bull. Soc. chim. Belge*, 1957, **66**, 640–649.
7. Taylor, J. H.; Woods, P. S., and Hughes, W. L. The organization and duplication of chromosomes as revealed by autoradiographic studies using tritium-labeled thymidine. *Proc. Nat. Acad. Sc.*, 1957, **43**, 122–128.
8. Messier, B. Histological Localization of Newly Formed Deoxyribonucleic Acid by Means of Tritium-Labeled Thymidine. Canadian Cancer Conference. Begg, R. W. (ed.). Academic Press, Inc., New York, 1959, pp. 23–30.
9. Hughes, W. L.; Bond, V. P.; Brecher, G.; Cronkite, E. P.; Painter, R. B.; Quastler, H., and Sherman, F. G. Cellular proliferation in the mouse as revealed by autoradiography with tritiated thymidine. *Proc. Nat. Acad. Sc.*, 1958, **44**, 476–483.

10. HUGHES, W. L. Autoradiography with Tritium. Second United Nations International Conference on the Peaceful Uses of Atomic Energy. Isotopes in Biochemistry and Physiology, Part 2, 1958, **25**, 203–210.

11. VERLY, W. G.; FIRKET, H., and HUNNEBELLE, G. Thymidine-H^3 in Studies of DNA Synthesis in Tissue Cultures. Second United Nations International Conference on the Peaceful Uses of Atomic Energy. Isotopes in Biochemistry and Physiology, Part 2, 1958, **25**, 181–185.

12. LEBLOND, C. P.; MESSIER, B. and KOPRIWA, B. Thymidine-H^3 as a tool for the investigation of the renewal of cell populations. *Lab. Invest.*, 1959, **8**, 296–308.

13. QUASTLER, H.; SHERMAN, F. G.; BRECHER, G., and CRONKITE, E. P. Cell Renewal, Maturation and Decay in Gastro-intestinal Epithelia of Normal and Irradiated Animals. Second United Nations International Conference on the Peaceful Uses of Atomic Energy. Biological Effects of Radiation, 1958, **22**, 202–205.

14. LEBLOND, C. P., and WALKER, B. E. Renewal of cell populations. *Physiol. Rev.*, 1956, **36**, 255–276.

15. LEBLOND, C. P.; STEVENS, C. E., and BOGOROCH, R. Histological localization of newly formed deoxyribonucleic acid. *Science*, 1948, **108**, 531–533.

16. THURINGER, J. M. Regeneration of stratified squamous epithelium. *Anat. Rec.*, 1924, **28**, 31–43.

17. BLUMENFELD, C. M. Normal and abnormal mitotic activity. I. A comparison of periodic mitotic activity in epidermis, renal cortex and submaxillary gland of the albino rat. *Arch. Path.*, 1942, **33**, 770–776.

18. HOFFMAN, J. G. The Size and Growth of Tissue Cells. Charles C Thomas, Springfield, Ill., 1953, 128 pp.

19. ABERCROMBIE, M. Estimation of nuclear population from microtome sections. *Anat. Rec.*, 1946, **94**, 239–247.

20. RIS, H. Cell Division. In: Analysis of Development. Willier, B. H.; Weiss, P. A., and Hamburger, V. (eds.). W. B. Saunders Co., Philadelphia, 1955, Chapt. 3, pp. 91–125.

21. BIZZOZERO, G. Ueber die Regeneration der Elemente der schlauchförmigen Drüsen und des Epithels der Magendarmkanals. *Anat. Anzeig.*, 1888, **3**, 781–784.

22. BULLOUGH, W. S. Mitotic activity in the adult male mouse, *Mus musculus L.* The diurnal cycles and their relation to waking and sleeping. *Proc. Royal Soc. London, s.B*, 1947–1948, **135**, 212–233.

23. BULLOUGH, W. S. The effects of experimentally induced rest and exercise on the epidermal mitotic activity of adult male mouse, *Mus musculus L. Proc. Royal Soc. London, s.B*, 1947–1948, **135**, 233–242.

24. PASTEELS, J., and LISON, L. Recherches histophotométriques sur la teneur en acide désoxyribosenucléique au cours de mitoses somatiques. *Arch. Biol.*, 1950, **61**, 445–474.

25. KNOWLTON, N. P., JR., and WIDNER, W. R. The use of x-rays to determine the mitotic and intermitotic time of various mouse tissues. *Cancer Res.*, 1950, **10**, 59–63.

26. HUGHES, A. The Mitotic Cycle; the Cytoplasm and Nucleus During Interphase and Mitosis. Butterworths, London, 1952, 232 pp.

27. WALKER, P. M. B. The mitotic index and interphase processes. *J. Exper. Biol.*, 1954, **31**, 8–15.

28. HOWARD, A., and PELC, S. R. Synthesis of desoxyribonucleic acid in normal and irradiated cells and its relation to chromosome breakage. *Heredity*, 1953, **6**, Suppl., 261–273.

29. PATT, H. M.; BLACKFORD, M. E., and DRALLMEIER, J. L. Growth characteristics of the Krebs ascites tumor. *Proc. Soc. Exper. Biol. & Med.*, 1953, **83**, 520–524.

30. LAJTHA, L. G. Detection of adenine carbon-14 in deoxyribonucleic acid by autoradiography. (Letter to the editor) *Nature, London*, 1954, **173**, 587–588.

31. LAJTHA, L. G.; OLIVER, R., and ELLIS, F. Incorporation of ^{32}P and adenine ^{14}C into DNA by human bone marrow cells *in vitro*. *Brit. J. Cancer*, 1954, **8**, 367–379.

32. HORNSEY, S., and HOWARD, A. Autoradiograph studies with mouse Ehrlich ascites tumor. *Ann. New York Acad. Sc.*, 1956, **63**, 915–928.

33. ASHBY, W. The determination of the length of life of transfused blood corpuscles in man. *J. Exper. Med.*, 1919, **29**, 267–281.

34. YOFFEY, J. M. The quantitative study of lymphocyte production. *J. Anat.*, 1932–1933, **67**, 250–262.

35. YOFFEY, J. M., and COURTICE, F. C. Lymphatics, Lymph and Lymphoid Tissue. Edward Arnold Ltd., London, 1956, ed. 2, 510 pp.

36. SANDERS, A. G.; FLOREY, H. W., and BARNES, J. M. The output of lymphocytes from the thoracic duct in cats and rabbits. *Brit. J. Exper. Path.*, 1940, **21**, 254–263.

37. DIXON, W. E., and MALDEN, W. Colchicine: with special reference to its mode of action and effect on bone-marrow. *J. Physiol.*, 1908, **37**, 50–76.

38. LEBLOND, C. P., and ALLEN, E. Emphasis of the growth effect of prolactin on the crop gland of the pigeon by arrest of mitoses with colchicine. *Endocrinology*, 1937, **21**, 455–460.

39. ALLEN, E.; SMITH, G. M., and GARDNER, W. U. Accentuation of the growth effect of theelin on genital tissues of ovariectomized mice by arrest of mitosis with colchicine. *Am. J. Anat.*, 1937, **61**, 321–341.

40. ASHBY, W. The span of life of the red blood cell: a résumé. *Blood*, 1948, **3**, 486–500.

41. Second United Nations International Conference on the Peaceful Uses of Atomic Energy. Isotopes in Biochemistry and Physiology, Part 2, 1958, **25**.

42. STOHLMAN, F., JR. (ed.) The Kinetics of Cellular Proliferation. Grune & Stratton, New York, 1959, 456 pp.

43. Conference on autoradiography. *Lab. Invest.*, 1959, **8**, 59–333.

44. DONIACH, I., and PELC, S. R. Autoradiographic technique. *Brit. J. Radiol.*, 1950, **23**, 184–192.

45. GRISHAM, J. W. Lobular distribution of hepatic nuclei labeled with tritiated thymidine in partially hepatectomized rats. (Abstract) *Fed Proc.*, 1959, **18**, Part 1, 478.

46. MACDONALD, R. A., and MALLORY, G. K. Life span of liver cells: autoradiographic studies in normal and fatty rat liver. (Abstract) *Am. J. Path.*, 1959, **35**, 690.

47. EDWARDS, J. L. Thymidine incorporation into cells of rat liver during regeneration. (In preparation)

48. HOWARD, A., and PELC, S. R. P^{32} autoradiographs of mouse testis: preliminary observations of the timing of spermatogenic stages. *Brit. J. Radiol.*, 1950, **23**, 634–641.

49. FRIEDMAN, N. B. Cellular dynamics in the intestinal mucosa: the effect of irradiation on epithelial maturation and migration. *J. Exper. Med.*, 1945, **81**, 553–558.

50. BERTALANFFY, F. D. The mitotic activity and cell renewal in the lung. M.Sc. thesis, McGill University, Montreal, 1951.

[*Illustrations follow*]

Legends for Figures

All photomicrographs were prepared from sections stained with hematoxylin and eosin.

Fig. 1. A radioautograph of an ovary and fallopian tube. Patches of ovarian follicular cells are heavily labeled. × 115.

Fig. 2. A radioautograph of seminiferous tubules in cross section. Primary spermatogonia in different segments are either all labeled or not labeled at all. × 750.

Fig. 3. A radioautograph of crypt glands of the small intestine. Distribution of labeled cells is not random. These tend to occur in adjacent pairs or patches. × 300.

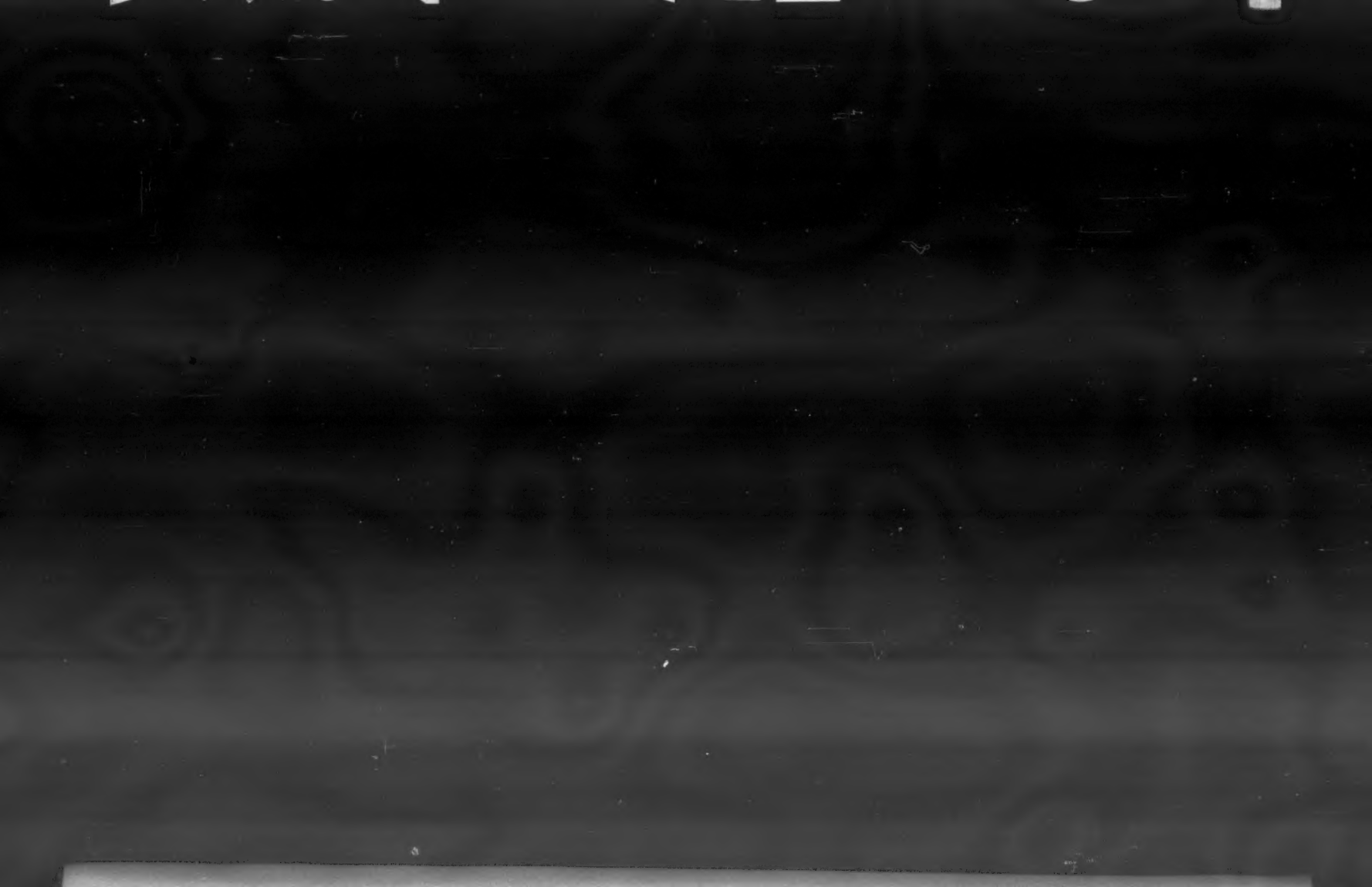

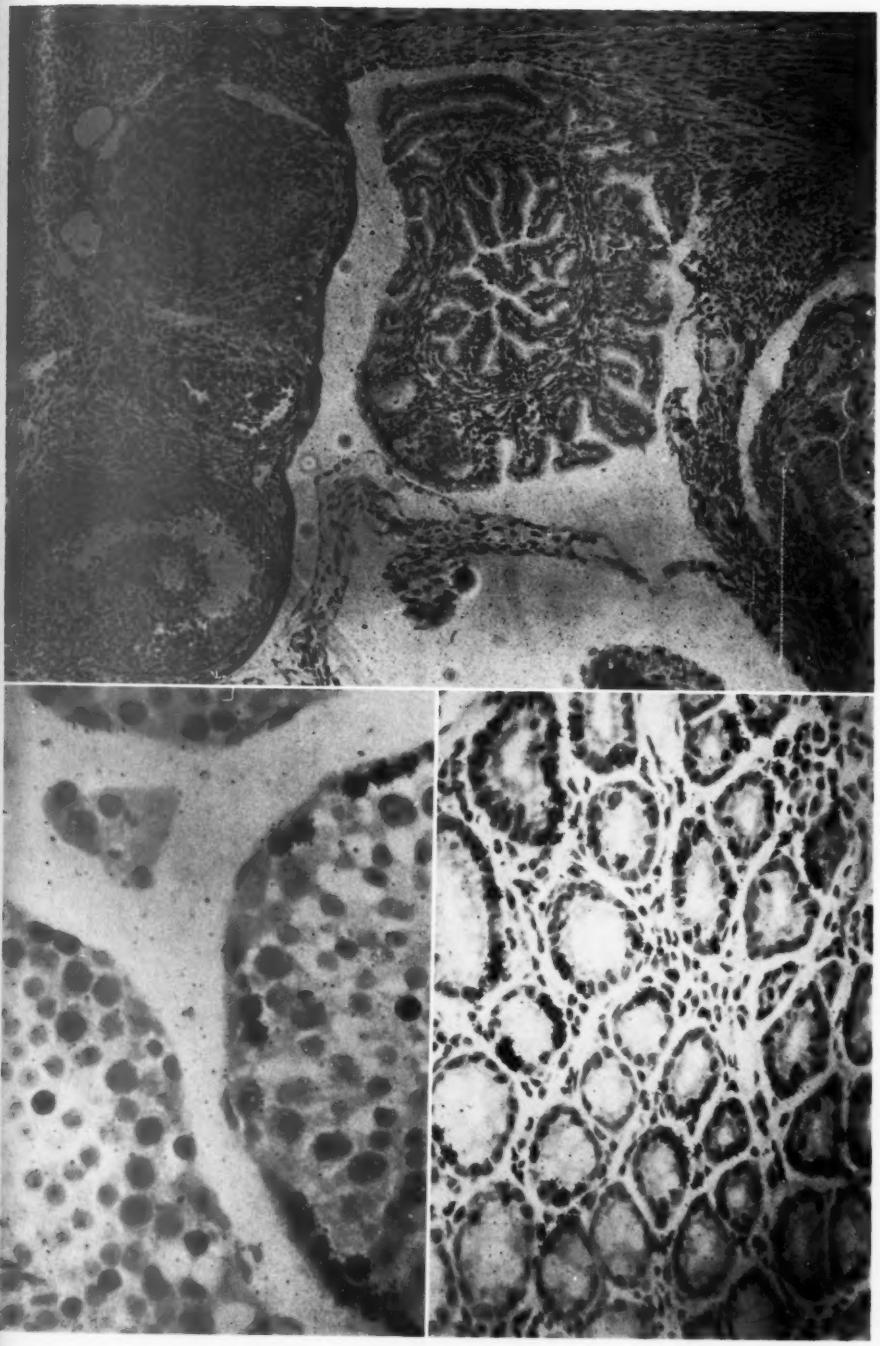

1

2

3

ACUTE DISEASE OF THE SUBMAXILLARY AND HARDERIAN GLANDS (SIALO-DACRYOADENITIS) OF RATS WITH CYTOMEGALY AND NO INCLUSION BODIES

With Comments on Normal Gross and Microscopic Structure of the Exocrine Glands in the Head and Neck of Rats

J. R. M Innes, Sc.D. (Cantab), Ph.D. (Cantab), D.Sc., M.R.C.V.S., and Mearl F. Stanton, M.D.

From the Biology Department, Brookhaven National Laboratory, Upton, L.I., N.Y., and the Laboratory of Pathology, National Cancer Institute, National Institutes of Health, United States Public Health Service, Department of Health, Education and Welfare, Bethesda, Md.

Many papers dealing with disorders of the salivary glands in laboratory rodents have been read; no description has been found of clinical and pathologic features comparable to those recorded in this article. Further, in the course of lecturing (J.R.M.I.) many times in the United States and Great Britain on disease of laboratory animals, slides illustrating the macroscopic and microscopic lesions have been shown to hundreds of workers interested in laboratory animal diseases without any indication that others have recognized the condition.* There are no data on this "new disease" in texts on diseases of laboratory animals.[1] It is thus remarkable that the disorder has been seen on two separate occasions (1957 and 1960), affecting many rats in two institutions hundreds of miles apart, and involving two different commercial strains of

Research carried out at Brookhaven National Laboratory under the auspices of the United States Atomic Energy Commission and the National Institutes of Health, United States Public Health Service.

Accepted for publication, October 13, 1960.

* Since writing this paper, we have learned that two other workers have found the disease in their rat colonies. The first, V. J. Rosen, M.D. (United States Naval Radiological Defense Laboratory, San Francisco) presented us with a section, in which all the changes described by us were found. Later, Dr. Hans Meier (Jackson Memorial Laboratory, Bar Harbor, Maine) intimated in a letter that he had seen the condition. Meier published a letter in *Nature, London* (1960, **188**, 506), on "Spontaneous cytomegalic inclusion-body disease involving lacrimal glands of Caesarian-derived (so-called pathogen-free) rats." He pointed out that all male and female rats from this colony had evidence of inclusion-body disease at 6 months of age. Sections of our material were sent to him. He confirmed our opinion that the sialo-dacryoadenitis bore no resemblance to the cytomegalic inclusion-body disease in rats, nor did there seem to be any etiologic relationship. In some transmission experiments by him with the inclusion body virus, no sialo-dacryoadenitis was produced. He considered that the latter might be induced by an extraneous factor, possibly a toxic chemical. This latter thought was of interest, because in one of our outbreaks the commercial breeder suspected contamination of the food pellets or bedding by ethylene dioxide used in sterilization. However, my (J.R.M.I.) experience of previous years with the chronic exposure of rats to ethylene dioxide in a gassing chamber indicated that "red tears" were common, but no submaxillary gland involvement was ever noted.

rats. The condition has a low mortality and might not be detected in affected animals when alive. Thus the problem is important to workers who pursue transmission experiments in rats, especially with the virus of the cytomegalic inclusion-body disease, for it is impossible to believe the two outbreaks have been the only ones which have occurred. The disease is specific in that the lesions are distinct and easily recognizable, but the cause is unknown. It has some marks of infection. However, any relationship to salivary gland cytomegalic inclusion-body disease encountered in different laboratory species is speculative. The combination of involvement of the submaxillary (but not sublingual or parotid) and the harderian (and not exorbital or intra-orbital lacrimal) glands is an added bizarre feature.

Most of the papers on salivary gland infection of laboratory animals have dealt exclusively with infection by the salivary gland virus group.[2-9] The topic of salivary gland virus disease in human subjects was extensively reviewed by Nelson and Wyatt[10] and is a useful source of directional literature, but there is almost no reference to animals other than investigations concerned with transmission. Much of this work is concerned with cytologic changes in the acinar and duct epithelium, and with the acidophilic intranuclear inclusion bodies rather than pathologic alterations. Host specificity, at least in the case of the salivary gland virus of the guinea pig, seems to be established. In the guinea pig, our experience and that of others indicates that this disorder, under natural conditions, provokes few or no clinical signs, and morphologic changes are generally limited to mild inflammation and intracellular inclusions in the chronically involved salivary glands.[9]

Lyon, Christian and Miller[11] found cytomegalic inclusion bodies in both the intra- and extra-orbital lacrimal glands of adult male rats from 8 separate colonies in the United States; thus, this viral infection is widespread. The infection was mild, and although there was mention of increase in stromal cells and lymphocytic infiltration, the reaction could not have been very intense, for the authors did not stress this or any pathologic aspect of the condition. The salivary glands were not mentioned, so presumably they were not involved; this feature offers the first item that may distinguish the disease described by Lyon and coworkers[11] from the disease described here.

Structure of the Superficial Exocrine Glands of the Head and Neck of the Rat

It is appropriate to refer briefly to the normal anatomy and histologic structure of glands in the head and neck of rats because the facts are not well known except to those whose work has been concerned with

these structures (Figs. 1 to 7). Within the past year, two reports have been brought to our attention in which the exorbital lacrimal gland has been confused with the parotid gland in rodents.

Gross anatomic and histologic differences in the structure of the salivary glands of rats from that in other animals were described in the last century.[12–13] Greene[14] has supplemented these descriptions with modern terminology and excellent diagrams. The paired submaxillary glands of rats are the largest salivary glands. Each gland is a lobulated, encapsulated ellipsoid that is flattened in a dorso-ventral direction. The caudad pole is broader than the cephalad, and the two glands are loosely bound together with connective tissue at the midline. A major sublingual gland is lateral and closely adherent to the cephalad pole of each submaxillary gland. Generally, 4 lymph nodes lie superficial to the two pairs of ventral glands. Lateral to each submaxillary gland is the finely lobulated, uncircumscribed flat tissue of the parotid gland. This may extend laterally from the submaxillary glands to the ear and is partially enveloped by fatty areolar tissue. The latter can be separated from the parotid and is distinguished by its pale white color, in contrast to the gray-pink color of parotid tissue. Well circumscribed lymph nodes may be found also in this region. Lateral to the parotid tissue and just ventral to the ear canal is the encapsulated exorbital lacrimal gland. This is second in size only to the submaxillary gland and can be distinguished from adjacent lymph nodes by this fact; it is also a much darker shade of brown. In location and cell structure, the exorbital lacrimal gland of rodents resembles somewhat the parotid gland of man; hence the confusion sometimes noted in the literature. The remaining pair of intra-orbital lacrimal glands lies at the rim of the bony orbit. They are triangular in shape and similar in color to the exorbital lacrimal glands. Each lies superficial to the bony orbit but immediately adjacent to its more caudad margin.

We could find little information on the normal histologic features of the harderian glands, and nothing on their pathologic anatomy. There is very brief mention in von Möllendorff's text[15] that these structures are more developed in rodents and ruminants (see also Wolff[16]). We could not find any word to denote inflammation of the gland. However, as it is really an accessory lacrimal structure, there is no reason to object to the use of the term "dacryoadenitis" to refer to its inflammation. The harderian glands are yellow-orange in color and occupy much of the orbit deep to the eyeball. The histologic pattern in each gland is briefly described in the legends to Figures 2 to 7.

References to age changes in the parotid glands of rats will be found in Andrew.[17] Appleton[18] referred to the high variability in the size of

the submaxillary glands, not only in untreated control rats of the same sex and litter, but also between the right and left glands. This was also apparent to us after examination of some 40 normal rats.

The Disease

Two separate outbreaks were seen, no whit different from each other from any angle. In the first one, a large number of animals were affected, and over 10 animals were examined at necropsy. In the second outbreak the condition occurred in another strain of rats purchased from another commercial source. Unfortunately, the groups of rats in the second outbreak had been received both in November, 1959, and in January, 1960, and by the time the disease was noticed, the groups had been mixed and some had been treated with whole body x-irradiation. We do not know, thus, whether the condition was present in both groups, whether they acquired it in our own laboratory, or even whether the irradiation had ignited some latent infection brought in or indigenous to our own experimental animals. No rats were bred in our laboratory. Transmission experiments and bacteriologic studies could not be done. There were certainly no deaths in the outbreak in our laboratory, and if any deaths occurred in the first outbreak, they must have been few or had occurred before the condition was detected. No comparable process has been identified in guinea pigs or mice housed in the same animal quarters.

In the well developed stage, the disease was clinically unmistakable. The rats (all immature, noninbred, albino males and females) remained active and seemed to eat well. The neck was grossly swollen, with the head sunk into the neck, so that the rats had the short, hunched head-and-neck appearance of guinea pigs. Many showed "red tears" and red staining around the eyelids due to porphyrin excretion presumably from the harderian glands. The neck was thickened by obviously enlarged submaxillary glands and pronounced edema; both of these combined to produce a "mumps-like" appearance.

Macroscopically, gross gelatinous edema involved the intermandibular space from the front to the base of the neck (in the midst of which lay the swollen, tense submaxillary glands; Fig. 8). Pressure on the great veins entering the thorax caused them to be enormously dilated. All other viscera were normal.

The salivary glands and the harderian glands from a number of affected rats in both outbreaks were examined histologically. Paraffin sections after formol-saline fixation were stained with hematoxylin and eosin, eosin and methylene blue, Lendrum's method, and by the periodic acid-Schiff (PAS) and Giemsa stains.

Histologically, involved submaxillary and harderian glands showed

an acute inflammatory process affecting all parts (Fig. 9). In a few sections the mucin-secreting lobules of the adjacent major sublingual gland were unaffected. The lobules were widely separated from each other by edema and fibrinous exudate; there was infiltration by neutrophils, lymphocytes, histiocytes, and stellate and spindle-shaped connective tissue cells (Figs. 10 and 11). Mast cells were present in small numbers. There was no hemorrhage. The same edematous cellular exudate involved the capsule and the periglandular fat and connective tissue. The parenchyma of the gland was almost unrecognizable. Massive cellular infiltration obscured degenerated alveolar epithelium, but there was no massive necrosis (Fig. 11). Cytologic alterations in the acinar cells were remarkable. The cells and their nuclei were sufficiently enlarged to be considered "cytomegalic." In the many sections studied, however, no inclusion bodies of the types characteristic of salivary gland virus infection could be found in either ductular or acinar epithelium, although some nucleoli were very prominent. The latter may not be unusual in rats of advanced age (see Figs. 7 and 8 in Andrew [17]). There were also remarkable deposits of dense basophilic material in the cytoplasm of the hypertrophied acinar cells. This commonly occurred adjacent to the nuclear membrane or in the basal portion of the cell (Fig. 11). Some degree of this change is normally present in the exorbital lacrimal gland, but it is not observed in the cytoplasm of the submaxillary gland under normal conditions.

One curious feature concerned both the intralobular and interlobular ducts (Figs. 12 and 13). In many areas, their usually well defined columnar epithelium was converted into a mosaic of stratified epithelium that appeared sufficiently extensive to occlude the lumens. This hyperplastic epithelium was not keratinized, and many mitotic figures were present. Some of the parenchymal changes may have resulted from the partial obstruction of these altered intralobular and interlobular ducts. One could postulate, in fact, that the bizarre cytologic alterations might be due to stasis induced by obstruction.

The only other lesion of note was an intense sinus edema and leukocytic infiltration of the regional lymph nodes. This presumably was a phenomenon reflecting drainage from the affected glands.

Why the harderian glands were examined particularly in the first group of affected rats cannot be remembered, except that the production of "red tears" in rats was noted years ago following the administration of different toxic chemical agents. In the rats in both outbreaks an acute inflammatory process also affected the harderian glands (Fig. 12) in the few examined; how frequently this was associated with the acute sialoadenitis is unknown.

Comments

This report is published primarily to draw attention to what we believe to be a new disease of rats. The disorder may be of interest to those in charge of rat colonies or interested in salivary gland virus (cytomegalic inclusion) disease. The cells and nuclei of some degenerated ducts and alveoli were certainly cytomegalic, but beyond this feature any resemblance to the salivary gland virus infection of laboratory rodents ceased. With the possibility in mind that the salivary gland virus still might be at work, and that infection had been introduced from a source of supply of rats, submaxillary glands from a large number of discarded adult breeders (provided by one commercial breeder) were examined; no additional information was forthcoming. However, it is difficult to believe the lesions are anything else but those due to some form of infection.

The metaplastic changes in the epithelium of the ducts and ductules have some similarity to those produced by vitamin A deficiency. However, vitamin A deficiency affects not only salivary glands but many organs.[19] Sections of submaxillary glands of vitamin A-deficient rats from work done many years ago[20] were re-examined with this in mind. Comparison of a gland from a rat, vitamin A-deficient for 3 months, is of interest. There is some resemblance in the parenchymal changes, but the duct alterations are different. In the present disease, metaplasia is complete without keratinization, and ducts are blocked by cell proliferation. In the vitamin A-deficient rat the epithelium shows keratinized metaplastic changes and gross dilation of lumens, perhaps from more distal duct obstruction. To our knowledge, there has been no report of any natural outbreaks of severe chronic vitamin A deficiency in rats. Further, if by chance batches of our pellet diet had been deficient in vitamin A, we would be at a loss to explain why all rats in the same room did not suffer to some degree. Moreover, in each outbreak, there was a sudden upsurge of cases and an equally precipitate disappearance. Furthermore, other manifestations of vitamin A deficiency in different tissues were absent. The same observations hold in the much larger first outbreak which occurred in a colony interbred for commercial rat production and in which thousands of rats of all ages were kept in one room.

To some extent, the appearance of the salivary glands in the present condition was like those at an early stage of ductal obstruction or those in which extracellular destructive phenomena prevented release of the gland secretion. It was totally unlike the progressive atrophy and sclerosis that followed chronic obstruction of major (salivary gland or pancreatic) ducts by stones or after experimental duct ligation.

From the comparative viewpoint the lesions are not without interest. In the colossal tomes written by Duke-Elder,[21] there is a lengthy chapter on conditions of the human lacrimal glands. Here it is stated that acute infection (dacryoadenitis) is very rare in man, and naturally pathologic reports are even more rare. The gland is, however, concomitantly involved in many specific infections, e.g., tuberculosis, syphilis, etc. It is of some moment that Duke-Elder illustrates an altered duct (his Fig. 4707) which shows considerable resemblance to the lesions in rat submaxillary glands.

It may be irrelevant, but Appleton[18] in his studies dealt with the simple hypertrophy of the submaxillary gland following experimental parathyroidectomy. The enlarged gland, other than its increase in actual size, showed no pathologic changes. The enlargement was due to an increase in the volume of individual parenchymal cells. This was estimated by nuclear counts and cell diameters, and by weighing the glands; the weight of the latter was about 0.212 gm. in the normal, and 0.3244 gm. in parathyroidectomized rats.

Summary

Two separate outbreaks of an acute disease (sialo-dacryoadenitis) with low mortality affected the submaxillary and harderian glands of rats. There was a marked swelling of the neck due to enlargement of the salivary glands and inflammation and edema of adjacent areolar tissues. Characteristically, the animals developed "red porphyrin tears" from the harderian part of the complex. Within the submaxillary glands the process was one of acute inflammation with enlargement of parenchymal cells and hyperplasia of duct epithelium but without inclusion bodies. The cause of the disease was not determined, but the inflammatory reaction and epidemic pattern suggested an infectious agent. The condition is distinct from the so-called cytomegalic or salivary gland virus diseases of rodents.

References

1. Cohrs, P.; Jaffé, R., and Meessen, H. Pathologie der Laboratoriumstiere. J. Springer, Berlin, 1958.
2. Cole, R., and Kuttner, A. G. A filterable virus present in the submaxillary glands of guinea pigs. *J. Exper. Med.*, 1926, **44**, 855–873.
3. Thompson, M. J. Intranuclear inclusions in the submaxillary gland of the rat. *J. Infect. Dis.*, 1932, **50**, 162–170.
4. Kuttner, A. G., and Wang, S. H. The problem of the significance of the inclusion bodies found in the salivary glands of infants, and the occurrence of inclusion bodies in the submaxillary glands of hamsters, white mice and wild rats (Peiping). *J. Exper. Med.*, 1934, **60**, 773–791.
5. Kuttner, A. G., and T'ung, T. Further studies on the submaxillary gland viruses of rats and guinea pigs. *J. Exper. Med.*, 1935, **62**, 805–822.

6. HUDSON, N. P., and MARKHAM, F. S. Brain to brain transmission of the submaxillary gland virus in young guinea pigs. *J. Exper. Med.*, 1932, **55**, 405–415.
7. ROSENBUSCH, C. T., and LUCAS, A. M. Studies on the pathogenicity and cytological reactions of the submaxillary gland virus of the guinea pig. *Am. J. Path.*, 1939, **15**, 303–340.
8. SMITH, M. G. Propagation in tissue cultures of a cytopathogenic virus from human salivary gland virus (SGV) disease. *Proc. Soc. Exper. Biol. & Med.*, 1956, **92**, 424–430.
9. COOK, J. E. Salivary-gland virus disease of guinea pigs. *J. Nat. Cancer Inst.*, 1958, **20**, 905–909.
10. NELSON, J. S., and WYATT, J. P. Salivary gland virus disease. *Medicine*, 1959, **38**, 223–241.
11. LYON, H. W.; CHRISTIAN, J. J., and MILLER, C. W. Cytomegalic inclusion disease of lacrimal glands in male laboratory rats. *Proc. Soc. Exper. Biol. & Med.*, 1959, **101**, 164–166.
12. RANVIER, L. Étude anatomique des glandes connues sous les nommes de sous-maxillaire et sublinguale, chez les mammifères. *Arch. de physiol.*, 1886, Ser. 3, **8**, 223–256.
13. LOEWENTHAL, N. Zur Kenntnis der Glandula submaxillaris einiger Saeugetiere. *Anat. Anzeig.*, 1894, **9**, 223–229.
14. GREENE, E. C. Anatomy of the Rat. Hafner Publishing Co., Inc., New York, 1955, 370 pp.
15. LAUBER, H. Die Tränenorgane (Org. lacrimalia). In: Handbuch der mikroskopischen Anatomie des Menschen. Von Möllendorff, W. (ed.) J. Springer, Berlin, 1936, Vol. 3, part 2, pp. 582–601.
16. WOLFF, E. The Anatomy of the Eye and Orbit, Including the Central Connections, Development and Comparative Anatomy of the Visual Apparatus. H. K. Lewis, London, 1948, ed. 3, pp. 410–412.
17. ANDREW, W. Age changes in the parotid glands of Wistar Institute rats with special reference to the occurrence of oncocytes in senility. *Am. J. Anat.*, 1949, **85**, 157–197.
18. APPLETON, J. L. The hypertrophy of the submaxillary gland in the albino rat, following parathyroidectomy. *Am. J. Path.*, 1925, **1**, 217–223.
19. FOLLIS, R. H. Deficiency Disease. Charles C Thomas, Springfield, Ill., 1958, ed. 2, pp. 126–140.
20. HARRIS, L. J.; INNES, J. R. M., and GRIFFITH, A. S. On the pathogenesis of avitaminosis A; vitamin A as an antikeratinizing factor. *Lancet*, 1932, **2**, 614–617.
21. DUKE-ELDER, S. Textbook of Ophthalmology. Vol. 5, The Ocular Adnexa. C. V. Mosby Co., St. Louis, 1952, pp. 5214–5234.

Thanks are due to Mr. R. F. Smith, Photographic Department, Brookhaven National Laboratory for preparation of the photographs in Figures 8 to 14. Figures 1 to 7 were prepared in the National Cancer Institute.

LEGENDS FOR FIGURES

Photomicrographs were prepared from sections stained with hematoxylin and eosin.

FIG. 1. Anatomy of the major exocrine glands of the neck, male rat, strain Osborn-Mendel, age 12 months. Ventral view, showing the lobulated submaxillary gland (SM), the major sublingual gland (SL), the parotid gland (P), the exorbital lacrimal gland (E), and lymph nodes (N). × ½.

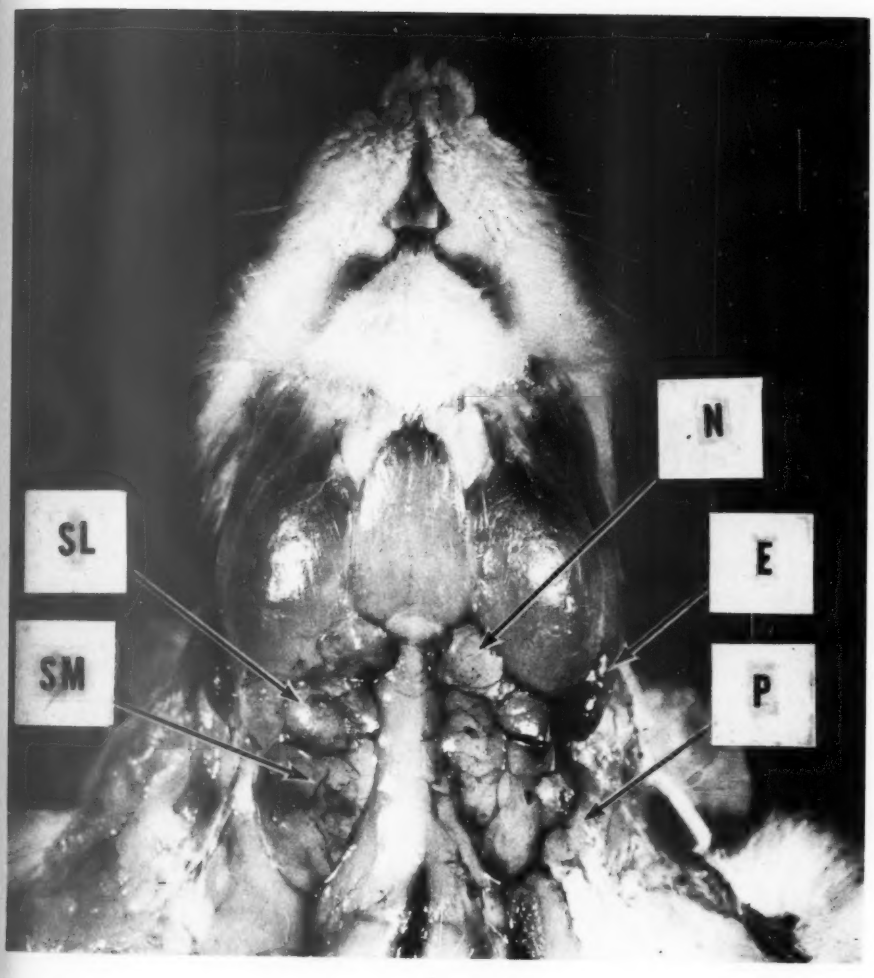

1

FIG. 2. Submaxillary gland. The serous cells of the acini contain a granular basophilic cytoplasm and basally placed chromatin-filled nuclei. The ducts are lined by columnar cells with basal striae and intensely eosinophilic cytoplasmic globules. × 340.

FIG. 3. Sublingual gland. The acini are composed of pyramidal-shaped, mucin-secreting (clear) cells with flattened basal nuclei. The intralobular ducts are lined by columnar cells with eosinophilic striated cytoplasm. × 340.

FIG. 4. Parotid gland. The acinar serous cells are smaller than those in the submaxillary gland and contain a more intensely basophilic cytoplasm that is basally striated and filled with chromophilic granules. The intralobular ducts are lined by striated, eosinophilic columnar cells. × 340.

FIG. 5. Harderian gland. The tubulo-alveolar gland is often confused histologically with the salivary and lacrimal glands. The acini are composed of tall clear cells with vacuolated fat-filled cytoplasm, and with much variation in nuclear size. The lumens of acini and ducts contain deposits and laminated concretions of golden brown pigment not shown in the picture. Ducts are lined by a pseudo-stratified epithelium. × 340.

FIG. 6. Exorbital lacrimal gland. A tubulo-alveolar gland like the major salivary glands, and rather similar to the parotid gland. The acinar cells are much larger, and the nuclei range in shape and size from small ovoid to multilobulated structures which occasionally show mitosis. Note some vacuolated nuclei, a common finding in the lacrimal acinar cells. Intralobular ducts are lined by flattened cuboidal epithelium. × 340.

FIG. 7. Intra-orbital lacrimal gland. The gland is identical in structure to that of the exorbital lacrimal gland. However, this section illustrates the degree of artifactual atypism which may occur in a gland left unfixed for 4 hours after death. Such changes have led to the mistaken identification of this gland as a tumor. × 340.

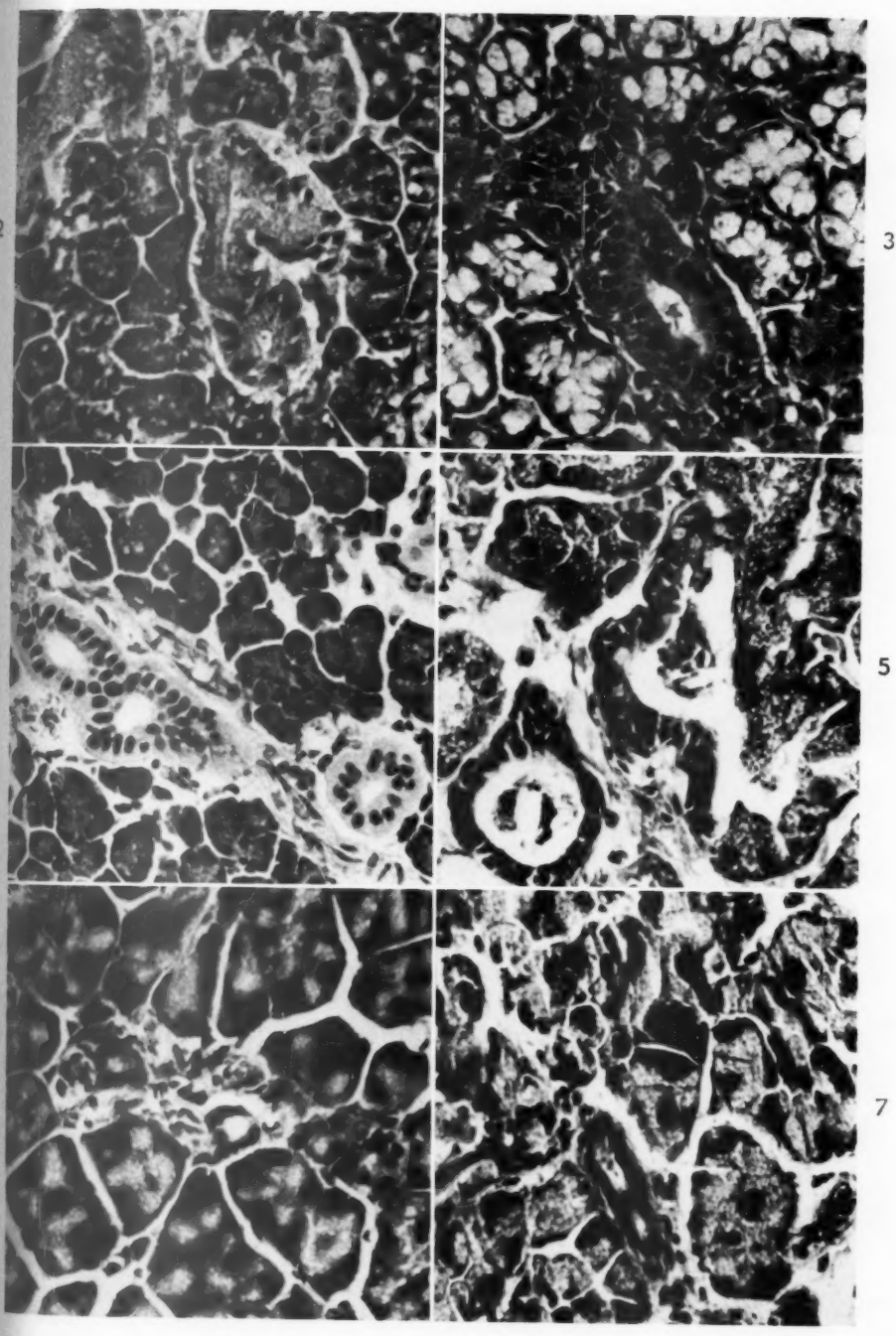

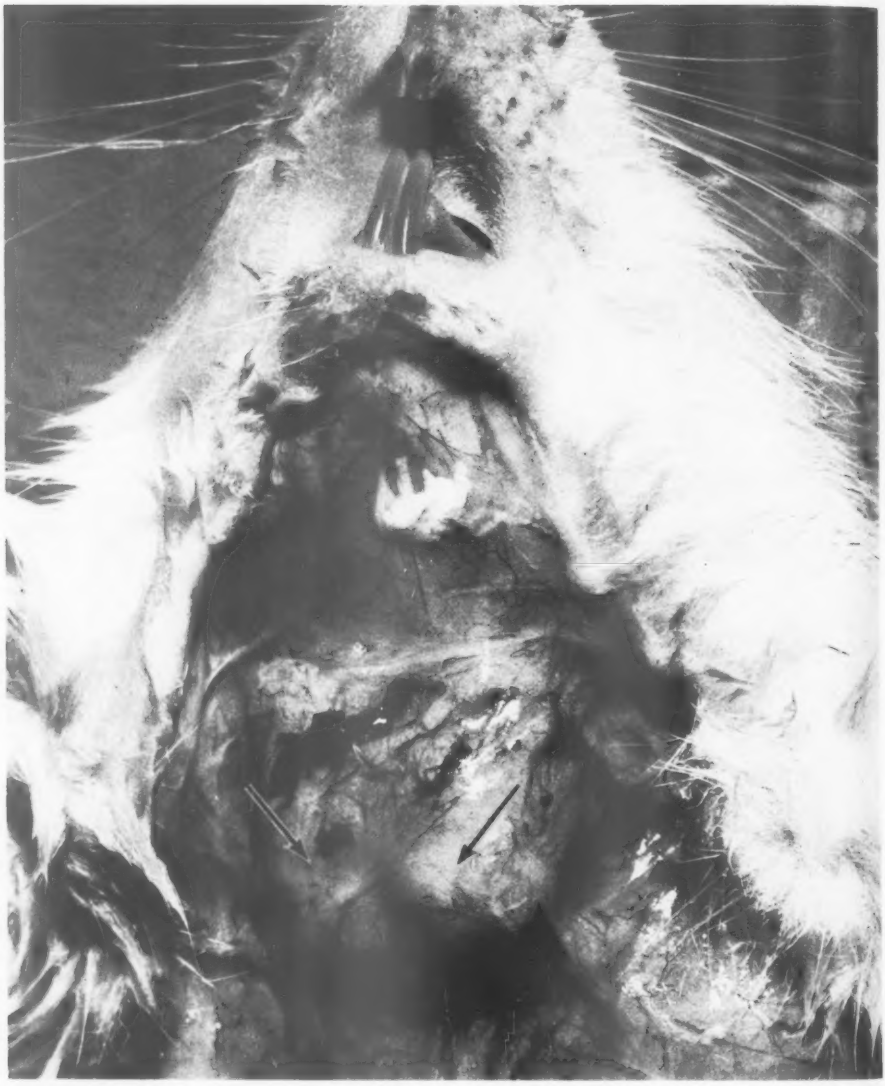

FIG. 8. Macroscopic appearance of the under jaw, showing edematous change and swelling of the submaxillary glands (arrows), lymph nodes, and interstitial tissues of a severely affected rat. Compare with Figure 1.

FIG. 9. Sialoadenitis, submaxillary gland. There is gross interlobular edema and inflammatory reaction; ducts (see Fig. 13) stand out as dark streaks. × 25.

FIGS. 10 and 11. Affected submaxillary glands (two separate outbreaks), showing diffuse inflammatory edema and cellular reaction. × 100.

FIG. 12. Affected harderian gland showing degenerating acini and interstitial inflammatory reaction. × 100.

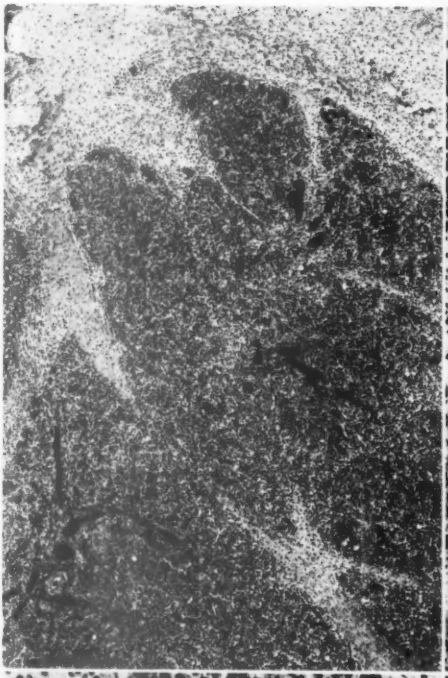

9

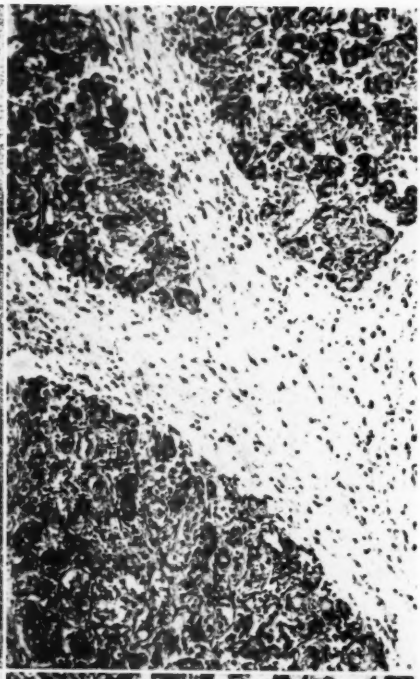

10

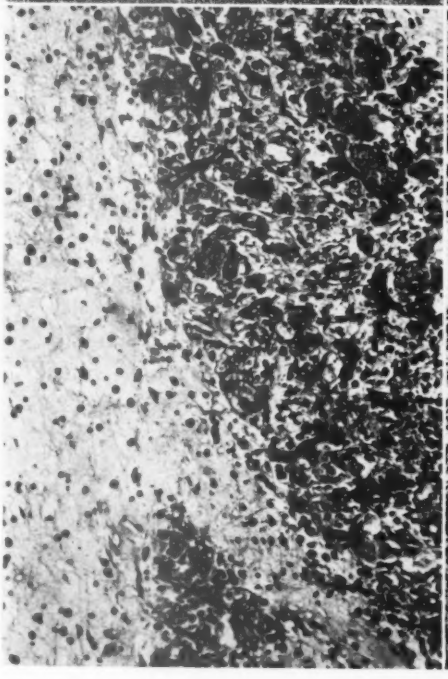

11

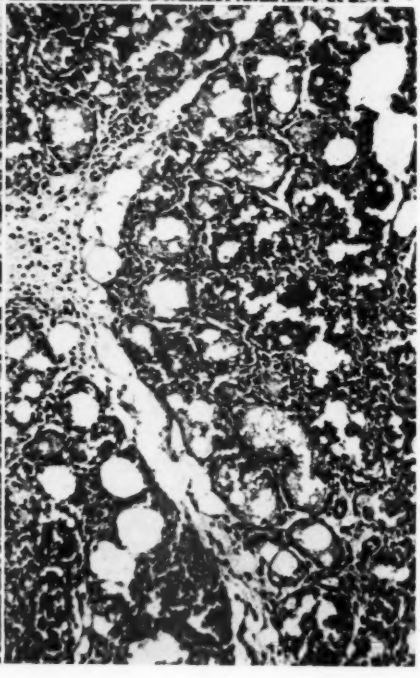

12

13

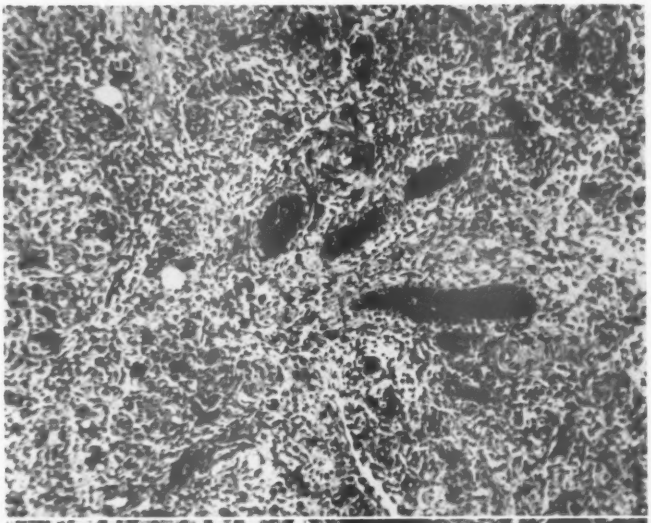

14

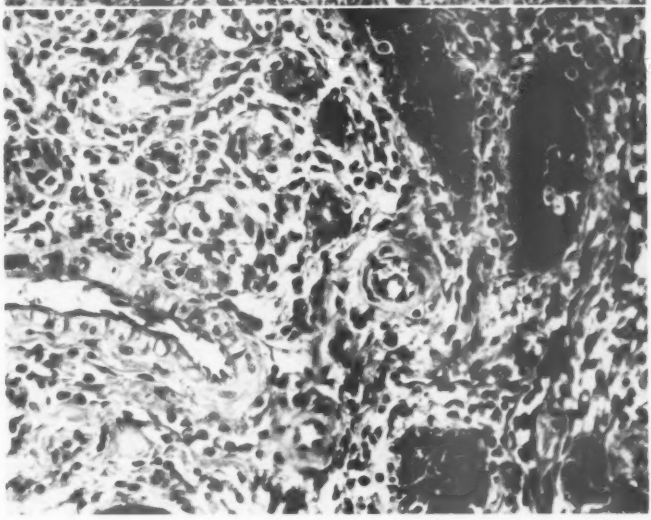

FIGS. 13 and 14. Affected submaxillary gland, showing degenerated and hypertrophied acinar cells and nonkeratinizing proliferation of duct epithelium with consequent blockage. Fig. 13, × 200; Fig. 14, × 400.

EXPERIMENTAL ANTHRAX IN THE RAT

I. The Rapid Increase of Natural Resistance Observed in Young Hosts

Martha J. Taylor, A.B.; George H. Kennedy, A.B.,*
and George P. Bundell, M.D.†

From the United States Army Chemical Corps Biological Laboratories, Fort Detrick, Frederick, Md.

The degree of natural resistance of an individual host to infectious disease reflects both the genetically determined development of cellular and humoral defense mechanisms and the responses of these mechanisms to a variety of experiences. Thus, it is generally true that mature hosts have greater resistance to many infectious organisms than do immature members of the same species. A measure of the rate of increase in resistance following birth, and of the age at which a high level of resistance is attained for any given host-parasite system, should provide useful information in the continuing search for host mechanisms that contribute to adult resistance. Few, if any, investigations have supplied data adequate for calculating such a rate over any extensive period after birth.

There are published reports that correlate the increasing age of the rat with its resistance to a wide variety of pathogens.[1–7] In 1890 Charrin and Roger [8] reported that the resistance of the white rat to infection with *Bacillus anthracis* varied with the age and weight of the host. This organism is unusually convenient for long-term studies because of its easily stored, relatively stable, highly virulent spores. Furthermore, the remote likelihood that specific immunity to anthrax would be acquired by chance encounter with the anthrax bacillus is advantageous.

Preliminary experiments, employing relatively wide variations in both age of host and dose of spores, indicated that *B. anthracis* and the albino rat might constitute a useful host-parasite system for the study of natural resistance. This paper reports an investigation of dose-age relationships in maturing rats. Survival values and hours between injection and death were determined for a number of litters of the genetically homo-

Presented in part at the Fifty-fifth Annual Meeting of the American Association of Pathologists and Bacteriologists, April 24, 1958, Cleveland.

Accepted for publication, December 9, 1960.

* Present address: Research Grants Branch, National Cancer Institute, National Institutes of Health, Bethesda, Md.

† Present address: Oscar B. Hunter Memorial Laboratory, 915 19th St., N.W., Washington, D.C.

geneous Fischer rat tested at 1 to 40 days of age with different numbers of spores. An average rate of increase in resistance was calculated from probit regression analysis estimates of the ages at which each dose level corresponded to 50 per cent survival. The data have been examined for certain host factors in addition to age that might have influenced survival.

Material and Methods

Breeding and Care of Hosts

Four pedigreed litters (filial generations 62 and 63) of the Fischer 344 strain of albino rat were obtained in 1957 from the Division of Research Services, National Institutes of Health, through Dr. George E. Jay, Jr. The system of brother by sister mating was continued for our colony. Filial generations 63, 64, 65, and 66 contributed the test rats for these experiments. Beginning with matings in generation 65, all animals of the same filial generation were derived from 1 brother-sister pair 3 generations earlier. Parentage, date of birth, sex, and weight at the time of injection for every rat were recorded.

Although there was no attempt to raise "pathogen-free" rats, certain precautions were observed: (1) Ultraviolet-lighted air locks separated the breeding room from laboratories and from rooms that held experimentally infected animals. (2) Ultraviolet lights burned continuously in the breeding room. (3) Other rats were excluded from the building, and other species from the rat rooms. (4) Human contact was restricted. Individuals working with the rats showered after handling other species, and dressed in freshly laundered clothes before entering the rat rooms. Purina Laboratory Pellets for Rats and tap water were available *ad libitum* to animals of all ages. Sucklings which had been inoculated were nursed by their mothers until death, or until they survived at least 2 weeks. Litters in the group tested with 10^7 spores were weaned on the day before injection, at 19 to 29 days of age. All others were weaned at 28 days.

Groups of Hosts

Four large groups of litters, for testing with 10^4, 10^7, 10^8, or 10^9 spores, were selected to provide ranges in age which responded with low through high survival per cents for each of these 4 doses. Two smaller groups were used to check responses of rats whose ages ranged between 10 and 20 days to doses of 10^5 and 10^6 spores. The age of rats at the time of inoculation was usually known to within 12 hours, always to within 24. There were nearly equal numbers of males and females in all except the oldest group plotted in Text-figure 1.

Pathogen, Dose, Injection Route

All spore inoculums were harvested from a single culture of a highly virulent strain of *B. anthracis*. This culture was prepared from the same parent stock as that used by Roth, DeArmon and Lively.[9] This stock is known as the 1B sib-progeny of the Vollum strain. The concentrated spore suspension, which contained 1 per cent phenol, was diluted 1/10 in distilled water, heat-shocked at 60° C. for 30 minutes, and stored in the refrigerator. (Viable counts varied between 7×10^9 and 9×10^9 per ml. during the experimental period.) The suspension was subjected to 3 types of tests to characterize its virulence: (a) the LD_{50} by intradermal route for guinea pigs, (b) the proportion of smooth (capsule-forming) colonies,[10] (c) the median survival time for mice inoculated intraperitoneally.[9] All responses were characteristic of highly virulent populations. The stock suspension was diluted in distilled water to the concentration required for the test. Each inoculum was counted for viable spores within 24 hours of injection, and did not differ from the intended dose by more than 20 per

cent. All doses, given in a volume of 0.1 ml., were injected either subcutaneously or intradermally. On the average, 3 independent tests were run for each combination of dose and age.

Time to Death

Inspection at 12 to 18 hours after injection revealed that all animals were alive and eating well. Frequent subsequent surveys insured a record of time to death that was accurate to plus or minus 6 hours.

Diagnosis

The first 366 rats that died were necropsied. The cut surfaces of liver, spleen, or subcutaneous edema at the inoculation site were touched to glass slides. The slides

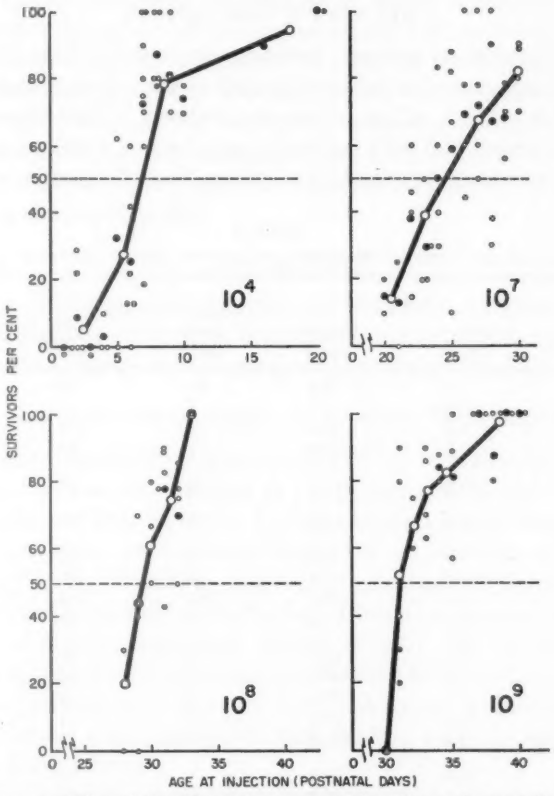

TEXT-FIGURE 1. The relationships between age at injection and proportion of Fischer rats surviving the indicated numbers (10^4, etc.) of spores of *B. anthracis*. The curves are drawn through points (large circles) obtained by combining data from litters of similar ages, and plotting per cent survivors at the mid-point of the ages of those litters combined. There were nearly equal numbers of males and females tested for each of these points except one. In the group plotted at 38.5 days and tested with 10^9 spores, there were 5 males and 35 females. If ages of combined litters differed by more than 24 hours, the per cent of survivors within each 24-hour group is shown by closed circles. The extent of variability among litters is indicated by small circles—one for each litter.

were then placed in 10 per cent formalin (phosphate-buffered at pH 7) overnight, washed in running water, air-dried and stained with the Jenner-Giemsa stain. Microscopic examination consistently revealed short chains of large, square-ended, thick-walled, encapsulated bacilli, morphologically characteristic of *B. anthracis* in tissue. Tissues from more than 200 of the same rats were streaked on plates of Difco blood agar base enriched with 5 to 7 per cent whole, fresh rabbit blood. Colonies characteristic of the injected organism were always recovered, usually in pure culture. Because of these consistent results, and the rarity of spontaneous deaths in the rat colony, necropsy and culture were discontinued. Death between 18 hours and 1 week following injection of spores was subsequently considered sufficient evidence of specific infection.

Results

Age and Per Cent Survival

The relationships between injection age and per cent survival for groups of rats of similar ages within each of the 4 large groups of litters tested with 10^4, 10^7, 10^8, or 10^9 spores are shown in Text-figure 1. These results indicated that with increasing age the rats rapidly acquired the ability to survive larger numbers of spores. From the graphs, 50 per cent

Table I

AVERAGE WEIGHTS AND NUMBERS OF FISCHER RATS FOR THE GROUPS PLOTTED IN TEXT-FIGURE 1

Log of spore dose	Age * (days)	Weight † (gm.)	No. of litters tested	No. of individuals	
				Tested	Surviving
4	2.5	6.7	10	97	5
	5.5	9.7	8	72	20
	8.5	12.6	18	170	133
	18.0	25.8	2	18	17
5	12.5	19.3	5	48	29
6	16.5	23.9	8	75	55
7	20.5	31.2	4	35	5
	23.0	35.4	12	120	47
	27.0	50.5	19	174	117
	30.0	62.4	4	39	32
8	28.0	57.8	2	15	3
	29.0	58.9	4	34	15
	30.0	62.9	3	18	11
	31.5	70.9	9	71	53
	33.0	74.8	1	10	10
9	30.0	62.0	1	10	0
	31.0	70.7	5	50	26
	32.0	74.9	2	18	12
	33.0	80.8	4	35	27
	34.5	83.0	5	40	33
	38.5	92.4	7	40	39

* Mid-point of injection ages represented. For days included, when more than one, see closed circles, Text-figure 1.

† Average weight per rat at injection.

survival would be expected when 10^4 spores are administered to 7-day-old rats, 10^7 spores to 24.5-day-old rats, 10^8 spores to 29.25-day-old rats, and 10^9 spores to 31-day-old rats. Additional information regarding these groups is recorded in Table I.

Rate of Resistance Increase

The methods of probit analysis [11] were used to compute the age at injection corresponding to 50 per cent survival for the dose used to challenge each of 6 groups of rats. The computed ages are plotted in Text-figure 2 against the log of the number of spores administered. These points were weighted for the unequal numbers of litters tested with each dose, and a straight line was fitted * to them for the interval from day 5.8 (10^4) to day 31.3 (10^9). The antilog (1.5) of the slope of this line estimates the average rate of increase in resistance during this interval. Thus, for each day of increasing age from 5.8 to 31.3 days, the 50 per cent survival level corresponded to 1.5 times the number of spores administered the previous day.

Time to Death

Animals of all ages died promptly (96 per cent in 72 hours, 99.8 per cent by the end of one week). With one exception, the deaths that occurred under 24 hours were in the groups of younger animals.

Variations Among Litters in Replicate Experiments

When litters the same age were tested with the same number of spores, there was considerable variation in the proportions of each litter that died of anthrax (Text-figure 1). Known variables among these genetically uniform litters were average weight per rat, numbers of each sex, age of mother at parturition, different preparations of inoculums, and degree of infestation with pinworms and of infection with an unidentified agent(s) of chronic respiratory disease (CRD). The severity of the CRD and pinworm infestation was not recorded for individuals or litters, but both conditions were observed to be widespread in the colony. Records did permit a compilation of data dealing with the other known variables listed above.

Weight. The close correlation between weight and age in the period of rapid growth makes it difficult to distinguish between their separate influences on increase in resistance. Table I shows the relationship between weight and age in the Fischer rat. Instances in which weight does

* Method of least squares. Equation: $Y = 2.77 + 0.1823X$, where $Y =$ log of dose corresponding to 50 per cent survival, and $X =$ age at injection in days.

not correlate with per cent survival follow:

(1) Within each dose group, the average weight per rat for each litter was calculated and plotted against per cent survival. No correlation could be detected between heavy litters and high per cent survival unless the heavy litters were also older. The responses and distribution

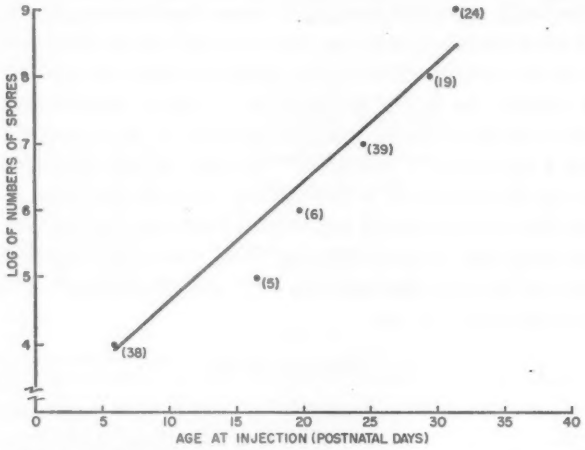

TEXT-FIGURE 2. Relationship, at 50 per cent survival for each dose group, between numbers of *B. anthracis* spores and injection age of Fischer rats. Each plotted point (obtained by regression analysis of probit per cent survival on age of all litters that were tested with each dose) was weighted for the number of litters, and the straight line fitted by the method of least squares. Numbers of litters are in parentheses. See text for further details, including use of the equation for this line to estimate the average rapidity of increase in resistance over this period.

of weights of litters included in the 10^7 dose group made possible the examination of the effect of age without regard to weight on the per cent survival of the 20 litters weighing between 25 and 45 gm. Again, the importance of age in determining response to challenge is apparent (Text-figure 3).

(2) A comparison of the weights of survivors with the average weight per rat for the litter revealed that among 94 litters there were 6 litters in which all survivors were average or below average weight, 85 litters in which the survivors were both above and below average weight, and 3 litters in which all survivors were average or above average weight. Furthermore, there was no correlation between time to death and heavy or light individuals within a litter.

(3) Table II presents several instances of closely equivalent average weights for groups of male and female litter mates with differences in

proportions of survivors varying from plus 21 to minus 37 per cent. These differences may or may not be due to sex, but they certainly are not due to weight.

Sex. The data for comparison of per cent survival among males and females (Table III) are from tests of each litter that fulfilled the following requirements: (a) The age-dose combination was one for which the

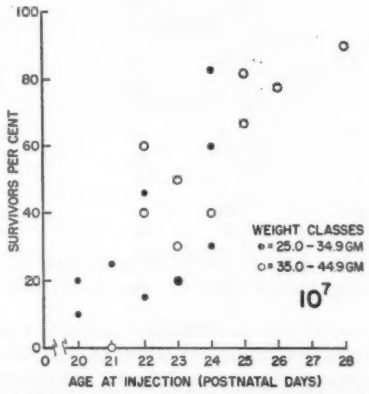

TEXT-FIGURE 3. Relationships of age at injection to per cent survivors among litters of closely similar weights (average weight per rat at time of injection).

average survival had been observed to be 10 to 90 per cent; (b) no less than 10 and no more than 90 per cent survived; and (c) at least two of each sex were included. Within each dose group, the data were combined from litters of similar age. It is concluded that (a) the expected correlation occurred within each sex between age and increase in per cent survival; (b) different sex ratios among litters the same age could not account for the observed variation among litters in survival per cent; and (c) statistically significant (chi-square) difference in response can be correlated with sex only among rats more than 4 weeks old at injection, at which time a larger proportion of females survived. This means that sex must be controlled in testing rats 4 weeks old or older, although when survival is high for both sexes, a difference need not show up (Table III, 10^9 dose).

Age of Mother. All litters were identified by age of mother at parturition. Table IV summarizes the number of litters, by mother's age, for which the per cent survival fell either below or above the average curves in Text-figure 1. No differences could be related to ages at parturition of 3 through 8 months. The number of litters with 9- to 13-month-old mothers was too small to render their superior survival values significant.

TABLE II

INJECTION WEIGHTS COMPARED WITH PER CENT SURVIVORS AMONG GROUPS OF FISCHER RATS INJECTED WITH SPORES OF *B. anthracis*

Group: Log of spore dose	Age * (days)	No. tested		Average wt. (gm.)	Survivors (%)
4	5.5	M	25	10.1	48
		F	30	9.4	27
		Difference		+0.7	+21
7	21.5	M	57	34.8	37
		F	55	33.3	24
		Difference		+1.5	+13
8	29.5	M	16	60.8	38
		F	23	58.8	61
		Difference		+2.0	−23
8	31.5	M	32	75.6	63
		F	29	68.5	86
		Difference		+7.1	−23
9	31.5	M	31	82.4	36
		F	37	72.1	73
		Difference		+10.3	−37

* Mid-point of injection ages for groups in Table III which showed a difference between per cent survivals of males and females.

TABLE III

COMPARISON OF SURVIVAL OF MALE AND FEMALE FISCHER RATS INJECTED WITH SPORES OF *B. anthracis* AT DIFFERENT AGES

Log of spore dose	Age * at injection (days)	No. tested: Litters †	M	F	Total	Survivors (%): M	F	Total	Chi square	P ‡
4	5.5	6	25	30	55	48	27	36	2.85	0.053
	7.0	6	28	28	55	39	64	62	0.15	
	9.0	5	23	25	48	78	72	75	0.22	
7	21.5	11	57	55	112	37	24	30	2.33	0.125
	25.0	10	46	47	93	54	58	56	0.86	
	28.5	11	52	53	105	64	64	64	0.01	
8	29.5	4	16	23	39	38	61	51	2.05	0.150
	31.5	7	32	29	61	63	86	74	4.41	0.035
8 §	30.5	11	48	52	100	54	75	65	4.79	0.029
9	31.5	7	31	37	68	36	73	56	9.30	0.002
	34.0	8	33	36	69	76	81	78	0.21	

* Mid-point of different ages represented.

† See text for bases for choosing the included litters.

‡ The probability that the observed proportions are no more different than could have occurred by chance, from those expected if males and females survived in the same proportions as the total population.

§ Data in this line are the result of combining the two preceding lines.

TABLE IV

NUMBERS OF LITTERS WITH BELOW- OR ABOVE-AVERAGE * PER CENT SURVIVAL (FOR THE PARTICULAR AGE-DOSE COMBINATION), CLASSIFIED BY AGE OF MOTHER AT PARTURITION

Age of mother at parturition (mo.)	Number of litters with per cent survivors	
	Below average	Above average
3	23	26
4	8	2
5	5	9
Total	36	37
6	5½ †	5½
7	8	7
8	3	3
Total	16½	15½
9	1½	4½
10	1½	3½
11	0	1
12	0	2
13	0	1
Total	3	12

* Here defined as falling below or above the lines drawn through the open circles on Text-figure 1.

† One-half used when a litter's response coincided with the average.

The observed trend, however, was above the average survival for litters from older mothers.

Inoculums. The ±20 per cent variation in viable spore counts among replicate dilutions of inoculums did not correlate with variations in survival responses. Experiments with above-average counts gave high survival as often as did experiments with below-average counts, and vice versa.

DISCUSSION

A rapid increase in the resistance of Fischer rats to spores of *B. anthracis* has been demonstrated during the first 40 postnatal days. This increase in resistance, as measured by per cent survival of 1- to 40-day-old rats after injection with differing numbers of spores, appears to be primarily an age-related phenomenon. Between ages 5.8 and 31.3 days the average rate of increase in resistance was estimated to be 1.5-fold per day. For the period between 10 and 20 days, the responses of the 13 litters tested on 10^5 or 10^6 spores confirmed a continuing increase in resistance between the ages of 5.8 and 24.5 days. The data are not sufficient to ascertain whether the rate during this age period is the same as the over-all average. Likewise, there were insufficient data to determine a rate for the observed increase in resistance from birth to 6 days, or after 31 days. It is of interest to note that Whitman,[12] studying yellow

fever in Swiss mice, demonstrated an age-correlated rate of resistance increase.

The high resistance exhibited by the adult laboratory rat for a miscellany of pathogens has usually been reported as being attained by age 21 to 30 days.[1–7] Unfortunately, high resistance means only that the animal is resistant to the highest practicable dose of the micro-organism in question. Full resistance to 10^9 spores of *B. anthracis* Vollum 1B injected intradermally appeared in females of the Fischer strain by the 40th postnatal day.[13] (Only 5 males were available for this oldest test group of 40 rats whose average age was 38.5 days.) The oldest group in which there were equal numbers of each sex averaged 34.5 days old and had a survival value of 83 per cent. A larger dose, another injection route, and equal numbers of each sex in the test group might reveal that Fischer rats are not fully resistant at age 40 days.

In spite of the close correlation between age and weight, there is good reason to believe that increase in resistance of the rat is not primarily related to weight (Text-figure 3 and Table II). Recently, studies with the germ-free rat demonstrated that increased weight does not enable 5-week-old rats to survive injection with anthrax spores.[14] Moreover, among species highly susceptible to anthrax, body weight as such bears no relationship whatsoever to lethal dose. The LD_{50} of intradermally or subcutaneously injected spores is approximately the same for adult albino mice, grasshopper mice, hamsters, guinea pigs, and rabbits.[15]

While it has been demonstrated that resistance of the rat to *B. anthracis* challenge does increase rapidly with age, the basic mechanisms involved in this phenomenon have not been investigated. One can only speculate on the possible importance of such factors as spontaneously occurring CRD, contact with other aerobic, spore-forming bacilli known to have antigens in common with the anthrax organism, and the little-understood processes of physiologic and morphologic maturation. Certain important stages in the maturation of the reticuloendothelial system of the rat have been reported,[16–19] and are compatible in time with the responses reported in this investigation.

Furthermore, the variations in response of individuals within a given litter, and among litters the same age, could not be related to sex, weight, or slight variations in spore doses when examined by multiple probit regression analysis,[11] and are without explanation. The possible effects of the age of the mother, and variations in protection afforded to suckling littermates by mothers' milk are suggested by reports of work using different host-parasite systems.[20–22]

Despite the paucity of information regarding the mechanisms involved, the responses over the age range reported are sufficiently pre-

dictable to indicate that the Fischer rat and *B. anthracis* may be useful as a standard testing system in which to evaluate factors that alter the resistance of the host or the virulence of the pathogen. Caution should be exercised regarding extrapolation from the data reported to untested age-dose combinations and routes of infection.

Summary

Responses have been determined for the genetically uniform Fischer 344 strain of albino rat, at different ages, to graded doses of the highly virulent Vollum 1B strain of *Bacillus anthracis*.

A rapid increase in resistance was related to age within each of 4 groups tested with appropriate doses. When the age at injection was increased by 4 to 10 days, the proportion of survivors at each dose level rose from less than 20 to more than 80 per cent.

Calculation of an average increase in resistance revealed that for every 1-day increase in injection age from the sixth through the 31st day, an increment of 1.5-fold in spore dose was required to maintain 50 per cent mortality.

The data were examined for possible influence on survival of the factors of age, weight, and sex of host, and of age of mother at parturition. No differences in per cent survival between litters could be related to mothers' age at parturition of 3 through 8 months. No significant differences between the responses of males and females were noted among animals tested during the first 4 weeks of life, but among animals tested during the 5th week, females exhibited a significantly higher per cent survival. Evidence was presented that indicated that increasing weight does not account for the increasing resistance between 1 and 40 days of age.

It was suggested that the information obtained provides a reliable basis for selecting useful age-of-host and dose-level combinations to screen various factors for their influence upon the virulence of the bacillus or upon the resistance of the rat.

References

1. Findlay, G. M., and Howard, E. M. The transmission of neurotropic yellow fever virus to rats. *Ann. Trop Med.*, 1951, **45**, 220–222.
2. Findlay, G. M., and Howard, E. M. The susceptibility of rats to encephalomyocarditis viruses. *Brit. J. Exper. Path.*, 1951, **32**, 569–572.
3. Duffy, C. E., and Sabin, A. E. Behavior of St. Louis encephalitis virus in rats. (Abstract) *J. Bact.*, 1942, **43**, 88–89.
4. Duffy, C. E. Japanese B encephalitis in the rat. *Proc. Soc. Exper. Biol. & Med.*, 1951, **76**, 566–569.
5. Meyer, H. M., Jr., and Duffy, C. E. Age susceptibility pattern of the rat to

epidemic keratoconjunctivitis virus. *Proc. Soc. Exper. Biol. & Med.*, 1953, **82**, 751–754.

6. Ross, V. Oral immunization against pneumococcus types II and III and the normal variation in resistance to these types among rats. *J. Exper. Med.*, 1931, **54**, 875–898.
7. Lainson, R. Toxoplasmosis in England. II. Variation factors in the pathogenesis of Toxoplasma infections; the sudden increase in virulence of a strain after passage in multimammate rats, and canaries. *Ann. Trop. Med.*, 1955, **49**, 397–416.
8. Charrin, A., and Roger, G. H. Contribution à l'étude expérimentale du surmenage; son influence sur l'infection. *Arch. physiol. norm. et path.*, 1890, **2**, 273–283.
9. Roth, N. G.; DeArmon, I. A., Jr., and Lively, D. H. Survival time as a rapid method of determining virulence with *Bacillus anthracis*. *J. Bact.*, 1956, **72**, 666–672.
10. Thorne, C. B. Capsule Formation and Glutamyl Polypeptide Synthesis by *Bacillus anthracis* and *Bacillus subtilis*. In: Bacterial Anatomy, Sixth Symposium of the Society for General Microbiology, held at the Royal Institution, London, 1956. Cambridge University Press, Cambridge, 1956, pp. 68–80.
11. Finney, D. J. Probit Analysis; a Statistical Treatment of the Sigmoid Response Curve. Cambridge University Press, Cambridge, 1952, ed. 2, 318 pp.
12. Whitman, L. A modified intraperitoneal protection test for yellow fever based on the greater susceptibility of immature white mice to the extraneural injection of yellow fever virus. *Am. J. Trop. Med.*, 1943, **23**, 17–36.
13. Taylor, M. J.; Kennedy, G. H., and Blundell, G. P. The correlation in the rat of age with its degree of resistance to anthrax. (Abstract) *Am. J. Path.*, 1958, **34**, 573.
14. Taylor, M. J.; Rooney, J. R., and Blundell, G. P. Experimental anthrax in the rat: the relative lack of natural resistance in germfree (Lobund) hosts. (Abstract) *Bact. Proc.*, 1960, pp. 129–130.
15. Unpublished observations.
16. Suzuki, H. K. Development of phagocytic activity in the reticuloendothelium of the albino rat: a comparison of prenatal, neonatal, juvenile, and adult periods. *Yale J. Biol. & Med.*, 1957, **29**, 504–524.
17. Culbertson, J. T. Phagocytosis of trypan blue in rats of different age groups. *Arch. Path.*, 1939, **27**, 212–217.
18. Andrew, W. Age changes in the vascular architecture and cell content in spleens of 100 Wistar Institute rats, including comparisons with human material. *Am. J. Anat.*, 1946, **79**, 1–73.
19. Andrew, W., and Andrew, N. V. Age changes in the deep cervical lymph nodes of 100 Wistar Institute rats. *Am. J. Anat.*, 1948, **82**, 105–165.
20. MacDowell, E. C., and Taylor, M. J. Mouse leukemia. XIII. A maternal influence that lowers the incidence of spontaneous cases. *Proc. Soc. Exper. Biol. & Med.*, 1948, **68**, 571–577.
21. MacDowell, E. C. Mouse leukemia. XVI. Spontaneous cases in strain C58 resisted by milk of old STOLI foster nurses. *Cancer Res.*, 1955, **15**, 23–25.
22. Halliday, R. Prenatal and postnatal transmission of passive immunity to young rats. *Proc. Royal Soc. London, s.B*, 1955, **144**, 427–430.

It is a pleasure to record the long-continued interest of Dr. Virginia G. McGann and Dr. George G. Wright in this work. We are indebted to Mr. Floyd H. Taylor for a multiple probit regression analysis of the data.

PREVENTION OF CROSS-RESISTANCE TO CARDIOTOXIC AGENTS BY LOW CHLORIDE INTAKE

HANS SELYE, M.D., PH.D., D.SC., AND EÖRS BAJUSZ, M.D.*

From the Institut de Médecine et de Chirurgie expérimentales, Université de Montréal, Montréal, Canada

In previous studies, it was demonstrated that sudden exposure to stressor agents—e.g., cold, muscular exercise, restraint, trauma, noradrenalin—elicited large infarct-like patches of myocardial necrosis in rats pretreated with certain corticoids and sodium salts.[1] However, more recently it has been established that this type of cardiac lesion was suppressed if, under otherwise similar conditions, the rats were gradually adapted to an alarming stimulus. Under these circumstances, the animals resisted subsequent exposure to the full, normally pathogenic dose of the same stressor[2] or even one different from that with which they had been pretreated.[3,4]

Similar cross-resistance of the heart can also be obtained against other types of experimental cardiopathies. For example, in rats sensitized with dihydrotachysterol (DHT) plus sodium biphosphate (NaH_2PO_4), the sudden stress of forced restraint or of bone fracture produced rapidly fatal suppurating myocarditis (Fig. 1) and nephrocalcinosis (Fig. 5). The nonspecificity of this protection was shown by the fact that the cardio- and nephrotoxic effects of restraint could be prevented by pretreatment with either restraint or noradrenalin, and those of bone fracture, by cold baths[5] (Figs. 2 and 6). Indeed, even the Mönckeberg type of arteriosclerosis due to DHT overdosage,[6] as well as the cardiopathy and the fatal outcome produced by the intravenous injection of a proteolytic enzyme, such as papain, or an antimalarial, such as plasmocid (Figs. 11 and 13), could be avoided by previous exposure to the stressor actions of forced restraint, muscular exercise, noradrenalin, cold baths, or reserpine[7,8] (Figs. 3 and 4). Further investigations have shown that both mineralo- and glucocorticoids participated in the development of this type of stress-induced resistance in the cardiac muscle. In adrenalectomized rats only combined treatment with both corticoids could re-establish the ability to develop this type of nonspecific tolerance.[9]

The experiments to be described show that in addition to the normal

This work was performed with the aid of grants (Nos. A-1641-C2, H-3688-C3, and B-2037-C1) from the National Institutes of Health, United States Public Health Service, and from the Gustavus and Louise Pfeiffer Research Foundation.

Accepted for publication, December 15, 1960.

* Fellow of the Gustavus and Louise Pfeiffer Research Foundation.

reactivity of the adrenal cortex, an adequate intake of certain electrolytes is necessary for the successful development of cross-resistance. More particularly, it will be seen that the acquisition of this type of insensitivity can be completely abolished by lowering the dietary chloride intake (Figs. 12 and 14). A magnesium-deficient diet, also known to sensitize the myocardium to stress,[10,11] does not abolish this form of cross-resistance. It may be concluded, therefore, that in this regard, the metabolic action of chloride deficiency is rather specific.

Methods

Two hundred forty female Sprague-Dawley rats from the Holtzman farm, with an average initial body weight of 96 gm. (range: 87 to 103 gm.), were used in 3 experimental series. Each group consisted of 10 animals. Some of the groups were kept on a low-chloride diet, others on a magnesium-deficient ration, while the control rats received a basic diet throughout the period of observation. (The diets used in these experiments were supplied by General Biochemicals, Inc., Chagrin Falls, Ohio.) In this manner, we hoped to eliminate any possible nonspecific effect that might have been due to the pure synthetic diets. Distilled water was given *ad libitum*. During sensitization with the diets, the animals were treated with various cardiotoxic agents (Tables I to III). Several stressor agents were used to induce cross-resistance in the heart; the manner of their application will be described later.

The percentage composition of the basic diet was as follows: sucrose, 70.65; vitamin-free test casein GBI, 18.3; butter fat (salt free) 5; vitamin supplement, 1.05; salt mixture, 5. The vitamin supplement (gm. per hundred pounds of diet) consisted of: alpha tocopherol, 10.215; calcium pantothenate, 2.043; carotene in oil (3,333 I.U. per gm.), 150; choline dihydrogen citrate, 272.4; i-inositol, 13.62; menadione, 0.102; niacin, 27.24; pyridoxine phosphate 0.953; riboflavin, 0.953; thiamine monophosphate, 0.953; viosterol (400,000 I. U. per gm.), 0.125. The percentage composition of the salt mixture was: calcium lactate, 20.4; calcium gluconate, 12; potassium phosphate (monobasic), 11.2; potassium chloride, 31.2; sodium phosphate (dibasic), 2.5; sodium chloride, 4.974; sodium bicarbonate, 2.5; ferric citrate, 9.5; magnesium chloride, 3.8; copper sulfate, 1.9; zinc acetate, 0.026.

The low-chloride diet differed from the basic diet only as regards the salt mixture; all the chlorides were replaced by the corresponding bicarbonate on a molar basis. The chloride content of this deficient diet was 0.035 per cent, that of the basic diet, 0.953 per cent (according to the data given by the suppliers). The magnesium-deficient diet also differed from the basic diet only in its salt mixture and was as follows (gm. per hundred pounds of diet): calcium carbonate, 905.84; calcium phosphate (monobasic), 266.44; cupric sulfate, 0.92; ferric ammonium citrate, 84.52; manganese sulfate, 12.08; potassium iodide, 2.4; potassium phosphate (dibasic), 226.44; sodium chloride, 507.2; zinc carbonate, 0.76.

The first experiment (Table I) dealt with the influence of low chloride intake upon the development of cross-resistance to the cardio- and nephrotoxic actions of DHT plus NaH_2PO_4, as well as the cardiac necrosis eliciting effect of stress. In order to induce increased resistance of the heart, some of the animals were pretreated with repeated restraint (groups 2, 4, 6, 8) while the remainder served as controls (groups 1, 3, 5, 7). Restraint was applied every second day by strapping prone rats to a board with adhesive tape, starting with 4 hours on the second day and then gradually increasing this time up to 7 hours. Treatment with various potentially cardiotoxic agents was initiated on the fourth day and continued until the termination of the experiment. Twenty μg. of DHT (dihydrotachysterol, "Calcamin," The Wander Company) was administered in the form of a microcrystal suspension together with

0.5 mM of NaH_2PO_4 in 2 ml. of water, twice daily, through a stomach tube (groups 1, 2, 5, 6). F-COL (fluorocortisol, or 9α-fluorohydrocortisone acetate, The Upjohn Company) was injected subcutaneously as a microcrystal suspension, 500 μg. daily in 0.2 ml. of water (groups 3, 4, 7, 8). Sodium acetate (Fisher Scientific Company) was administered by stomach tube, in a concentration of 1 mM in 2 ml. of water, twice daily (groups 3, 4, 7, 8). Since the combined administration of F-COL plus sodium acetate to rats on a normal diet does not produce cardiac necrosis, the rats kept on our basic ration were exposed to the stress of bone fracture in order to elicit the cardiac lesions. Multiple fractures of all 4 extremities were performed under light ether anesthesia on the tenth day (groups 3 and 4). This experimental series was terminated on the twelfth day by killing the survivors with chloroform.

The second experiment (Table II) dealt with the development of cross-resistance to the cardiotoxic actions of papain (a proteolytic enzyme) and plasmocid (a rather toxic, now obsolete antimalarial) under the influence of a lowered chloride intake. In order to activate stress defense, two stressor agents were applied on the 14th day (i.e., after 13 days' sensitization with the basic or chloride-deficient rations). These consisted of restraint for a period of 17 hours (groups 2, 5, 8, 11) and cold baths. The latter were accomplished by immersing the rats in ice water 3 times at 4-hour intervals for 4-minute periods (groups 3, 6, 9, 12). Groups 1, 4, 7 and 10 served as controls to show the intensity of the cardiotoxic effects of papain and plasmocid on the basic and chloride-deficient diets respectively, without previous exposure to stressors. The papain suspension was injected on the 15th day into all animals of groups 1 to 3 and 7 to 9. Five gm. of crude papain powder (Nutritional Biochemicals Corp.) were added to 50 ml. of distilled water; this turbid suspension was mixed in a Waring blender for 25 minutes, and 0.2 ml. of the unfiltered preparation was then slowly administered via the jugular vein under light ether anesthesia. Plasmocid, 6-methoxy-8-(diethyl-amino-propylamino)-quinoline dihydroiodide, was injected intraperitoneally in groups 4 to 6 and 10 to 12. This was carried out 3 times daily, at 4-hour intervals, on the 15th and 16th days, with a dose of 0.3 mg. in 0.2 ml. of water. This experiment was terminated on the 17th and 18th days, respectively, 48 hours after the papain or the last plasmocid injection.

The third experiment (Table III) dealt with the effect of magnesium deficiency upon stress-induced cross-resistance under experimental conditions comparable with those of the second experiment. Some of the animals on the magnesium-deficient ration were exposed to restraint (groups 2 and 4) and then treated with papain or plasmocid; controls, not pretreated, were also given these substances (groups 1 and 3). The duration and intensity of the exposure to restraint, as well as the doses of papain and plasmocid, were the same as in the second experiment. The survivors were killed on the 17th (groups 1 and 2) and 18th (groups 3 and 4) days.

At necropsy, the hearts were inspected with the aid of a dissecting loupe; they were then fixed in susa solution saturated with picric acid for subsequent staining with the periodic acid-Schiff (PAS) or hematoxylin-phloxine stains, and in alcohol-formol for the histochemical detection of calcium with von Kossa's silver nitrate technique as well as with celestin blue.[18] When necropsy findings were positive, the kidney sections were also examined for calcium. The severity of the myocardial lesions and nephrocalcinosis was assessed on an arbitrary scale of 0 to 3: 0 designating no lesion; 1, a just detectable lesion; 2, a moderate lesion; 3, a severe lesion. The incidence (per cent positive animals within the group) and the severity of the cardiac and renal lesions (with standard errors) as well as the mortality rate are listed in the Tables.

Results

All control rats, not pretreated, whether kept on the basic diet (group 1) or on the chloride-deficient ration (group 5), exhibited severe cardiac

TABLE I

INFLUENCE OF LOW CHLORIDE INTAKE UPON THE DEVELOPMENT OF CROSS-RESISTANCE TO CARDIOTOXIC AGENTS

Group	Treatment: Inducing cross-resistance	Treatment: Eliciting cardiac lesions	Cardiac necrosis: Grade (0–3) *	Cardiac necrosis: Incidence (%)	Nephrocalcinosis: Grade (0–3) *	Nephrocalcinosis: Incidence (%)	Mortality (%)
			On basic diet				
1	None	DHT + NaH_2PO_4	2.6 ± 0.23	100	2.5 ± 0.23	100	70
2	Restraint	DHT + NaH_2PO_4	0	0	0	0	10
3	None	F-COL + Na-acetate + bone fracture	1.1 ± 0.42	50	0.2 ± 0.20	10	80
4	Restraint	F-COL + Na-acetate + bone fracture	0	0	0	0	10
			On chloride-deficient diet				
5	None	DHT + NaH_2PO_4	3.0 ± 0	100	1.9 ± 0.10	100	100
6	Restraint	DHT + NaH_2PO_4	2.1 ± 0.40	80	1.7 ± 0.30	90	90
7	None	F-COL + Na-acetate	1.9 ± 0.43	78	0.5 ± 0.17	50	90
8	Restraint	F-COL + Na-acetate	1.7 ± 0.40	80	1.2 ± 0.42	60	90

* ± indicates standard errors of the mean.

lesions and intense nephrocalcinosis as a consequence of DHT + NaH_2PO_4 administration (Table I). Histologically, the cardiac muscle of these rats showed suppurating, inflammatory lesions, with extensive necrosis. In addition, there was calcification of the Mönckeberg-sclerosis type in the coronary arteries. Calcium deposition within the cardiac muscle or in the surrounding stroma was especially marked in the subendocardial layers of both ventricles. It is evident, furthermore, that in rats kept on the basic diet, adaptation to restraint afforded complete protection against acute DHT + NaH_2PO_4 intoxication (group 2); a similar pretreatment with stress was ineffective in the animals on a low-chloride intake (group 6).

It will be recalled that the combined adminstration of F-COL plus sodium acetate did not, in itself, usually (in animals on normal laboratory diets) produce any histologically detectable cardiac damage. It merely predisposed the heart to the necrotizing effect of subsequent exposure to stressors. However, chloride deficiency selectively sensitized the myocardium to this potentially cardiotoxic steroid-electrolyte interaction, so that massive and sometimes fatal cardiac necrosis developed.[13] Thus, in this regard, chloride deficiency replaced the effect of an acute stressor.

In accordance with these observations, bone fracture elicited severe cardiac lesions in 50 per cent of the F-COL + Na-acetate-conditioned rats on a basic diet (group 3). On the other hand, this steroid-electrolyte combination in itself produced cardiac necrosis in the chloride-deficient animals (group 7). Here again, pretreatment with restraint protected only the rats fed the basic diet (group 4); nearly all the animals on the chloride-deficient ration died, presumably as a consequence of the cardiac lesions (group 8).

It should be noted that this so-called electrolyte-steroid-cardiopathy with necrosis (ESCN) differed basically in its histologic characteristics from the myocarditis normally produced by DHT + NaH_2PO_4 administration. The former consisted of massive, necrotic patches in which the muscle fibers were gradually resorbed by histiocytes and neutrophils and later replaced by connective tissue. The slight degree of nephrocalcinosis produced by F-COL + Na-acetate in the animals maintained on a chloride-deficient diet was aggravated by pretreatment with restraint (groups 7 and 8). In addition, in 50 per cent of the restrained chloride-deficient animals (group 8), severe centrilobular hepatic necrosis occurred. This was not present in the chloride-deficient unrestrained controls (group 7).

In rats kept on the basic diet, the intensive disseminated cardiac fiber necrosis following papain injection (group 1) as well as the large patchy

cardiac necrosis (usually associated with diffuse myocarditis) ordinarily resulting from plasmocid administration (group 4) were both prevented by a previous period of restraint (groups 2 and 5) or by cold baths (groups 3 and 6) (Table II). This protective action of stressors

TABLE II

STRESS-INDUCED RESISTANCE OF THE HEART TO THE CARDIOTOXIC ACTIONS OF PAPAIN OR PLASMOCID, AND THE ABOLISHING EFFECT OF CHLORIDE DEFICIENCY

Group	Treatment: Inducing cross-resistance	Treatment: Eliciting cardiac lesions	Cardiac necrosis: Grade (0–3) *	Cardiac necrosis: Incidence (%)	Mortality (%)
		On basic diet			
1	None	Papain	1.5 ± 0.30	90	60
2	Restraint	Papain	0	0	0
3	Cold bath	Papain	0	0	0
4	None	Plasmocid	1.6 ± 0.33	89	90
5	Restraint	Plasmocid	0	0	0
6	Cold bath	Plasmocid	0	0	0
		On chloride-deficient diet			
7	None	Papain	2.1 ± 0.27	100	50
8	Restraint	Papain	0.6 ± 0.27	40	10
9	Cold bath	Papain	1.6 ± 0.40	70	10
10	None	Plasmocid	1.1 ± 0.28	70	90
11	Restraint	Plasmocid	1.5 ± 0.23	90	90
12	Cold bath	Plasmocid	2.2 ± 0.42	80	90

* ± indicates standard errors of the mean.

TABLE III

THE INABILITY OF MAGNESIUM-DEFICIENT DIET TO INFLUENCE THE DEVELOPMENT OF CROSS-RESISTANCE

Group	Treatment * : Inducing cross-resistance	Treatment * : Eliciting cardiac lesions	Cardiac necrosis: Grade (0–3) †	Cardiac necrosis: Incidence (%)	Mortality (%)
1	None	Papain	2.3 ± 0.30	90	0
2	Restraint	Papain	0	0	0
3	None	Plasmocid	1.2 ± 0.42	60	10
4	Restraint	Plasmocid	0	0	0

* In addition to the treatments listed here, all rats were kept on a magnesium-deficient diet throughout the experiment, as described in the text.

† ± indicates standard errors of the mean.

is also evident from the reduced mortality rates. However, in the rats kept on the chloride-deficient ration, only restraint offered significant protection against the development of papain necrosis (groups 7 and 8).

In some cases, stress not only failed to prevent but seemed actually to aggravate the lesions normally induced by such treatment (groups 10, 11 and 12).

Maintenance on a magnesium-deficient diet did not interfere with the protective effect of stress (groups 2 and 4) against the cardiac lesions normally induced by papain or by plasmocid (Table III).

Discussion

It is evident from these experiments that when rats were kept on a basic diet containing all the necessary electrolytes, various types of cardiac lesions (the DHT + NaH_2PO_4 myocarditis, the infarct-like cardiopathy produced by stress after sensitization with F-COL + Na-acetate, the cardiac necrosis caused by papain or plasmocid) could be prevented by pretreatment with stressors. Previous studies showed that this protective effect was shared by many diverse agents; e.g., forced restraint, cold baths, electric shock, adrenalin, noradrenalin, or reserpine.[3,5,8] Hence, this protection cannot be ascribed to any specific action of the prophylactic agents; it presumably reflects a rather nonspecific generalized defensive phenomenon. This view received further support from the present experiments.

We learned, however, that adaptation to stressors no longer increased resistance of cardiac and renal tissues when the dietary chloride intake was lowered from a basic 0.953 per cent to 0.035 per cent (Figs. 9 and 10). Nothing is known as yet about the mechanism through which a short period of chloride deficiency can thus block cross-resistance phenomena. Earlier investigations suggested that variations in dietary intake, not only of certain cations (such as K and Mg) but also of the anions (Cl), played an important role in the pathogenesis of some necrotizing cardiopathies. In particular, chloride deficiency was found to enhance the susceptibility of the myocardium to the production of various lesions (necrosis, inflammation or calcification) by a number of cardiotoxic agents, while dietary chloride excess proved to exert an opposite effect.[14] It is difficult to decide, therefore, on the basis of the present experiments, whether chloride deficiency specifically blocked the normal development of cross-resistance or whether it merely so raised the sensitivity of the heart that the defensive stress reactions were no longer effective. The first hypothesis appears to receive some support from the observation that the magnesium-deficient ration—well known to enhance disease susceptibility in the heart muscle—did not affect the normal development of cross-resistance.

Finally, it should be noted that the chloride-deficient diet differed from the basic diet; in the former the chloride was replaced on a molar

basis by corresponding bicarbonates. However, since bicarbonate is generally considered to be innocuous,[15,16] the detrimental effect of this diet may reasonably be attributed to its deficiency in chlorides. At any rate, it is significant that the effectiveness of defensive stress reactions, as well as the disease susceptibility of the heart muscle, were so basically altered by changes in the dietary intake of certain anions.

Summary

Experiments on rats indicated that acute overdosage with dihydrotachysterol plus sodium biphosphate produced rapidly fatal myocarditis and nephrocalcinosis, while exposure to restraint elicited an infarct-like cardiopathy and high mortality, following sensitization with fluorocortisol plus sodium acetate. Yet both types of lesions, like the cardiac necrosis normally induced by papain or plasmocid, were equally prevented by previous exposure to a stressor agent. These were additional examples of nonspecific cross-resistance, showing that increased resistance of the myocardium could be obtained against the most diverse cardiotoxic agents through pretreatment with the same stressor (e.g., restraint).

Stress failed to exert this protective effect upon the myocardium if the dietary chloride intake was markedly lowered. On the other hand, sensitization with a magnesium-deficient ration—also known to enhance the disease-susceptibility of the heart muscle—did not influence the normal development of cross-resistance.

Apparently, the reactivity of the myocardium, as regards defensive reactions, largely depends upon the dietary intake of certain anions.

References

1. Selye, H. The Chemical Prevention of Cardiac Necroses. Ronald Press, New York, 1958, 235 pp.
2. Selye, H. Wechselwirkungen zwischen Stress, Elektrolyten und Steroiden beim Entstehen verschiedener Kardiopathien und Myopathien. *Endokrinologie*, 1959, **38**, 195–217.
3. Bajusz, E., and Selye, H. Adaptation to the cardiac necrosis-eliciting effect of stress. *Am. J. Physiol.*, 1960, **199**, 453–456.
4. Selye, H.; Bajusz, E., and Strebel, R. Cross-resistance to cardiotoxic agents. *Canad. J. Biochem. & Physiol.* (In press)
5. Bajusz, E., and Selye, H. ¿Como alteran las reacciones inespecificas de adaptacion, la susceptibilidad para enfermedades renales y cardiovaculares? Un estudio experimental de la resistencia cruzada. *Folia clin. internac.*, 1960, **10**, 260–264.
6. Selye, H.; Jean, P., and Bajusz, E. Résistance croisée et prévention des cardiopathies expérimentales produites par un dérivé de la vitamine D. *Semaine hôp. Paris.* (In press)

7. BAJUSZ, E., and SELYE, H. Ueber die durch Stress bedingte Nekroseresistenz des Herzens. *Naturwissenschaften,* 1960, **22,** 520–521.

8. SELYE, H., and BAJUSZ, E. Protection Afforded by Stress Against Humorally Induced Cardiac Necroses. In: Sodi-Pallares' Memorial Volume, Mexico. (In press)

9. SELYE, H., and BAJUSZ, E. Participation of corticoids in the development of stress-induced cross-resistance. *Am. J. Physiol.* (In press)

10. MISHRA, R. K. Studies on experimental magnesium deficiency in the albino rat. *Rev. canad. biol.,* 1960, **19,** 122–180.

11. BAJUSZ, E., and SELYE, H. Conditioning factors for cardiac necroses. *Tr. New York Acad. Sc.,* 1959, **21,** 659–667.

12. SELYE, H., and NIELSEN, K. Histogenesis of experimental cutaneous calcinosis. *Acta morphol. Acad. sc. Hungar.* (In press)

13. BAJUSZ, E., and SELYE, H. Sensitization by chloride deficiency to corticoid-induced cardiac necroses. *Acta endocrinol.* (In press)

14. BAJUSZ, E., and SELYE, H. Influence of variations in dietary intake of chlorides upon diverse necrotizing cardiopathies. *Am. Heart J.,* 1960, **60,** 266–280.

15. VORIS, L., and THACKER, E. J. The effects of the substitution of bicarbonate for chloride in the diet of rats on growth, energy and protein metabolism. *J. Nutrition,* 1942, **23,** 365–374.

16. THACKER, E. J. The mineral composition of the albino rat as affected by chloride deficiency. *J. Nutrition,* 1943, **26,** 431–441.

The authors are grateful to The Upjohn Company, Kalamazoo, for the fluorocortisol and to Dr. R. C. Elderfield, University of Michigan, Ann Arbor, for the plasmocid.

[*Illustrations follow*]

Legends for Figures

Fig. 1. Focus of necrosis, inflammation and calcification in the left ventricular wall of a rat maintained on the basic diet and given DHT+NaH_2PO_4. Von Kossa stain. × 120.

Fig. 2. Absence of lesions in the heart of a rat treated as in the animal shown in Figure 1 but, in addition, adapted to forced restraint. Von Kossa stain. × 120.

Fig. 3. Mönckeberg type of coronary sclerosis resulting from DHT+NaH_2PO_4 overdosage in a rat maintained on the basic diet. Von Kossa stain. × 120.

Fig. 4. Prevention of coronary sclerosis by adaptation to restraint. Coronary vessels of this stress-adapted rat are protected, as compared with those in the previous figure, although both animals received the same amount of DHT+NaH_2PO_4. Von Kossa stain. × 120.

Fig. 5. Intense nephrocalcinosis produced by combined DHT+NaH_2PO_4 administration in a rat fed the basic diet. Von Kossa stain. × 120.

Fig. 6. Absence of nephrocalcinosis in a rat treated similarly to that shown in the previous figure, but adapted by the stressor effect of restraint. Von Kossa stain. × 120.

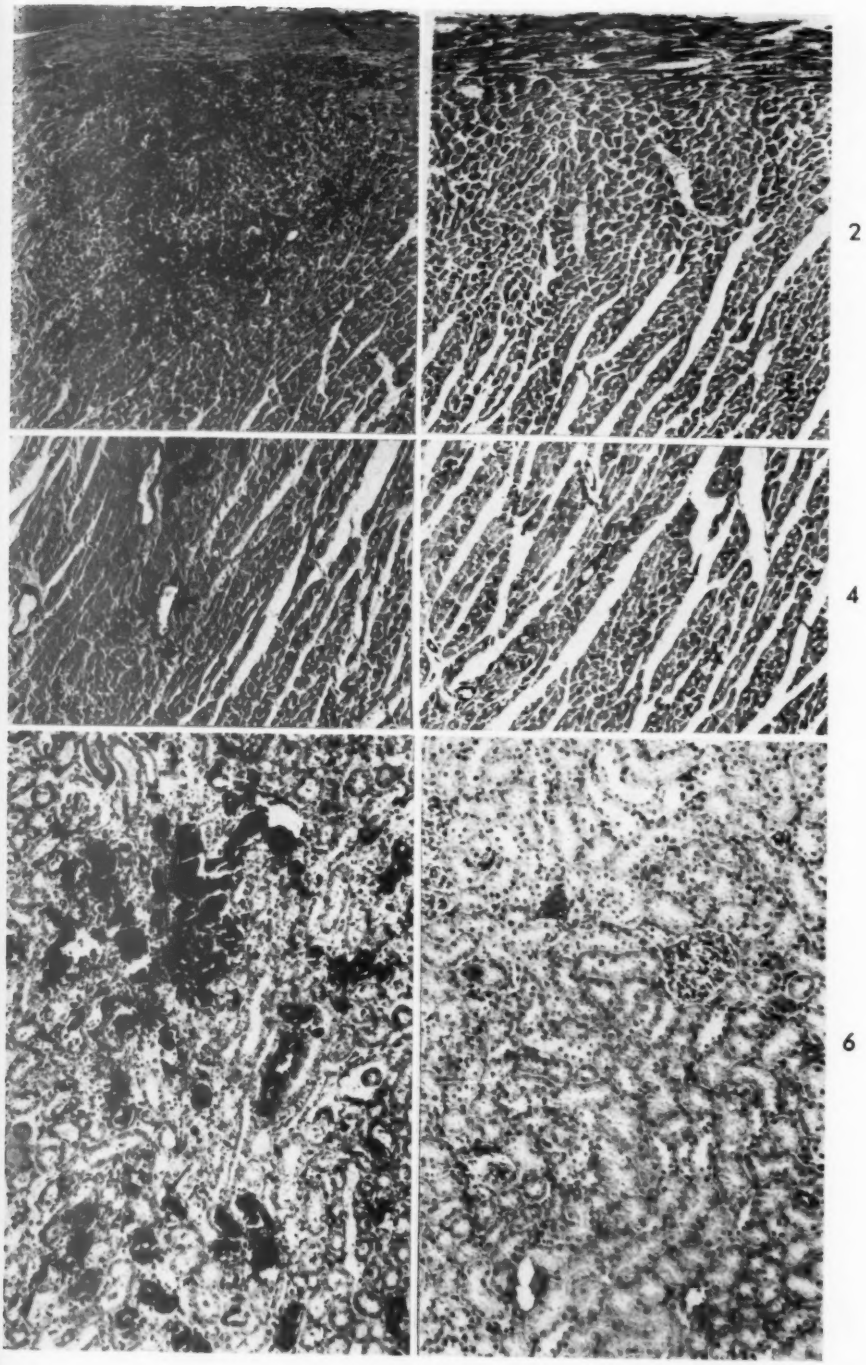
1
2
3
4
5
6

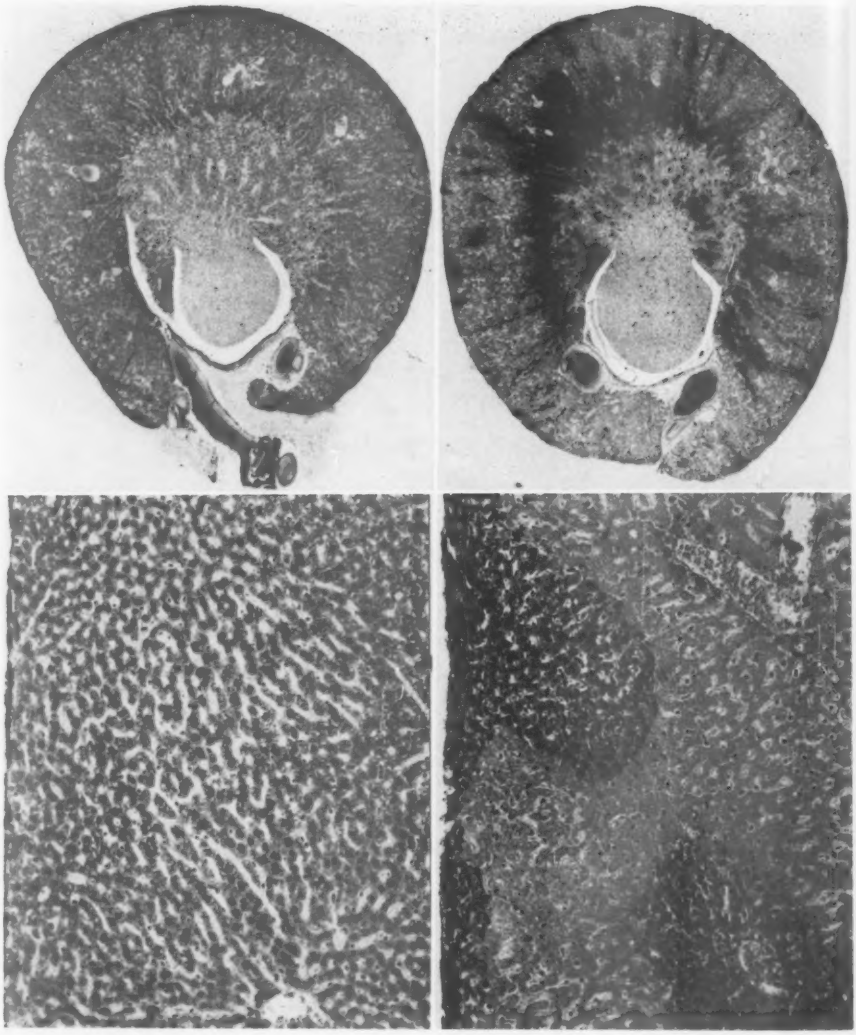

FIG. 7. Just detectable, slight nephrocalcinosis at the corticomedullary juncture, in a rat maintained on a low chloride diet and treated with F-COL+Na-acetate. Von Kossa stain. × 12.

FIG. 8. Intense nephrocalcinosis in a rat treated as in the animal shown in Figure 7. In addition, this rat was repeatedly restrained. Von Kossa stain. × 12.

FIG. 9. Normal appearance of hepatic tissue in a rat maintained on a low chloride diet, showing that combined F-COL+Na-acetate administration does not usually produce any detectable morphologic abnormality in the liver. Hematoxylin-phloxine stain. × 120.

FIG. 10. Diffuse hepatic necrosis in a rat kept on the same low chloride diet and treated similarly to the rat shown in the previous figure. In addition, this animal was repeatedly restrained. Hematoxylin-phloxine stain. × 120.

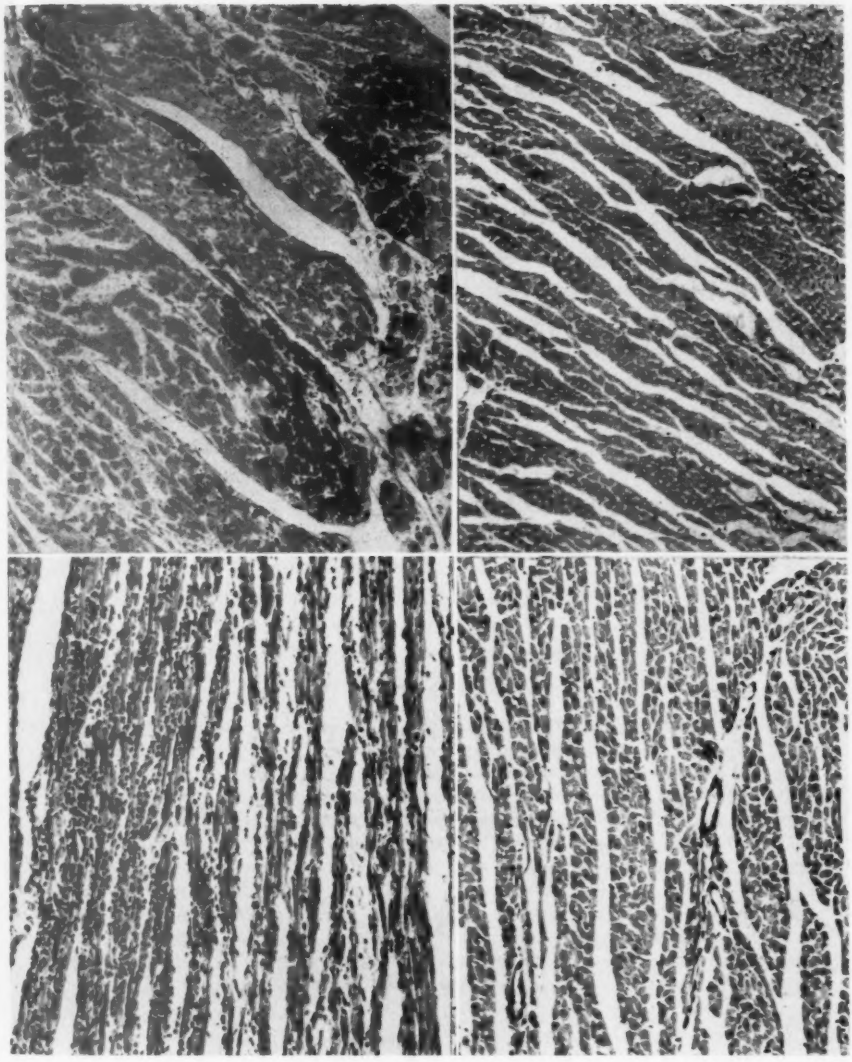

FIG. 11. Calcified necrotic foci in the heart of a rat kept on a basic diet and given a single intravenous injection of papain. Celestin blue stain. × 120.

FIG. 12. Prevention of papain necrosis by stress. This rat received the same amount of papain as did the animal shown in the previous photograph. Here, however, cross-resistance was induced by the stressor actions of cold baths. Celestin blue stain. × 120.

FIG. 13. Diffuse necrosis and myocarditis in the left ventricle of a rat treated with plasmocid and maintained on a basic diet. Von Kossa stain. × 120.

FIG. 14. Absence of myocardial lesions in rat treated with plasmocid while maintained on a basic diet but adapted to cold baths. Von Kossa stain. × 120.

A LIGHT AND ELECTRON OPTICAL STUDY OF REGENERATING TENDON

R. Peach, Ph.D.*; G. Williams, M.D.†, and J. A. Chapman, Ph.D.

From the Departments of Rheumatism Research and Pathology, Manchester University, Manchester, England

Tendon regeneration has been investigated at the histologic level by several workers.[1-3] Apart from its intrinsic interest as a form of connective tissue repair, regenerating tendon provides a useful experimental model for the study of connective tissue metabolism. It has advantages in that the newly formed tissue is free from necrosis and contaminant injection materials, is easily reproducible and relatively homogeneous.

In the present investigation the principal flexor tendons of the hind limbs of the guinea pig were removed, and the regenerating connective tissue was examined histologically and electron optically. This enabled the appearances of the over-all regenerative process to be correlated with the ultrastructure of the fibroblasts. Particular attention was given to the cellular structure in the early stages of repair.

Material and Methods

Treatment of Animals

Guinea pigs of both sexes, weighing 250 to 350 gm. were used. The skin on the medial aspect of both hind limbs was shaved, and incisions 2 cm. long were made in each limb under ether anesthesia and aseptic conditions. The 4 tendons in the posterior aspect (Fig. 1), the principal ones being the Achilles and the long flexor of the toes, were exposed. The tendons were removed *in toto* following division near their proximal origin in muscle and distal insertion in bone. The empty compartment so formed partly filled with blood clot. When bleeding had ceased, the overlying skin wound was closed with interrupted sutures.

Animals were sacrificed in pairs, by a blow on the head, at various time intervals after operation, ranging from 4 days to 6 months. Some tissue was also obtained 2 years after operation. The newly formed tissue was rapidly removed from one limb and taken for electron microscopy. The remaining limb was taken for conventional histologic examination.

Histologic Techniques

The tissues for histologic investigation consisted of either whole limbs or, in some cases, excised portions of the regenerating tissue. Whole limbs were fixed for 5 to 7 days in 10 per cent formol saline; penetration of the fixative was encouraged by incising the skin and muscle. Following decalcification in 6 per cent nitric acid and thorough washing, the limbs were embedded in paraffin and serial sections cut at 7 μ.

Accepted for publication, December 2, 1960.

* Supported by a grant from the Nuffield Foundation.

† Temporary address: Department of Pathology, University of Vermont College of Medicine, Burlington, Vt.

These were stained with hemalum and eosin, silver impregnation combined with van Gieson counterstain, and Mallory's trichrome stain.

Excised portions were allowed to harden in the deep freeze, then divided into two. One half was fixed and stained in the same way as the whole limbs except that, in the absence of bone, no decalcification was required. The other half was fixed in an acridine-ethanol mixture[4] to preserve acid mucopolysaccharides. Paraffin sections were stained with hemalum and eosin, the periodic acid-Schiff (PAS) technique (modified McManus[5]), and toluidine blue (Grübler).

Whole limb sections were used to investigate the all-over topography of the lesions and to establish the relationship of the various tissues during regeneration. This was especially important in the early stages.

Excised portions were used mainly in the later stages when the regenerating tissue was more homogeneous in composition.

Electron-Optical Techniques

The excised tissue was immersed in a drop of fixative, sliced into small pieces with a razor blade, transferred to further fixative in a weighing bottle and fixed, usually for a period of one hour. Two fixatives were used: Either an ice-cold 1 per cent solution of osmium tetroxide (OsO_4) in acetate veronal buffer[6] made isotonic by the addition of sodium chloride,[7] or an ice-cold 0.6 per cent solution of potassium permanganate[8] ($KMnO_4$) in the same isotonic buffer. After fixation the tissue was washed and dehydrated through increasing concentrations of alcohol before embedding. Some tissue was embedded in a 4:1 mixture of n-butyl methacrylate and methyl methacrylate with benzoyl peroxide as catalyst.[9] A prepolymerized mixture was used in the final stage and polymerization carried out at 60° C.[10] The remaining tissue was embedded in araldite.[11] The following soaking times, all at 48° C., were used: 50:50 araldite mixture (no accelerator): 100 per cent alcohol, 18 hours; araldite mixture (no accelerator), 48 hours; araldite mixture (plus accelerator), 9 hours with changes every 2 to 3 hours.

Staining. Some specimens embedded in araldite were stained in 2 per cent phosphotungstic acid (PTA) in the absolute alcohol used in the dehydration series.[12] This provided an over-all increase in contrast, particularly of collagen fibrils. Other specimens were stained with PTA after sectioning, by the method of Watson.[13] This proved an unsatisfactory method for araldite-embedded tissue.

Selection of Tissue for Electron Microscopy. Although relatively homogeneous, the granulation tissue removed for electron microscopy was sometimes contaminated by muscle, adipose tissue and strands of preformed connective tissue. In the very early stages of the regenerative process, there were regions consisting solely of blood cells and fibrin clot. To enable selection of required tissue for electron microscopy, thick sections were cut from the methacrylate- or araldite-embedded specimens and examined by conventional microscopy. Methacrylate-embedded tissue was stained with Weigert's iron hematoxylin and van Gieson's reagents. The results of staining araldite-embedded tissue were variable, and sections from this embedding medium were usually examined by phase contrast techniques. Euparol[14] was found to be a very satisfactory mounting medium for examining araldite sections by this method.

Thin Sectioning. Thin sections were cut on either a Haanstra thermal advance ultramicrotome or a Huxley mechanical advance instrument, using a glass knife. It was necessary during the course of the work to examine relatively large areas of tissue, and sections up to 2 mm. square were sometimes obtained on the Huxley ultramicrotome. Spreading of sections was encouraged by application of xylene vapor. Sections were usually mounted on carbon-filmed Athene electron microscope grids. Some of the larger araldite sections were mounted without a supporting film. Sections were examined in a Siemens Elmiskop I operated at an accelerating voltage of 80 kv. Micrographs were taken on Ilford Special Lantern Plates (Contrasty) at magnifications ranging from 300 to 80,000.

Observations

Behavior of Animals

Postoperatively the condition of the animals was good; they maintained their normal feeding habits and did not lose weight. In no case did sepsis occur. For the first few days the animals lost the use of their hind limbs and dragged their hind quarters, but use was gradually regained, and within 4 weeks of the operation the animals were using the affected limbs quite freely. By this time a tendinous cord of new tissue had formed (Fig. 2) and could be felt through the skin. In most animals slight ulceration of the feet occurred within a few days of operation, but this gradually healed.

Histologic Observations

Three days after operation the space formerly occupied by the tendons was filled by a loose fibrin clot (Fig. 3) which included red and white blood cells in its meshwork. Macrophages were active within the exudate but were mainly concentrated around dilated capillaries at the periphery of the lesion. The connective tissue cells of the divided tendon sheaths were proliferating, and new capillaries were forming among them. By the fifth day the connective tissue cells were organized into cellular sheets invading the clot from all sides, particularly from the proximal and distal extremities. The most prominent cells were the fibroblasts although macrophages and endothelial cells were also present.

It was significant that two types of fibroblast could be distinguished in this early granulation tissue. Those at the advancing edge of the cellular sheet, noticeably where the exudate was less dense, possessed elongated nuclei with dense, uniformly distributed chromatin (Fig. 4). The cells were spindle-shaped with tapering eosinophilic cytoplasmic processes blending with fine reticulin fibers in a loosely textured matrix. Some PAS-positive granules (diameters $\sim 1\mu$) could be detected in the cytoplasm. Mitotic figures were not common. It will be convenient to describe these spindle-shaped fibroblasts at the advancing edge as "migratory" fibroblasts.

In the deeper aspects of the invading cellular tissue (further removed from the center of the clot) a second type of fibroblast appeared. These were characterized by ovoid, vesicular nuclei, finely stippled with chromatin (Fig. 5). Where their outlines could be distinguished, the cells appeared rounder in over-all shape than those of the first type although cytoplasmic processes could still be detected. The nuclei, which occupied much of the cell, were surrounded by a narrow rim of rather basophilic cytoplasm in which PAS-positive granules could be demonstrated. These

cells, showing numerous mitotic figures, lay in a basophilic matrix in which the connective tissue fibers were thicker and more numerous than those associated with the spindle-shaped fibroblasts. The rounder fibroblasts will be referred to as "synthesizing" fibroblasts.

The terms "migratory" and "synthesizing" are not intended to imply that the cells were entirely restricted in function to one or the other of these two categories. The histologic evidence does suggest, however, that the spindle-shaped cells were predominantly migratory in character while the rounder cells, forming a more compact syncytium, were engaged in synthesis. It will be shown that the electron optical evidence also indicates a morphologic difference between the two cell types.

By the seventh day the exudate was largely replaced by new connective tissue in which the predominant fibroblasts were of the rounder form. The intercellular fibers had thickened and stained preferentially red with the acid fuchsin of the combined silver and van Gieson preparation. Simultaneously the basophilia of the matrix had diminished. By the 14th day the fibroblasts were still predominantly rounded, with basophilic cytoplasm and vesicular nuclei. Mitotic figures were still fairly numerous. The matrix showed a patchy metachromasia, and collagen fibers, now aggregated into bundles, showed the characteristic wavy arrangement of tendinous tissue (Fig. 6).

Thereafter the histologic picture suggested a gradual settling down of metabolism. After 6 weeks (Fig. 7) most of the fibroblasts appeared elongated, with eosinophilic cytoplasm. Only a few contained PAS-positive granules. The matrix was uniformly fibrillar and devoid of basophilic areas. By the end of 6 months the connective tissue closely resembled normal tendon; the cellularity was reduced, and most of the fibroblasts appeared elongated. The matrix, now homogeneous, consisted mainly of eosinophilic tendinous bundles, in some of which foci of calcification and even of ossification could be identified. This pattern was repeated in the tissue obtained 2 years after tendon removal (Fig. 8).

Electron Microscopy

With minor exceptions, the features described were present in both OsO_4 and $KMnO_4$ fixed tissue. As observed by Luft,[8] attached particles were absent from the membranes of the endoplasmic reticulum in tissue fixed in $KMnO_4$.

Early Stages. The early granulation tissue (4 to 5 days) contained regions of structureless extracellular space, presumably occupied before fixation by the fluid exudate. Collagen fibrils, blood cells and remnants of the fibrin clot were identified.

The fibroblasts contained extensively developed, rough-surfaced profiles of endoplasmic reticulum. It was observed that, depending on the form of endoplasmic reticulum, the fibroblasts could be classified into two types. These will be referred to as type A and type B. Their distribution, determined from study of the thick sections taken from the blocks before ultramicrotomy and from the examination of relatively large areas (up to 2 mm. square) with the electron microscope, indicated that the type A fibroblasts corresponded to the migratory cells and the type B fibroblasts to the synthesizing cells distinguished at the conventional histologic level.

The type A fibroblasts (Fig. 9) were found only in the very early stages (4 to 5 days) and usually at the edge of the fibrin clot. The cells tended to be elongated in cross section although rounder forms were also encountered. Their most marked characteristic was the ordered relative distribution of the rough-surfaced profiles of endoplasmic reticulum. The profiles were elongated, tending to lie parallel to each other and to the long axis of the cell. Individual profiles extended for several μ in the plane of section and were rarely interconnected. The width of a given profile was relatively constant although the width of different profiles varied between 400 Å and 2,000 Å. They occupied variable proportions of the cytoplasm at any particular level of section. In some cells they were restricted to a region near a centrally placed nucleus or to one end of the cell. In others, the profiles occupied all regions of the cytoplasm. Irrespective of the method of fixation or of PTA staining, the contents of the profiles were of higher electron density than the rest of the cytoplasm but appeared quite structureless.

The type B fibroblasts (Fig. 10) were found in greater numbers in the deeper aspects of the tissue. Their appearance varied considerably, and the rough-surfaced profiles, in marked contrast to those of the type A cells, were of irregular shape, variable size, showed no particular relative arrangement and were often interconnected. Their contents were of much lower electron density than those of the type A cells and included a fine fibrillar material in tissue stained with PTA before embedding.

There were other differences between the two types of cell. Type A cells usually showed a well defined cell membrane (Fig. 9) and elongated mitochondria, in contrast to type B cells which often lacked a limiting membrane and possessed shorter mitochondria (Fig. 10). Evidence of transition forms between the two cell types was occasionally encountered (Fig. 11). In such cells, the profiles of the endoplasmic reticulum, although still retaining interiors of high electron density and tending to be elongated, were more irregular in both shape and relative distribution than those in the type A cells.

The nuclei in both types of cell did not differ significantly although a double nuclear membrane was more common in type B cells; nucleoli were frequently seen in both. In OsO_4 fixed tissue, numerous cytoplasmic particles similar to those on the membranes of the endoplasmic reticulum were present singly and in groups in the cytoplasm of both cell types. No granules were found corresponding in size to the PAS-positive granules observed with the light microscope.

Later Stages. By the 14th day the tissue was compact and the extracellular space contained numerous closely packed collagen fibrils. The endoplasmic reticulum of the fibroblasts was exclusively of the type B category (Fig. 12). In later tissue the profiles of the endoplasmic reticulum tended to increase in size. In some cells they occupied most of the cytoplasmic volume. The cell membrane was sometimes well defined, but frequently the cytoplasm merged so closely with the adjacent collagen fibrils that a limiting membrane could not be detected (Fig. 13).

Collagen Fibrils. As early as 4 days after tendon removal, collagen fibrils in varying numbers were recognized in close proximity to the type B cells and, to a lesser extent, the type A cells. Striated collagen fibrils were often observed in contact with the cell surface but were never found in intracellular locations. Fine filaments (diameters $\sim$ 100 Å), sometimes showing suggestions of a periodic structure, were occasionally observed in close association with striated collagen fibrils. Groups of filaments often showed a close association with each other (Fig. 14). The early collagen fibrils were randomly oriented but later assumed a more orderly array. In some of the larger fibrils up to 8 striations per period were resolved (Fig. 15).

Discussion

Detailed histologic accounts of tendon repair have been given by previous workers,[1,3] but so far as is known, no adequate electron optical study dealing with the cellular components has been published. Wasserman[15] described electron microscopic observations following simple tenotomy of the Achilles tendon of the rat but concentrated mainly on the fibrillar constituents. Furthermore, the techniques of fixation were unsatisfactory by present standards.

In the present work, histologic studies were used primarily as a general background for a detailed study of fibroblast structure, particularly in the early stages of tendon regeneration. Removal of a group of tendons, as in this investigation, as opposed to simple tendon division, has the advantage of producing adequate amounts of fairly homogeneous granulation tissue suitable for electron optical examination and, as shown by Kodicek and Loewi,[16] for biochemical investigation.

The observations on migratory and synthesizing fibroblasts are in agreement with those of Stearns.[17,18] She examined living fibroblasts in transparent chambers in rabbits' ears, and noted that elongated fibroblasts underwent changes in form and arrangement as they migrated centrally. These cells became rounder, formed a syncytium and appeared to engage in fibrogenesis. Penney and Balfour[19] also noted morphologic changes of the fibroblasts in the early stages of wound healing in their nonscorbutic (control) guinea pigs. Edwards and Dunphy[20] visualized 3 phases of functional activity of fibroblasts in the healing wound; namely, proliferative, synthesizing, and finally one of maturation in which "their blast potential, according to present evidence, vanishes." The differences in fine structure of the connective tissue cell described in the present work may well reflect functional differences such as these authors describe.

Intracytoplasmic PAS-positive granules were most prominent in the synthesizing fibroblasts, where they varied in number, size and distribution from cell to cell. They were observed by Gersh and Catchpole[21] and Catchpole[22] in proliferating fibroblasts where they were noted for their "resistance to most solvents." They have been found in tissue culture fibroblasts[23] and are also widely distributed throughout the cells of the reticuloendothelial system in experimental amyloidosis.[24] According to LeBlond, Glegg and Eidinger[25] and Hooghwinkel and Smits,[26] only neutral polysaccharides can be demonstrated by the PAS technique. Hence, these granules have been regarded as glycoprotein, but their role in the formation of new connective tissue is not known; nor is their relationship, if any, to serum mucoproteins established. This is of interest in view of the recent work of Jackson, Flickinger and Dunphy,[27] whose analysis of 8-day-old granulation tissue in implanted sponges in rats indicated that the hexosamine content in the early stages of connective tissue formation was derived mainly from serum mucoprotein and not from sulfated acid mucopolysaccharide. Similar findings regarding hexosamine content were reported by Grillo, Watts and Gross[28] in studies of healing wounds in guinea pigs.

The proliferating fibroblasts in the regenerating tendon appeared to be derived mainly from the cells of the subcutaneous fatty reticulum and from the fascial sheaths surrounding the muscle bellies adjacent to the wound area. The periosteal contribution to new fibroblast population was small by comparison, but new bone formation was quite commonly seen on the tibial shaft in the wound area from the seventh day onward. The overlying true dermis appeared relatively inert throughout the entire regenerating process. In contrast to Buck's findings,[3] after single

tendon division, intramembranous ossification was commonly seen in the reformed tendinous tissue in the last stages.

The ultrastructural component showing the most interesting features was the endoplasmic reticulum. The concept of this cytoplasmic structure as a cell-wide system of membrane-bounded cavities has been stated by Palade.[29] Since the rough-surfaced profiles of the endoplasmic reticulum are associated with synthesis of secretory protein in many cell types,[30] it might be expected that in the fibroblast they would be involved in the synthesis of collagen. Evidence showing that newly synthesized collagen protein is closely associated with the rough-surfaced profiles of the endoplasmic reticulum of fibroblasts in carrageenin granulomas has been obtained by Lowther, Green and Chapman.[31] These workers, using tissue slices of the granulomas, incubated with labeled amino acids, found a high degree of radioactivity in the neutral-salt-soluble collagen from the microsomal fraction. This fraction was shown to be derived from the rough-surfaced profiles of the endoplasmic reticulum.

The present work demonstrates differences in the endoplasmic reticulum among the fibroblasts in regenerating tendon. The significance of these differences cannot be fully assessed at the moment. In the early stages the fibroblasts could be classified into two types (A and B) according to the form of their endoplasmic reticulum. The evidence indicated that this difference in appearance was associated with the differences between the migratory and synthesizing cells. The type A cell appeared to correspond to the migratory cell and the type B cell to the synthesizing cell. As the tissue aged and synthetic activity apparently decreased, the size of the profiles of the endoplasmic reticulum tended to increase.

The type A cell resembles fibroblasts in embryonic chick tissues. Structures corresponding to the endoplasmic reticulum in fibroblasts of embryonic chick tendon[32] and dermis[33] and in osteoblasts of embryonic chick bone[34] are similar to the endoplasmic reticulum of the type A cell. This similarity has been confirmed by the authors' own observations on embryonic chick fibroblasts.

The structure of the type B cell on the other hand resembles that of fibroblasts in amphibian skin reforming after wounding.[35] These cells were described as being "densely filled with endoplasmic reticulum in the form of distended 'cisternae.'" It may be significant that in both the reforming amphibian skin and the regenerating tendon the stimulus to cellular activity was provided by tissue injury.

If a transition from a migratory to a synthesizing state is accompanied by a transition from the type A to the type B cell, then these differences in the endoplasmic reticulum could be associated with differences in the

rate of synthesis of collagen or other secretory product. Similarly, the increase in size of the profiles in the later tissue could be associated with the decrease in synthetic activity. The 3-dimensional change involved in the cells of the later tissue would appear to be an increased regularity of the cavities. This signifies a decrease in membrane surface area. The transition from a type A to a type B cell on the other hand would involve an increase in membrane surface area. These interpretations accord with the view [29] that one of the functions of the endoplasmic reticulum is to provide a large surface area for metabolic reactions. However, other factors may also influence the size of the cavities. For example the cavities may enlarge to accommodate synthesized material as in the exocrine cells of the guinea pig pancreas.[36]

It is significant that granules corresponding in size to the PAS-positive granules were not observed with the electron microscope. Jackson [32] made similar observations on embryonic chick tendon. The granules may have low electron density or may not be preserved by the methods of preparation used for electron microscopy. The absence of a cell membrane from many cells emphasizes the labile nature of the cell surface during collagen fibril formation as pointed out by previous workers.[37] The observations on striated collagen fibrils and in particular their absence from intracellular locations confirm those of previous workers.[33] The fine filaments (diameters ~ 100 Å) probably represent early stages in the formation of collagen fibrils.

Summary

Light and electron optical studies were made on tendon regeneration in guinea pigs following removal of the flexor tendons of the knee. A general histologic survey of the regenerating process served as a background for more detailed study of fibroblast structure.

With both forms of microscopy two types of fibroblast were distinguished in the early stages of regeneration. At the light optical level, one type appeared elongated and tapering, with fine eosinophilic cytoplasmic processes and a compact, uniformly dense nucleus. Located both at the advancing edge of the invading granulation tissue and at varying depths of penetration of the fibrin clot, this form was regarded as a "migratory" fibroblast. The other type, a rounder cell with a vesicular nucleus and more basophilic cytoplasm constituted the main cellular component of the early granulation tissue and was arranged in syncytial sheets behind the advancing edge. In these cells, mitotic figures and intracytoplasmic PAS-positive granules were frequently seen. This type was regarded as a "synthesizing" fibroblast.

The two types of fibroblast (A and B) were also distinguishable at

the electron optical level. Type A cells possessed an endoplasmic reticulum with orderly distribution; the rough-surfaced profiles were elongated, of uniform width, and tended to lie parallel to each other and to the long axis of the cell. The interiors of the cavities were homogeneous and of high electron density. Type B cells possessed an endoplasmic reticulum of which the profiles were of variable shape, irregular size, and showed no particular relative arrangement. The interiors were of low electron density and contained a fine fibrillar material in PTA-stained tissue. Cells suggesting an intermediate form between A and B were also seen. The distribution of the cells indicated that the migratory fibroblast corresponded to the type A cell and the synthesizing fibroblast to the type B cell.

The findings indicate that in this process of connective tissue repair the fibroblast undergoes a cyclical change from a resting to a resting state via migratory and synthesizing phases and that these changes in function are reflected in the fine structure of the cell.

References

1. Cameron, G. R. Pathology of the Cell. Charles C Thomas, Springfield, Ill., 1951, pp. 461–463.
2. Mason, M. L., and Shearon, C. G. The process of tendon repair; experimental study of tendon suture and tendon graft. *Arch. Surg.*, 1932, **25**, 615–692.
3. Buck, R. C. Regeneration of tendon. *J. Path. & Bact.*, 1953, **66**, 1–18.
4. Williams, G., and Jackson, D. S. Two organic fixatives for acid mucopolysaccharides. *Stain Technol.*, 1956, **31**, 189–191.
5. McManus, J. F. A. Histological demonstration of mucin after periodic acid. *Nature, London*, 1946, **158**, 202.
6. Palade, G. E. A study of fixation for electron microscopy. *J. Exper. Med.*, 1952, **95**, 285–298.
7. Sjöstrand, F. S. Electron Microscopy of Cells and Tissues. In: Physical Techniques in Biological Research. Oster, G., and Pollister, A. W. (eds.). Academic Press, Inc., New York, 1956, Vol. 3, Cells and Tissues, Chapt. 6, pp. 241–298.
8. Luft, J. H. Permanganate—a new fixative for electron microscopy. (Brief note) *J. Biophys. & Biochem. Cytol.*, 1956, **2**, 799–801.
9. Newman, S. B.; Borysko, E., and Swerdlow, M. Ultra-microtomy by a new method. *J. Res. Nat. Bur. Stand.*, 1949, **43**, 183–199.
10. Borysko, E. Recent developments in methacrylate embedding. I. A study of the polymerization damage phenomenon by phase contrast microscopy. *J. Biophys. & Biochem. Cytol.*, 1956, **2**, Suppl. to No. 4, 3–14.
11. Glauert, A. M., and Glauert, R. H. Araldite as an embedding medium for electron microscopy. *J. Biophys. & Biochem. Cytol.*, 1958, **4**, 191–194.
12. Huxley, H. E. The double array of filaments in cross-striated muscle. *J. Biophys. & Biochem. Cytol.*, 1957, **3**, 631–648.
13. Watson, M. L. Staining of tissue sections for electron microscopy with heavy metals. *J. Biophys. & Biochem. Cytol.*, 1958, **4**, 475–478.

14. GATENBY, J. B., and BEAMS, H. W. (eds.). The Microtomist's Vade-Mecum (Bolles-Lee). A Handbook of the Methods of Animal and Plant Microscopic Anatomy. J. & A. Churchill Ltd., London, 1950, ed. 11, pp. 214–215.

15. WASSERMAN, F. Fibrogenesis in the regenerating rat tendon with special reference to growth and composition of the collagenous fibril. *Am. J. Anat.*, 1954, **94**, 399–437.

16. KODICEK, E., and LOEWI, G. The uptake of (^{35}S) sulphate by mucopolysaccharides of granulation tissue. *Proc. Royal Soc. London, s.B*, 1955, **144**, 100–115.

17. STEARNS, M. L. Studies on the development of connective tissue in transparent chambers in the rabbit's ear. I. *Am. J. Anat.*, 1940, **66**, 133–176.

18. STEARNS, M. L. Studies on the development of connective tissue in transparent chambers in the rabbit's ear. II. *Am. J. Anat.*, 1940, **67**, 55–97.

19. PENNEY, J. R., and BALFOUR, B. M. The effect of vitamin C on mucopolysaccharide production in wound healing. *J. Path. & Bact.*, 1949, **61**, 171–178.

20. EDWARDS, L. C., and DUNPHY, J. E. Wound healing. I. Injury and normal repair. II. Injury and abnormal repair. *New England J. Med.*, 1958, **259**, 224–233; 275–285.

21. GERSH, I., and CATCHPOLE, H. R. The organization of ground substance and basement membrane and its significance in tissue injury, disease and growth. *Am. J. Anat.*, 1949, **85**, 457–521.

22. CATCHPOLE, H. R. Role of the Ground Substance in Wound Healing. In: The Healing of Wounds. A Symposium on Recent Trends and Studies. WILLIAMSON, M. B. (ed.). Blakiston Div., McGraw-Hill Book Co., Inc. New York, 1957, pp. 29–46.

23. ROBBINS, W. C.; WATSON, R. F.; PAPPAS, G. D., and PORTER, K. R. Some effects of anti-collagen serum on collagen formation in tissue culture; a preliminary report. (Brief note) *J. Biophys. & Biochem. Cytol.*, 1955, **1**, 381–384.

24. TEILUM, G. Periodic acid-Schiff-positive reticulo-endothelial cells producing glycoprotein. Functional significance during formation of amyloid. *Am. J. Path.*, 1956, **32**, 945–959.

25. LEBLOND, C. P.; GLEGG, R. E., and EIDINGER, D. Presence of carbohydrates with free 1,2-glycol groups in sites stained by the periodic acid-Schiff technique. *J. Histochem.*, 1957, **5**, 445–458.

26. HOOGHWINKEL, G. J. M., and SMITS, G. The specificity of the periodic acid-Schiff technique studied by a quantitative test-tube method. *J. Histochem.*, 1957, **5**, 120–126.

27. JACKSON, D. S.; FLICKINGER, D. B., and DUNPHY, J. E. Biochemical studies of connective tissue repair. *Ann. New York Acad. Sc.*, 1960, **86**, 943–947.

28. GRILLO, H. C.; WATTS, G. T., and GROSS, J. Studies in wound healing. I. Contraction and the wound contents. *Ann. Surg.*, 1958, **148**, 145–160.

29. PALADE, G. E. The endoplasmic reticulum. *J. Biophys. & Biochem. Cytol.*, 1956, **2**, Suppl. to No. 4, 85–98.

30. PALADE, G. E. Microsomes and Ribonucleoprotein Particles. In: Microsomal Particles and Protein Synthesis. ROBERTS, R. B. (ed.). Pergamon Press, London, 1958, pp. 36–49.

31. LOWTHER, D. A.; GREEN, N. M., and CHAPMAN, J. A. (To be published)

32. JACKSON, S. F. The morphogenesis of avian tendon. *Proc. Royal Soc. London, s.B*, 1956, **144**, 556–572.

33. PORTER, K. R., and PAPPAS, G. D. Collagen formation by fibroblasts of the chick embryo dermis. *J. Biophys. & Biochem. Cytol.*, 1959, **5**, 153–166.

34. JACKSON, S. F. The fine structure of developing bone in the embryonic fowl. *Proc. Royal Soc. London, s.B.*, 1957, **146**, 270–280.

35. WEISS, P., and FERRIS, W. The basement lamella of amphibian skin. Its reconstruction after wounding. *J. Biophys. & Biochem. Cytol.*, 1956, **2**, Suppl. to No. 4, 275–282.

36. SIEKEVITZ, P., and PALADE, G. E. A cytochemical study on the pancreas of the guinea pig. II. Functional variations in the enzymatic activity of microsomes. *J. Biophys. & Biochem. Cytol.*, 1958, **4**, 309–318.

37. JACKSON, S. F. Fibrogenesis and the Formation of Matrix. In: Bone as a Tissue. RODAHL, K.; NICHOLSON, J. T., and BROWN, E. M. (eds.). McGraw-Hill Book Co., Inc., New York, 1960, pp. 165–185.

We wish to thank Professor J. H. Kellgren for his interest and encouragement and for reading the manuscript.

LEGENDS FOR FIGURES

Photomicrographs were prepared from sections stained with hemalum and eosin.

FIG. 1. Hind limb of guinea pig; skin resected to show the 4 tendons removed during operation.

FIG. 2. Hind limb of guinea pig 4 weeks after tendon removal. A tendinous cord of new connective tissue (T) has formed behind the bone (B).

FIG. 3. The wound area 3 days after operation. The space behind the bone (B) contains a loose fibrin clot (F). The removal of one tendon has, in this case, been incomplete, and the stump remains (T). × 45.

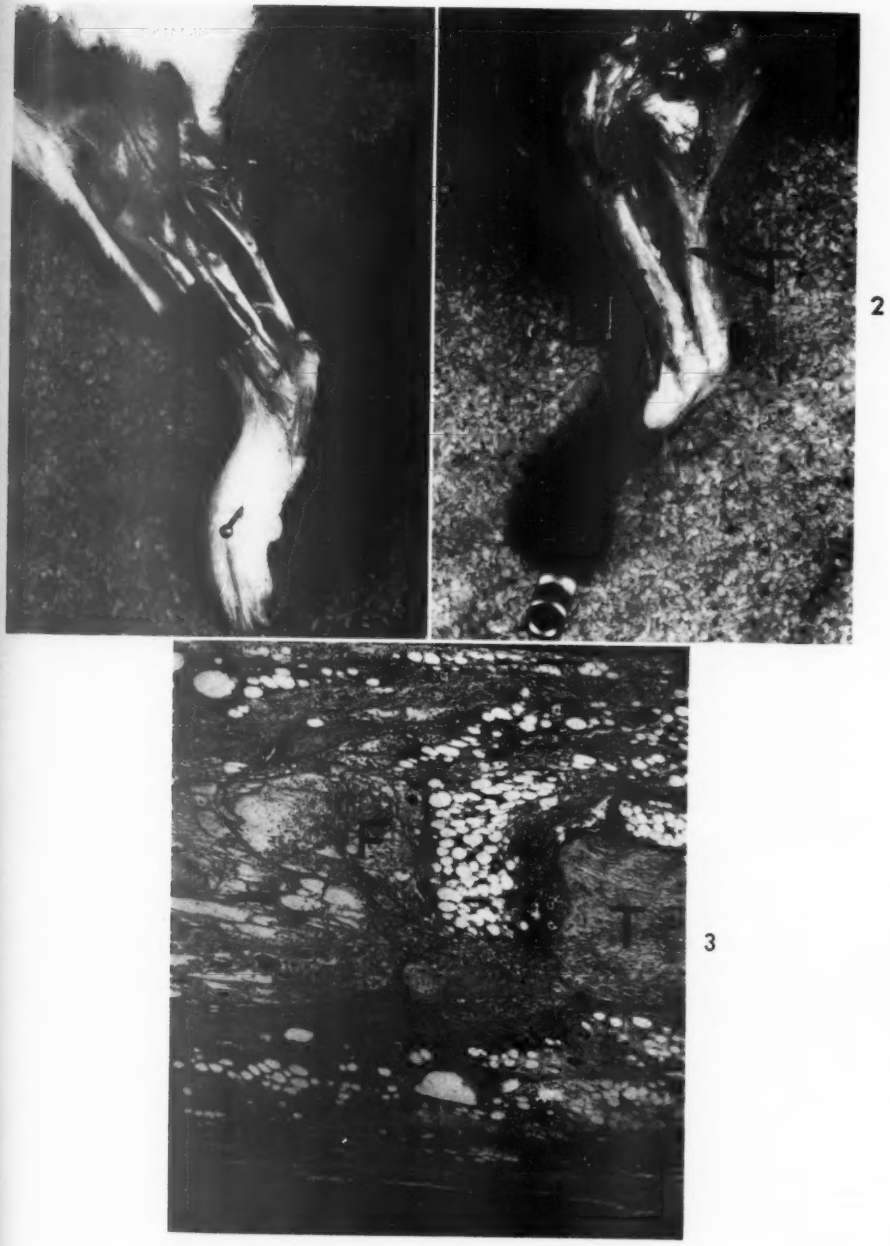

FIG. 4. Fibroblasts at the advancing edge of the granulation tissue 5 days after tendon removal. The cells are spindle-shaped and contain elongated nuclei with dense, uniformly distributed chromatin. These fibroblasts are regarded as being mainly "migratory" in character. × 250.

FIG. 5. Fibroblasts in the deeper aspects of the 5-day granulation tissue. The matrix consists of thicker and more numerous collagen fibers than that associated with the migratory fibroblasts. The cells are rounder with ovoid vesicular nuclei and are regarded as "synthesizing" fibroblasts. × 250.

FIG. 6. Regenerating tissue 14 days after tendon removal. The fibroblasts are surrounded by collagen fibers beginning to show the characteristic arrangement of tendinous tissue. × 125.

FIG. 7. Six weeks after tendon removal. The fibroblasts are elongated and the degree of cellularity reduced. The tissue resembles normal tendon. × 125.

FIG. 8. Bone formation in regenerated tissue 2 years after tendon removal. × 100.

4

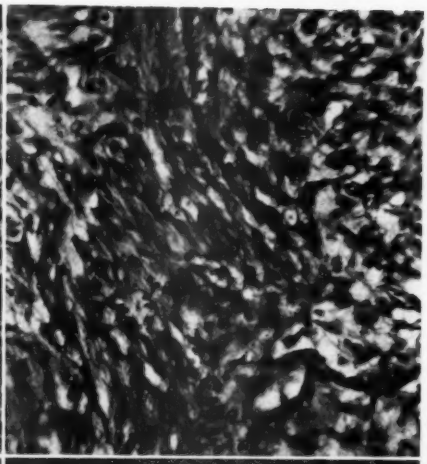

5

6

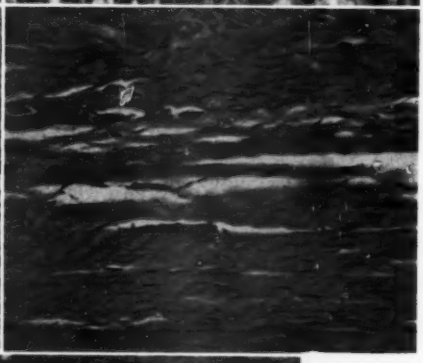

7

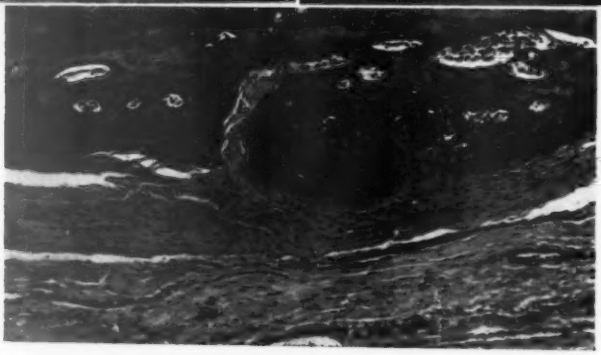

8

Figures 9 to 15 are electron micrographs of tissue fixed in OsO_4. The tissue was then stained with phosphotungstic acid and embedded in araldite except for Figure 9 where the tissue was embedded in methacrylate without staining.

FIG. 9. Part of a type A fibroblast from 5-day repair. This type, found only in the early stages and mainly at the advancing edge of the granulation tissue, is considered to correspond to the migratory fibroblasts observed with conventional microscopy. The rough-surfaced profiles of the endoplasmic reticulum tend to lie parallel to each other and are of fairly uniform width. Their contents are homogeneous and of high electron density. Several mitochondria are included, and the cell membrane is well defined, as is common with this type of cell. A small bundle of collagen fibrils is closely adjacent to the cell membrane in the lower left of the micrograph (arrow). × 30,000.

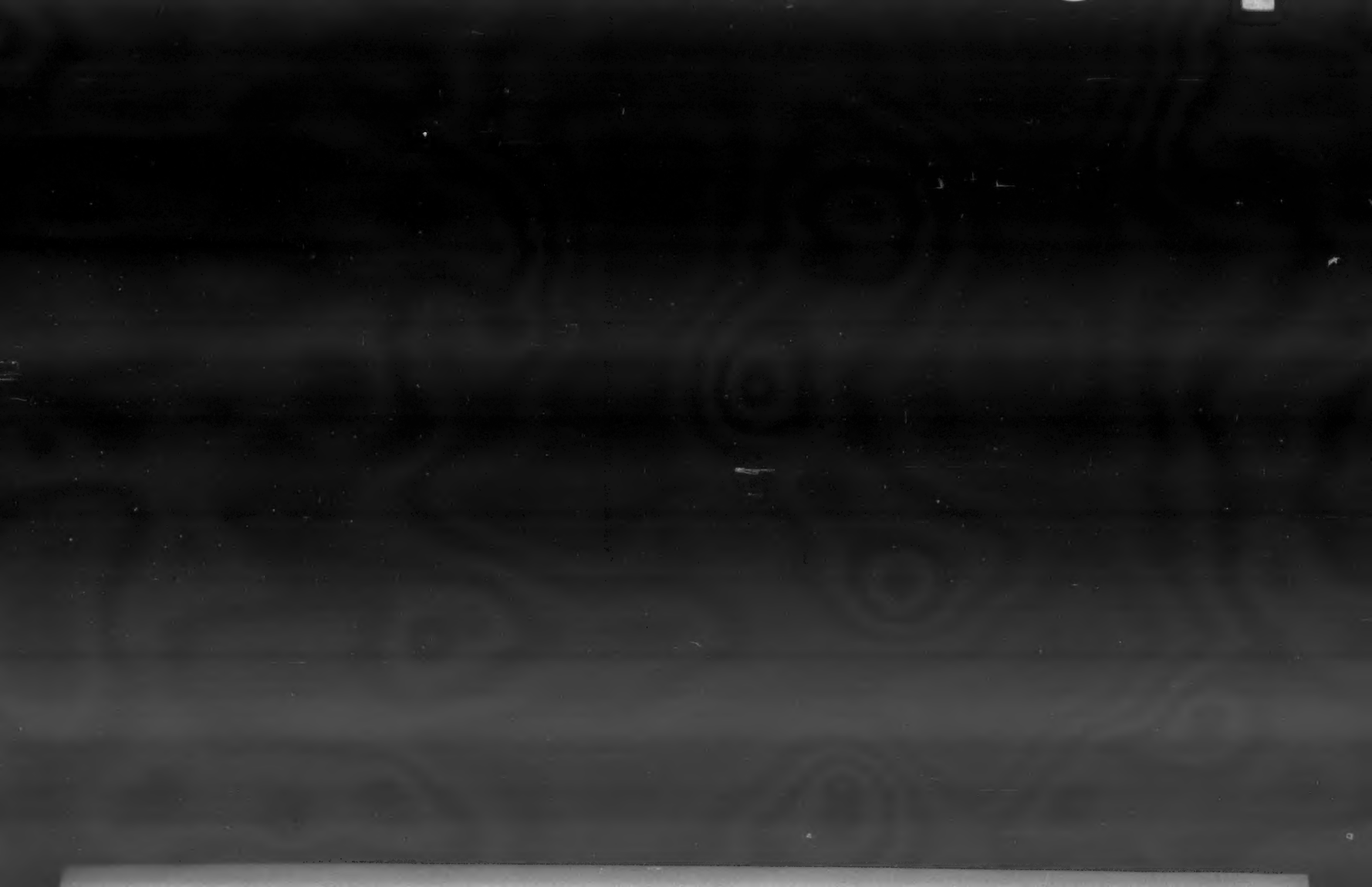

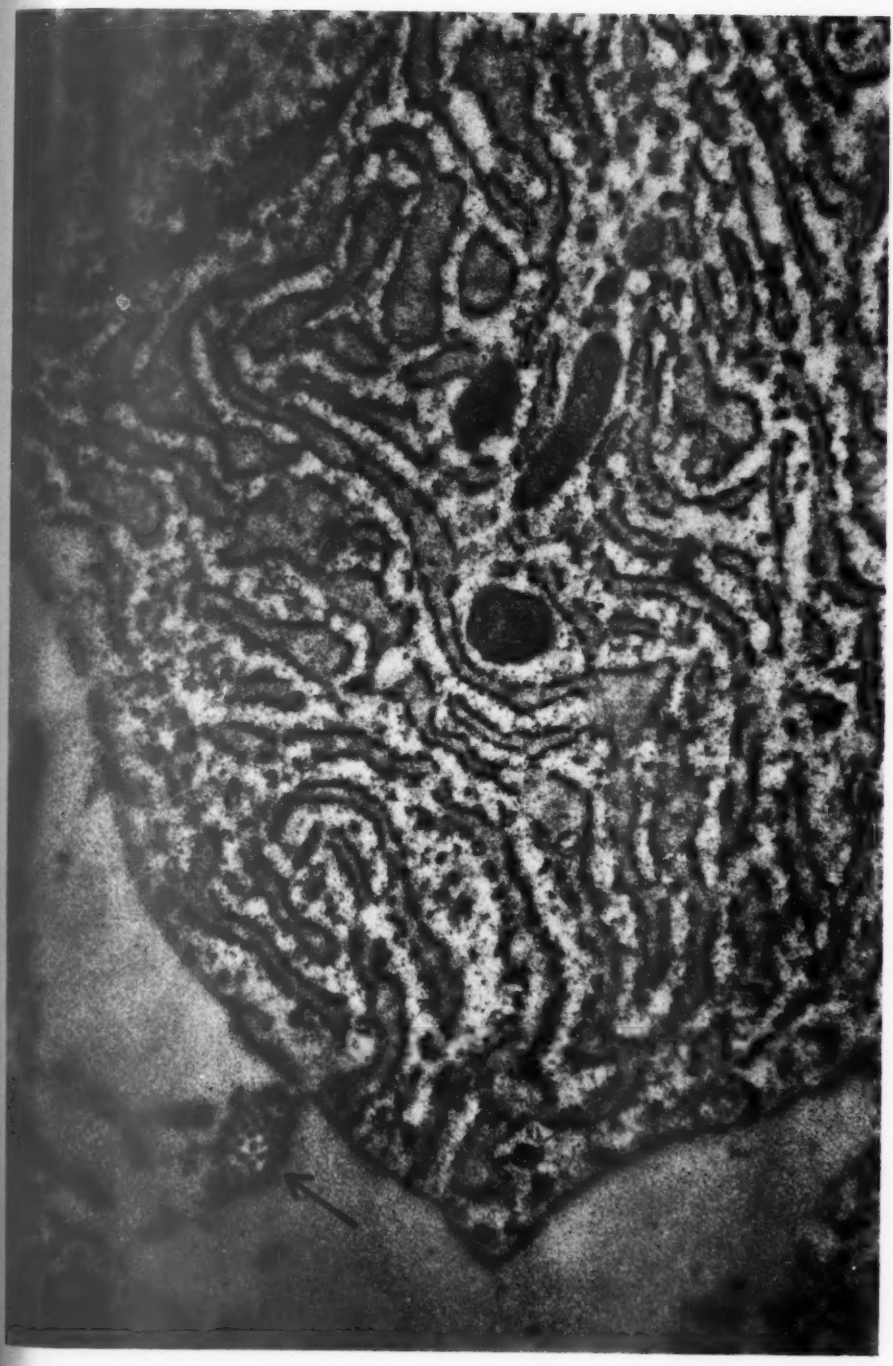

9

10

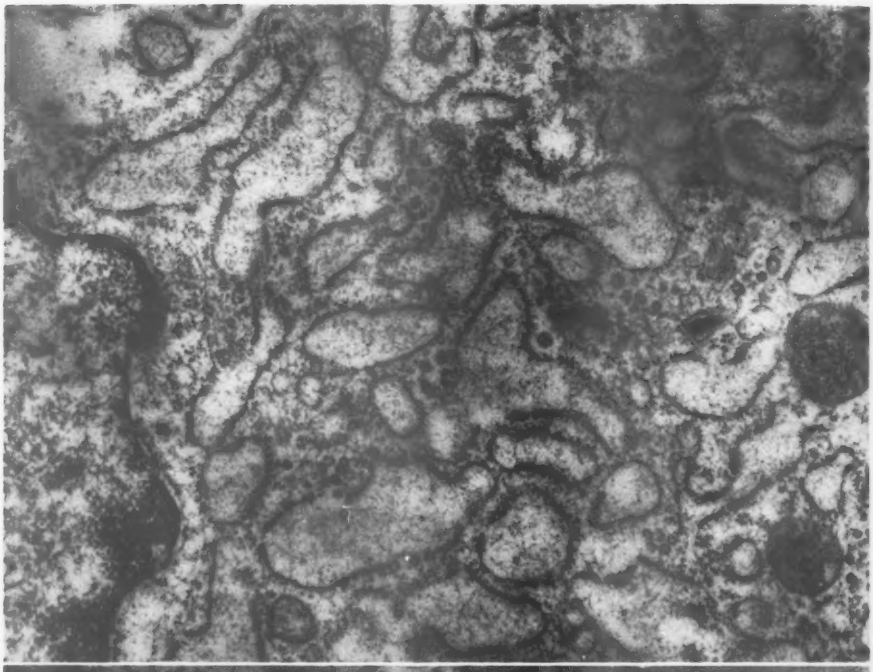

11

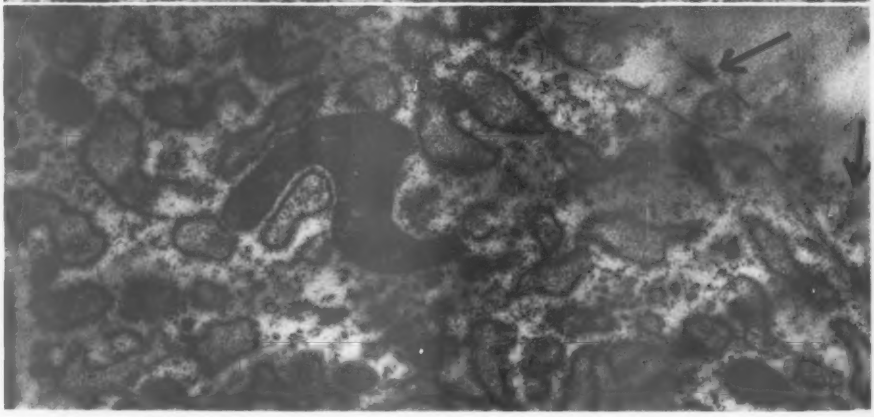

FIG. 10. Part of a type B fibroblast from the 5-day repair tissue. This type, found in greater numbers in the deeper aspects of the tissue, is considered to correspond to the synthesizing fibroblasts. Note the irregular size and distribution of the rough-surfaced profiles of the endoplasmic reticulum. They contain a fine fibrillar material. Two mitochondria are included. × 30,000.

FIG. 11. Part of a fibroblast from the 5-day repair tissue. The appearance of the endoplasmic reticulum is intermediate between that of the type A and type B fibroblasts. The rough-surfaced profiles tend to be elongated but are more irregular in both shape and relative distribution than in the type A cells. Collagen fibrils are indicated by arrows. × 20,000.

12

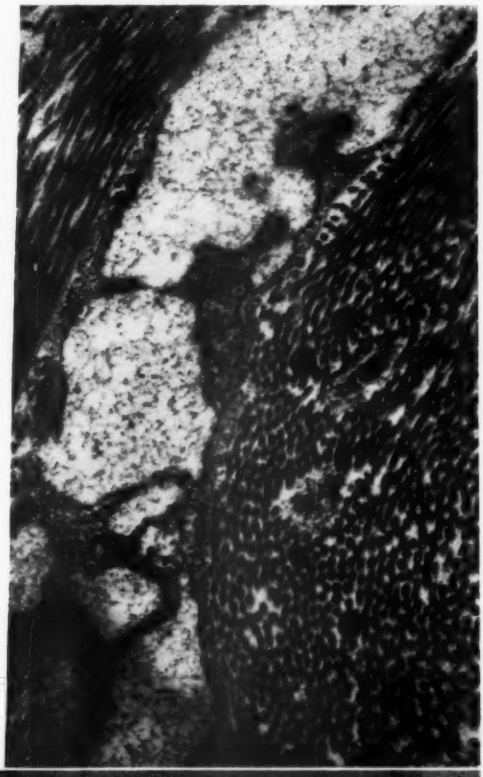

13

14

15

FIG. 12. A type B fibroblast from 14-day repair tissue. × 20,000.

FIG. 13. Part of a fibroblast from 6-week repair tissue, showing the increase in size of the profiles of endoplasmic reticulum with increasing age of the tissue. The cytoplasm merges with the closely adjacent collagen fibrils. × 20,000.

FIG. 14. A group of fine filaments (diameter~100 Å), showing suggestions of a periodic structure and probably representing an early stage in the formation of collagen fibrils. Fourteen-day repair. × 150,000.

FIG. 15. Collagen fibril from 6-week repair tissue. Eight intra-period striations are resolved. × 150,000.